Pelagic Nitrogen Dynamics in Plankton of the Vietnamese Upwelling Area According to Stable Nitrogen and Carbon Isotope Distribution

Dissertation

zur Erlangung des akademischen Grades
Doktor der Naturwissenschaften
(doctor rerum naturalium)

vorgelegt der
Mathematisch-Naturwissenschaftlichen Fakultät
der Universität Rostock

von
Natalie Loick
geb. am 03. Juli 1976 in Bottrop

Rostock 2006

Die vorliegende Arbeit wurde von der Mathematisch-Naturwissenschaftlichen Fakultät der Universität Rostock als Dissertation angenommen und am 15. September 2006 erfolgreich verteidigt.

Die Gutachter waren: PD Dr. Maren Voß, Leibniz-Institut für Ostseeforschung Warnemünde an der Universität Rostock

Prof. Dr. Karin Lochte, Leibniz-Institut für Meereswissenschaften an der Universität Kiel

Summary

Aim of this PhD-thesis was the identification and quantification of the principal nitrogen sources for primary production and to trace these nitrogen sources into higher trophic levels during upwelling and non-upwelling seasons off Vietnam. Furthermore, different food sources for mesozooplankton were investigated. This study is based on the analysis of stable nitrogen and/or carbon isotopes in different pelagic compounds like nitrate and plankton size fractions. In a new approach, nitrogen limitation in zooplankton was investigated based on the analysis of stable nitrogen isotopes in amino acids of plankton size fractions. The samples were collected during three cruises with RV *Nghien Cuu Bien* in the central area of Vietnamese upwelling, two during southwest monsoon (SWM) and one during spring intermonsoon season (SpIM) in 2003 and 2004.

This work is part of the interdisciplinary Vietnamese-German DFG-project Pelagic Processes and Biogeochemical Fluxes in the South China Sea.

Dissolved inorganic nutrients and chlorophyll *a* measurements are discussed with respect to exchange processes between different water masses. Four water masses were identified which are different in the composition of nutrients. Surface waters including Mekong River and the Gulf of Thailand waters and Open Sea Water showed nutrient depletion, whereas Maximum Salinity Water, the supposed upwelling water, had high nutrient concentrations. The subsurface chlorophyll maximum was located between 20 and 40 m water depth in the mixing zone of these three water bodies and fertilized by nutrients due to the dynamical upwelling. Deflection from the Redfield ratio in the C:N ratio and negative excess nitrogen identifies the region as nitrogen limited.

Atmospheric nitrogen (N_2) was identified as important new N-source for primary production. It was found that nitrogen fixation rates are app. 10 times higher during the monsoon season. However, this was not the case in the actual upwelling region – a 40–50 km wide strip along the coast – but further offshore, where the Mekong plume was noticeable. Therefore, it is hypothesized that the stability of the water column, micronutrients and/or trace metals in the Mekong river plume may be responsible for enhanced cyanobacterial growth. These cyanobacteria may be either Trichodesmium, unicellular, or diatom-associated symbionts, the latter are known from other river plumes like the Amazon.

The roles of NO_3^- and N_2 as new nitrogen sources for primary production were evaluated for zooplankton nutrition by comparing $\delta^{15}N$ and $\delta^{13}C$ values in nitrate, particulate organic matter (POM), and six net-plankton size fractions. The $\delta^{13}C$ values in POM and the net-

plankton size fractions differed by 2 to 4 ‰ at any time. It is assumed that plankton from the filters was dominated by nano-and picoplankton opposed to micro-and mesoplankton in the net-samples. This implicates size differential pathways of carbon and nitrogen in the planktonic food web.

We used $\delta^{15}N$ to estimate the differences in N-nutrition between the actual upwelling region and the oligotrophic area further offshore. The $\delta^{15}N$ values of the net-plankton size fractions were depleted in $\delta^{15}N$ by ca. 2 ‰ outside compared to inside the upwelling area during monsoon season. We attribute these patterns to the additional utilization of nitrogen derived from nitrogen fixation. The concomitant findings of high nitrogen fixation rates and low subthermocline nitrate (nitrate$_{sub}$) values of 2.9 to 3.6 ‰ support this conclusion. Net-plankton $\delta^{15}N$ values increased with size pointing to the dominance of higher trophic levels in the larger size fractions. According to a two source mixing model nitrogen fixation may have provided up to 13 % of the nitrogen demand in higher trophic levels and between 14 to 29 % to nitrate$_{sub}$.

Higher Chl. a values within compared to outside the upwelling area point to less favourable feeding conditions for zooplankton further offshore. It is hypothesized that zooplankton is nitrogen or food limited outside the upwelling area. Nitrogen limitation was investigated by comparing $\delta^{15}N$ values of the amino acids leucine (leu), alanine (ala), glutamic acid (glu), aspartic acid (asp), proline (pro), glycine (gly) and tyrosine (tyr) in net plankton size fractions from stations within and outside the upwelling area. In consensus with laboratory and field studies the observed increases in $\delta^{15}N$ in ala, asp, glu, and leu reflected the trophic enrichment in $\delta^{15}N$ with plankton size, whereas gly was not fractionated. Highly significant linear correlations were found between the $\delta^{15}N$ ratios of leu, glu, pro, ala, and asp from six different plankton size fractions at the offshore sites. In contrast no such correlations were found in the upwelling area, except for $\delta^{15}N_{leu}$: $\delta^{15}N_{ala}$ and $\delta^{15}N_{leu}$: $\delta^{15}N_{asp}$. Supported by physiological starvation studies and similarities between the SCS data and data from the North Atlantic Ocean we interpret the strong correlations found at the offshore stations as indication for N- or food limitation.

1.   Introduction

The Vietnamese upwelling area is the most productive region in the South China Sea, however, despite its far-reaching importance very little is known about its biogeochemistry (Liu et al. 2002). Therefore a bilateral Vietnamese-German project "Land-Ocean-Atmospheric Interactions in the Coastal Zone of Southern Vietnam" including the sub-project "Pelagic Processes and Biogeochemical Fluxes in the South China Sea" was launched in 2003. The participating institutes are the Institute of Oceanography in Nha Trang, Vietnam, the Institute of Oceanology in Hai Phong, Vietnam, the Institute of Oceanography in Hamburg, the Institute of Biogeochemistry and Marine Chemistry in Hamburg, the Institute of Geosciences in Kiel, the Center for Tropical Marine Ecology in Bremen, and the Baltic Sea Research Institute Warnemünde in Rostock. The emphasis of the latter project, of which this PhD was part of, is to investigate the marine nitrogen cycle in context to the hydro-chemical conditions in the tropical upwelling area off southern central Vietnam. Main focus of this PhD thesis was to identify and quantify the principal nitrogen sources for primary production (chapters 3.1 and 3.2) and to trace different nitrogen sources into higher trophic levels during upwelling and non-upwelling seasons off Vietnam (chapter 3.3). Furthermore, the structure of the pelagic food web was revealed (chapter 3.3) and the extent of nitrogen limitation was investigated (chapter 3.4). The study was based on the analysis of stable nitrogen and/or carbon isotopes in different pelagic compounds like nitrate, particulate organic matter (POM) or plankton size fractions as well as on the analysis of stable nitrogen isotopes in amino acids of plankton size fractions.

In the following chapters of the introduction a state-of-the-art description of the investigation area as well as a detailed description of the processes that determine stable nitrogen and carbon isotope signatures in a pelagic ecosystem is given. At the end of the introduction the aims of the study are addressed including cross-references to the respective chapters of the results and discussion section.

1.1   The Upwelling Area off Vietnam

The Vietnamese upwelling area is located in the southern part of the South China Sea (SCS) north of the Sunda Shelf and south of the Gulf of Tonkin (Fig. 1.1). Its geographic position lies between 11.0 to 16.0 °N and 109.0 to 111.0 °E where it covers an area of 2.0 to 2.2 x 10^6 km^2 and accounts for 7 % of the SCS (Liu et al. 2002). The topography is characterized by a steep continental shelf of only 20 km width in the northern and of 90 km width in the southern

part. The maximum water depth in the upwelling area off the shelf is 2500 m. There have been seven different water masses described off southern central Vietnam. During spring intermonsoon these have been Continental Shelf Waters (CSW) and Open Sea Water (OSW) at the surface, Seasonal Thermocline Water (STW), Maximum Salinity Water (MSW), Permanent Thermocline Water (PTW), and Deep Water (DW, Rojana-anawat et al. 2001). During southwest monsoon Mekong Water and Gulf of Thailand Water with a salinity above 32 psu have been described to enter the upwelling region from the south (Nguyen 1990).
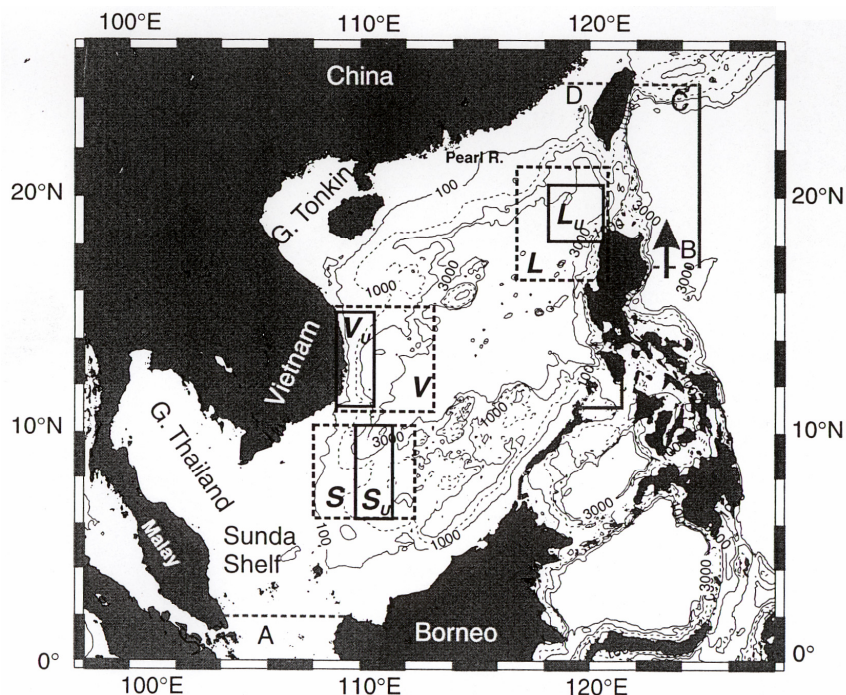
Fig. 1.1: Map of the SCS with isobaths (in meters). Rectangles show the three regions of high sea-surface chlorophyll concentrations: V, east of Vietnam; L, north-west of Luzon; S, north of Sunda Shelf. Subareas representing upwelling centres inside the three regions are V_U, L_U, and S_U. The dashed lines (A, B, C, and D) indicate open, the solid lines (A1, A2 and B1) closed ocean boundaries of the biogeochemical model domain from Liu et al. (2002).

The only effective water mass exchange in the SCS occurs with waters from the western Pacific Ocean through the Strait of Luzon (Xue et al. 2004). Pacific waters enter the SCS from May to January with a net flow through the strait of ca 3.3 Sv or 3.3×10^6 m^3 s^{-1} (Xue et al. 2004). More Kuroshio water reaches the western SCS at deep levels of approximately 1000 m, especially during summer and fall. The transport of waters from the SCS to the Pacific occurs between February to April with a flux of 1.8 Sv or 1.8×10^6 m^3 s^{-1}. The seasonal variation in the net transport appears to be closely related to the east-west sea level difference between Vietnam coast and the Luzon Strait with an approximate 2-month delay. Xue et al (2004) suggested that the elevated net influx during fall is to compensate the summertime coastal upwelling along the Vietnam and southern China coasts. In the deep basin, the Pacific water becomes the deep-water mass of the SCS (Broecker et al. 1986) which upwells and mixes with surface waters to form intermediate water (Gong et al. 1992).

The residence time for the deep water in the basin has been suggested to be 50 to 150 years (Gong et al. 1992).

The circulation in the central SCS is governed by monsoon winds and interaction between the circulation systems in the northern and southern SCS (Hu et al. 2000). The SCS Southern Anticyclonic Gyre occupies most of the southern SCS in summer while the SCS Southern Cyclonic Gyre exists in winter (Fig. 1.2).
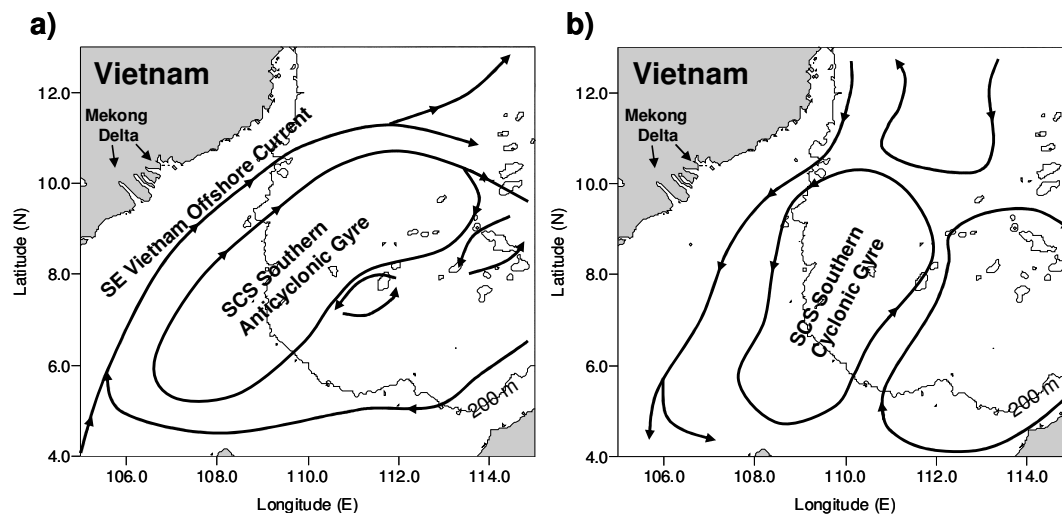
Fig. 1.2: Schematic diagrams of the upper layer circulation in the southern SCS. (a) Southwest monsoon, (b) Northeast monsoon. Redrawn after Hu et al. (2000).

The anticyclonic gyre in the southern part of the SCS is caused by the spatial heterogeneity of the wind stress also causing the cyclonic gyre in the northern SCS (Chao et al. 1996). This circulation pattern forms a dipole and is associated with an eastward offshore jet off the coast of Vietnam at ca. 12.0 °N in summer (Wu et al. 1998). In winter the southward current follows the western boundary throughout (Hu et al. 2000).

Upwelling off Vietnam occurs during southwest monsoon season from July to September and is due to wind induced Ekman transport and the clockwise rotation of the near coastal northward undercurrent that causes dynamical upwelling (Yoshida and Mao 1957, Yoshida 1967). A third upwelling mechanism is a special feature of the Vietnamese upwelling area and leads to the formation of a local maximum in upwelling at ca. 12 °N (Dippner et al. subm.). It is called "stretching deformation induced upwelling" and appears where the northward undercurrent meets the southward current in approximately 70 m depths. This causes a stretching deformation of the flow field leading to additional upwelling as well as to the formation of the aforementioned offshore jet (Dippner et al. subm.). Upwelling events off Vietnam last for 2 to 9 days (Hu et al. 2001). Nutrient rich waters arise from approximately 125 m depth to the surface and are advected offshore into the central SCS due to the general

circulation pattern (Fig. 1.2, Vo 1997, Dippner et al. subm). It appears that after an upwelling event the complete consumption of nutrients re-establishes the oligotrophic conditions described by Pham et al. (2002) and Dippner et al. (subm.). If the southeast monsoon is weak only subsurface layers will get fertilized by upwelling nutrients as documented for post ENSO years (Chao et al. 1996, Dippner et al. subm.).

Besides upwelling, the Mekong river influences the sea area off southern central Vietnam. The Mekong delivers annually about 160 Mt of suspended sediment, and around 5.0, 0.1 and 0.6 Mt of dissolved silica, phosphate and nitrate into the southern SCS (Meybeck and Carbonnel 1975, Milliman 1991). The river plume flows into the Gulf of Thailand and the Sunda Shelf during most of the year but turns northward in summer due to the SWM and the anticyclonic gyre in the southern basin of the SCS (Hu et al. 2000). Although the river delta lies ca 260 km southwest of the actual upwelling area the river plume's less saline waters may be still detectable. However, most of the riverine sediment load is deposed close to the river delta and not carried onto the Vietnamese shelf (Wu et al. 1999).

The biogeochemical model from Liu et al. (2002) computes chlorophyll *a* concentrations of maximum 0.9 mg m^{-3} in August and levels between 0.1 to 0.4 mg m^{-3} during the rest of the year (Fig. 1.3).
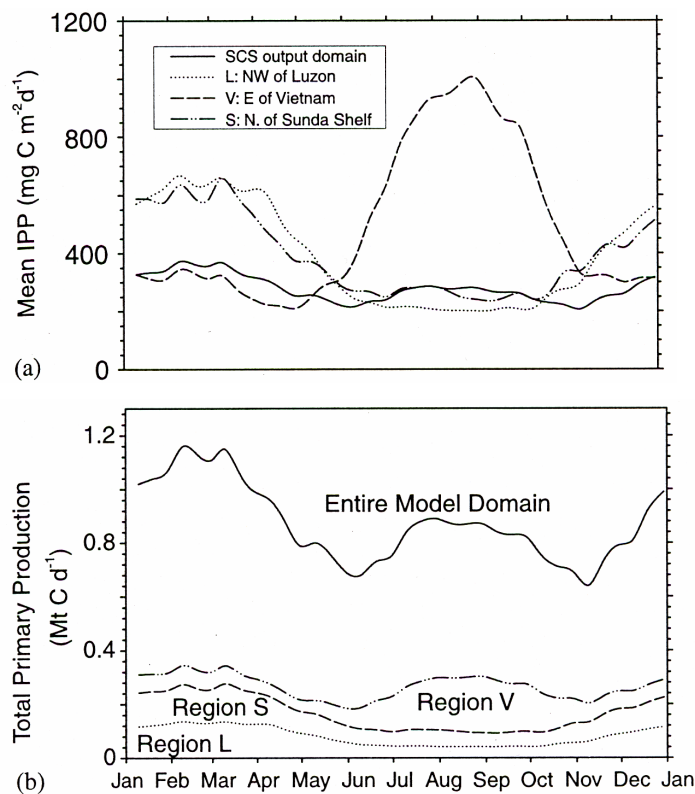
Fig. 1.3: (a) Annual variation of area-averaged depth-integrated primary production (IPP) in the three upwelling regions and the whole output domain for the top 135 m. Timer series model outputs at 10-day intervals. (b) Corresponding volume-integrated primary production in the three upwelling regions and the entire basin. Note: Identical x-axis labelling for a and b. Source: Liu et al. (2002)

This is in good accordance with *in-situ* measurements during summer monsoon (Dippner et al. subm.) and spring intermonsoon (Deetae and Wisespongpand 2001, unpubl. data). Model-derived maximum primary production rates are 1 g C m^{-2} d^{-1} (or 365 g C m^{-2} yr^{-1}, Fig. 1.3a) whereas in the other two upwelling areas northwest of Luzon and north of the Sunda Shelf (Fig. 1.1) maximum rates of 650 mg C m^{-2}d^{-1} (or 237 g C m^{-2} yr^{-1}) have been estimated. Taken together, the three upwelling areas account for 30 % of the annual basin wide total primary production of which the Vietnamese upwelling area contributes 40 Mt (or 40 %) of phytoplankton carbon (Fig. 1.3b). Nevertheless, primary production in the Vietnamese upwelling area is supposed to be nitrogen limited according to N:P ratios < 16 (Chen et al. 2001, Pham et al. 2002).

The only descriptions of phytoplankton distribution off southern central Vietnam are based on the SEAFDEC (Southeast Asian Fisheries Development Center) cruise during intermonsoon season 1999 (Nguyen and Vu 2001, Shamsudin et al. 2001). During this cruise microphytoplankton (> 20 µm) was dominated by the cyanobacteria *Trichodesmium* spp. followed by Bacillariophyta of the species *Bacteriastrum* spp, *Chaetoceros* spp., *Coscinodiscus* spp., *Hemiaulus* spp., *Nitschia* spp., *Rhizosolenia* spp., *Thalassionema* spp., and *Thalassiosira* spp. (Nguyen and Vu 2001). Shamsudin et al. (2001) investigated nanoplankton < 20 µm and found significantly higher nanodiatom cell densities nearshore than away from the coast, while nanodinoflagellates had significantely higher cell numbers offshore. Dominant diatom species were *Thalassiosira* spp., *Minidiscus* spp., *Chaetoceros* spp., *Cyclotella* spp., *Stephanodiscus* spp. and *Asterionella* spp., dinoflagellates were dominated by *Protoperidinium* spp., *Peridinium* spp., *Gonyaulax* spp., and *Prorocentrum* spp. (Shamsudin et al. 2001). Other phytoplankton observations include mass occurrences of *Trichodesmium erythraeum* in Apil 1993 and May 1995 (Nguyen and Doan 1996) and nearshore blooms of *Noctiluca scintillans*. The phytoplankton distribution associated with upwelling conditions off Vietnam has not been investigated in detail so far (Nguyen 1996). Tang et al. (2004) evaluated SeaWiFS-derived Chl. *a* images during summer monsoon 2002 and proposed that upwelling events, eutrophication and river discharge were among the most significant nutrient enrichment phenomena causing elevated Chl. *a* concentrations in the Vietnamese upwelling area. However, their suggestion was relativized by the study from Dippner et al. (subm.) to that effect, that phytoplankton fertilization was due to upwelling of nutrient rich MSW water during summer monsoon 2003. So far, no seasonal succession of algal species has been documented although a shift from diatom to flagellate dominated communities during monsoon and intermonsoon seasons may be expected as well as an in-

offshore trend during upwelling season due to the strong seasonal changes in hydro-chemical conditions.

The zooplankton distribution described for the Vietnamese upwelling area is based on the SEAFDEC cruise described above and on some results from samples that have been taken along a transect between Vietnam and the Philippines in late intermonsoon (May-June) 2000 (Jivaluk 2001, Nguyen and Nguyen 2002). Zooplankton was more abundant in the coastal region than at the offshore sites during both studies and was dominated by copepods, followed by chaetognats and ostracods (Jivaluk 2001, Nguyen and Nguyen 2002). Unpublished data from Cho Ngyuen (Institute of Oceanography Nha Trang, Vietnam) from summer 2003 show that coastal near zooplankton was dominated namely by copepods of the species *Eucalanus subcrassus*, *Canthocalanus pauper*, *Centropages furcatus*, *Oithona plumifera*, *Temora discuadata*, *Arcatia erythraea*, *Undinula vulgaris*, *Eucalanus subtenuis*, and *Acrocalanus gracilis*. Offshore species exceeding 25 ind. m^{-3} included *Acartia amboinensis*, *Nanocalanus minor*, *Pleuromamma robusta* and *P. borealis*. However, as for phytoplankton distribution, no seasonal succession of zooplankton species has been documented so far. Nevertheless it may be expected that along with changing water bodies and nutrient availability during monsoon and intermonsoon seasons an alteration in the phytoplankton community may cause a subsequent change in zooplankton species.

1.2   Nitrogen Supply in Plankton

There are two significant processes that have to be considered when using stable nitrogen isotopes to characterize the nitrogen dynamics in a planktonic food web. These are the mixing and fractionation effects. Different nitrogen sources like nitrate or atmospheric nitrogen can be distinguished because they have different isotopic signatures. Depending on the nitrogen source taken up, phytoplankton will reflect the isotopic signature or a mixture of signatures from different nitrogen sources. The original source values may be modified by the distinct uptake processes for different nitrogen species and lead to additional variations in the stable isotope signature in an algal cell. This process is called fractionation. Stable isotope values are given by the "delta (δ) notation" and have the unit per mil (‰). Descriptions on the definition of the δ-notation and of the isotope theory of fractionation are given in chapter 1.4. In order to understand how nitrogen isotope patterns are produced in phytoplankton and zooplankton it is necessary to know the potential N-sources in the study area as well as the potential uptake mechanisms for these N-sources by the organism and how they influence the isotope distribution. For zooplankton the excretion of nitrogen is also important for the determination

of the isotopic signature in the animal. In the following these N-uptake mechanisms will be described.

Nitrate (NO_3^-) is the most important bioavailable nitrogen form in the ocean and is accumulated below the euphotic zone. It may reach surface layers either by upwelling or via diffusion (Fig. 1.4). Whereas upwelling may be a temporally limited event, diffusion of NO_3^- through the nutricline is a permanent process. Diffusion leads to subthermocline chlorophyll peaks in depths where nutrient and light limitation are balanced, in contrast upwelling causes surface or subsurface chlorophyll peaks. Besides subthermocline nitrate, riverine nitrate may be an important nitrogen source in coastal areas. Therefore the influence of the Mekong River on the dissolved inorganic nitrogen (DIN) distribution has been investigated in chapter 3.1.
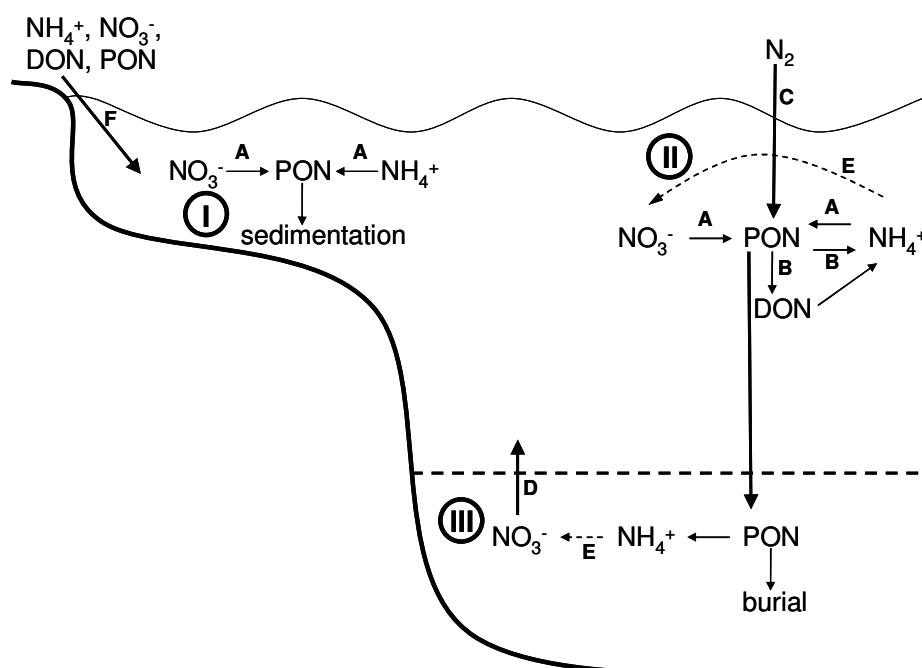
Fig. **1.4**: Conceptual diagram of major features of the nitrogen cycle in coastal shelf and upwelling (I), surface waters of the open ocean (II), and deep water (III). PON, particulate organic nitrogen; DON, dissolved organic nitrogen. Dashed arrows indicate transformations involving multiple steps. Dashed line indicates the nutricline. Pathways: A, DIN assimilation; B, ammonium regeneration; C, nitrogen fixation; D, nitrate diffusion/ upwelling from deep water; E, nitrification; F, continental inputs. Modified after Zehr and Ward (2002) and Sigman and Casciotti (2001).

Fixation of dissolved atmospheric nitrogen (N_2) is an additional new nitrogen source to the euphotic zone of the oligotrophic ocean (Karl et al. 1997). N_2-fixing cyanobacteria dominate these nitrogen limited areas and may form huge mats that can be seen from space in many oligotrophic regions. Ammonium (NH_4^+) is another important nitrogen source for marine phytoplankton. It is the principal end product of the oxidative decomposition of amino acids of ammonotelic zooplankton and the microbial catabolic end product of the remineralization of decaying organic material (Fig. 1.4). Different to NO_3^- and N_2 there is no NH_4^+-reservoir in

the pelagial or atmosphere and production relying on NH_4^+, called regenerated production, cannot produce net-increases in biomass (Dugdale and Göring 1967).

The success of phytoplankton species depends on their potential to quickly take up nitrogenous compounds from the environment. Phytoplankton have a nitrate-protone-symport-carrier in their cell membrane through which NO_3^- is transported from the surrounding waters into the cytosol (Fig. 1.5).
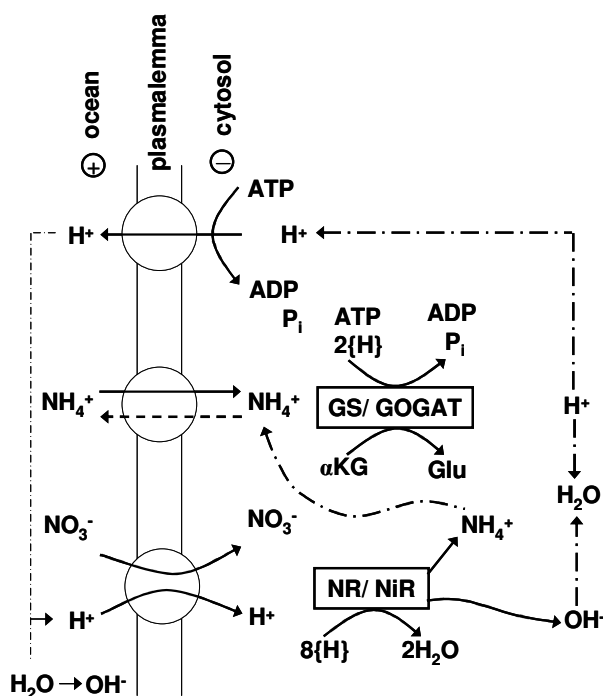
Fig. 1.5: Schematic picture of the hypothesized mechanism of ammonium and nitrate uptake by phytoplankton including the H^+/OH^--budget during uptake and assimilation of these N-compounds. Redrawn from Kohl and Nicklisch (1988).

In cyanobacteria and diatoms additionally evidence for a sodium/nitrate co-transport was found (Tischner 2000). Uptake velocity of NO_3^- into the cell depends on the k_m-value (= Michaelis-Menten half saturation constant in μmol L^{-1}) of the carrier protein which is habitat specific. Phytoplankton from oligotrophic environments have lower k_m-values for NO_3^- uptake than phytoplankton from eutrophic environments (Kohl and Nicklisch 1988). In oligotrophic oceans the maximum uptake velocity (v_m, e.g. in nmol colony^{-1} min^{-1}) of the carrier system is also depending on the maximum uptake rate (= maximum capacity, u_m, e.g. in h^{-1}) that in turn depends on the distinct number of NO_3^- carriers (Tischner 2000). Phytoplankton whose NO_3^- carrier systems have a high specific NO_3^- uptake rate and a low NO_3^- half saturation constant have the highest affinity parameter (u_m/k_m) for NO_3^- and out compete other primary producers (Kohl and Nicklisch 1988). This is the case in oligotrophic, tropical oceans e.g. for *Chaetoceros gracilis* ($u_m/k_m = 83$) which dominates over *Asterionella japonica* ($u_m/k_m = 3.8$).

Once transported into the cytosol NO_3^- is reduced to nitrite (NO_2^-) by the enzyme nitrate reductase (NR) and is further reduced to NH_4^+ by nitrite reductase (NiR, Fig. 1.5). However, there is a growing evidence that NR can also be located at the outside of the plasma membrane (acronym PM-NR) e.g. in the diatom *Thalassiosira* (Tischner 2000). Tischner (2000) assumes that PM-NR may function as blue-light or NO_3^- sensor. Factors controlling the activity of NR are not fully understood yet (Tischner 2000). McCarthy et al. (1977) showed that NO_3^- uptake was reduced by 90 % if NH_4^+ exceeded 0.5 µmol L^{-1}, whereas when NH_4^+ concentrations dropped below this threshold, NO_3^- uptake contributed up to 90 % of N-utilization. Similar NH_4^+ repression of NR has been reported by different authors, but the temporal kinetics and magnitude of NR repression are not consistent among diatoms and other phytoplankton species (Lomas 2004). Song and Ward (2004) found that NR transcription in the marine green algae *Dunaliella tertiolecta* was enhanced by NO_3^- and inhibited by NH_4^+ or N-limitation and that the induction of NR transcript responded to the diel cycle. Their results confirm the hypothesis that the induction and repression of NR transcript may be related to the size of internal nitrogen pools (Tischner 2000) that are described in the following paragraph.

For a cell it is energetically more advantageous to directly grow on NH_4^+ than on NO_3^- because no reduction is necessary before NH_4^+ is fixed. Therefore, natural phytoplankton assemblages may compete for NH_4^+ as preferred nitrogen source. Different studies showed that small pico- and nanophytoplankton (0.2 to 20 µm) may be more successful in utilizing the limited amount of NH_4^+ compared to larger microphytoplankton (20 to 200 µm) that in contrast seems to benefit from growing on NO_3^- (Wafar et al. 2004). NH_4^+ diffuses passively along the ion-gradient into the cytoplasm via nonselective cation channels (White 1996) or high and low affinity NH_4^+ transporters (Javelle and Merrick 2005). Plant cells must keep the intracellular NH_4^+ concentrations low, because NH_4^+ accumulation in the cell may cause protone extrusion, cytosolic pH disturbances, displacement of cations such as K^+ and Mg^{2+}, shifts in plant carbohydrate status and an uncoupling of photophosphorylation (Kronzucker et al. 2001). There are two enzymes that control the intracellular NH_4^+ concentration by synthesis of primary amino acids, glutamate-dehydrogenase (GDH) and glutaminsynthetase (GS). GS has a K_m for NH_4^+ of 29 µmol L^{-1}; GDH has a K_m for NH_4^+ of 10000 to 20000 µmol L^{-1} (Syrett 1981, Kohl and Nicklisch 1988). Therefore, GS is much more capable to keep the intracellular NH_4^+ level low. Although it is energetically more costly than GDH (1 mol ATP per mol glutamate for GDH) it is believed to be the principal NH_4^+ fixing enzyme (Miflin and Lea 1977, Tischner 2000). More recently different GS isoenzymes have been identified, one

is located in the cytosol and assimilates NH_4^+ from external sources and from catabolic processes and one is found in the chloroplasts and assimilates NH_4^+ produced from nitrate reduction (Takabayashi et al. 2005). GS is coupled with glutamate:oxo-glutarate amino-transferase (acronym GOGAT). Together these two enzymes catalyze the reaction from NH_4^+ to glutamine (via GS) to glutamate (via GOGAT, Fig. 1.5).

Atmospheric nitrogen (N_2) is a new nitrogen source for marine phytoplankton, however only cyanobacteria are capable to utilize it. They contain the N_2-fixing enzyme nitrogenase that reduces dissolved N_2 to NH_4^+ which in turn is transaminated via the GS/GOGAT pathway. Natural populations of the cyanobacteria *Trichodesmium* spp. showed a high capacity for NH_4^+ uptake and a low capacity for NO_3^- uptake (Mulholland and Capone 1999). Although N_2-fixation rates were highest and accounted for the majority of the total measured N-utilization during mid-day, rates of NH_4^+ uptake exceeded rates of N_2-fixation throughout much of the diel cycle (Mulholland and Capone 1999). So far *Trichodesmium* spp. is the best described cyanobacteria species due to its large size and high abundances in oligotrophic, tropical, and subtropical oceans (Capone et al. 1997). Other marine cyanobacteria include unicellular cyanobacteria (Zehr et al. 2001, Montoya et al. 2004), diatom-associated symbionts like *Richelia* (Carpenter et al. 1999), and copepod associated symbionts (Proctor 1997, Zehr et al. 2000). Different to most other N_2-fixers, *Trichodesmium* spp. is a nonheterocystous, aerobic N_2-fixer. Nitrogenase is inactivated by oxygen, therefore most cyanobacteria have specialized cells, called heterocysts, in which the enzymes are located. Heterocysts are characterized by thick cell walls to limit oxygen diffusion into the cell and are lacking photosystem II (PSII) so no intracellular oxygen is produced. Without heterocysts, *Trichodesmium* spp. simultaneously performs photosynthesis and N_2-fixation. Some evidence has been found that nitrogenase may be resistant to oxygen inactivation, transiently modified to protect from permanent O_2 deactivation (via conformational changes or covalent modification), or in other cases permanently synthesized to replace inactivated enzymes (Capone et al. 1997). Another study found experimental evidence that intracellular O_2-consumptive processes maintain O_2 at concentrations compatible with N_2-fixation. Even evidence for spatial segregation, analogous to heterocysts, has been given. Despite these strategies, a general mechanism allowing nitrogenase acitivity during photosynthesis has not been described yet (Capone et al. 1997).

The different uptake mechanisms for the nitrogen species NO_3^-, NH_4^+ and N_2 lead to distinct isotopic patterns in phytoplankton compared to the isotope signature of its nitrogen source. Generally, if enough nitrogen is available, algae are depleted in $\delta^{15}N$ compared to the nitrogen

source due to the preferential uptake of the light ^{14}N-molecule compared to the heavier ^{15}N-molecule. In contrast if nitrogen is limiting, phytoplankton will not discriminate against ^{15}N-compounds but will take up all the available nitrogen and therefore will have the same isotope signature as the N-source. For example, in laboratory studies when growing under non-limiting NO_3^- concentrations (> 100 µmol L^{-1}) the diatom *Thalassiosira pseudonana* had a δ^{15}N value of 0.8 ‰ and was 3 ‰ depleted compared to the nitrate δ^{15}N value of 3.8 ‰ (Waser et al. 1998). When nitrate becomes depleted during growth of the algae, also the residual nitrate, enriched in δ^{15}N, will be taken up. This lead to the increase in the δ^{15}N of *T. pseudonana* to the source nitrate value of 3.8 ‰. Similar observations have been made in a laboratory study by Montoya and McCarthy (1995) in which *Thallassiosira weissflogii* was 5 ‰ and *Sceletonema costatum* was 6 ‰ depleted in δ^{15}N compared to the initial NO_3^-. The flagellates *Isochrysis galbana* and *Pavlova lutheri* were 2 ‰ and the flagellates *Dunaliella tertiolecta* and *Chroomonas salina* were 1 ‰ and 1.7 ‰ depleted compared to the NO_3^--source. When all nitrate was used up in the experiments, the δ^{15}N in all algae was equal to 4 ‰ which was the δ^{15}N of the NO_3^- used in preparing the growth medium. The different fractionations of nitrate by diatoms and flagellates were attributed to different uptake mechanisms for nitrate between flagellates and diatoms which however are still not well understood. Recent laboratory studies showed that isotope fractionation of nitrate by three different Thalassiosira species and *Emiliania huxleyi* was caused by NR and the leaking of isotopically heavy NO_3^- out of the cell (Needoba and Harrison 2004, Needoba et al. 2004).

When growing under non-limiting NH_4^+ concentrations (> 150 µmol L^{-1}) *T. pseudonana* had a δ^{15}N value of - 20 ‰ compared to 0 ‰ of the NH_4^+ -source (Waser et al. 1998). It is not known whether the active or passive transport of ammonium into the cytoplasma or the subsequent synthesis of amino acids via GS/GOGAT are responsible for the large discrimination of $^{15}NH_4^+$ compared to $^{14}NH_4^+$ in marine phytoplankton. However, a similar fractionation of -27 ‰ in natural samples of *Skeletonema coastatum* and laboratory cultures of the marine bacterium *Vibrio harveyi* under similar initial NH_4^+ concentrations around 150 µmol L^{-1} has been found (Hoch et al. 1992). This has been taken as indication that in the diatom active transport of NH_4^+ may have caused the fractionation as identified for the bacterium (Hoch et al. 1992).

Laboratory cultures of *Trichodesmium* spp. had δ^{15}N values that varied between -3.6 to -1.3 ‰ when growing on N_2 with a δ^{15}N value of 0 ‰ (Carpenter et al. 1997). Fractionation during N_2-uptake therefore is small compared to the discrimination found during NO_3^- and NH_4^+uptake. Fractionation during N_2 fixation is most likely attributed to the slightly higher

preference of $^{14}N_2$ over $^{15}N_2$ by the nitrogenase complex that is found in all N_2-fixing cyanobacteria.

The isotopic fractionation factors determined during laboratory studies also apply to a large degree for natural phytoplankton assemblages. However, in contrast to the controlled laboratory conditions a natural system is never really closed. That means that a mixture of different N-sources may have to be considered and isotopically altered N-source pools may be replenished e.g. by upwelling impulses. Furthermore natural marine systems are often dominated by different phytoplankton species that cannot be separated. Nevertheless distinct patterns in isotopic distribution can be found in different marine areas. For example the isotopic value of deep nitrate is 5 ‰ in most parts of the ocean (Liu and Kaplan 1989). Only where denitrification takes place, like in oxygen minimum zones, the $\delta^{15}N$ in NO_3^- increase up to values of 20 ‰ (Liu and Kaplan 1989, Voss et al. 2001). On the other hand, in oligotrophic tropical areas like the East China Sea, nitrate in subsurface waters of 100 to 300 m depth was found to have $\delta^{15}N$ value of 3.3 ‰ presumably due to the input of isotopically light N_2 by cyanobacteria (Liu et al. 1996).

Natural phytoplankton communities dominated by diatoms were found to be 4 to 7 ‰ depleted in $\delta^{15}N$ values compared to the surrounding nitrate as found in the laboratory cultures when nitrate is not limiting (Goering et al. 1990, Horrigan et al. 1990, Wu et al. 1997). This was for example the case along a transect in the subarctic northeast Pacific, where *Corethron criochilum*, *Skeletonema* spp., and *Chaetoceros* spp. were dominating (Wu et al. 1997). The $\delta^{15}N$ values in the phytoplankton was always 5 ‰ lower compared to the $\delta^{15}N$ in the surrounding nitrate. $\delta^{15}N$ values in surface NO_3^- were 8 to 12 ‰ and $\delta^{15}N$ values in algae were 4 to 8 ‰. Surface nitrate therefore was 4 to 8 ‰ enriched in ^{15}N compared to NO_3^- in 400 m depth that had $\delta^{15}N$ values of 4 - 5 ‰. The high $\delta^{15}N$ values in phytoplankton, therefore, were the result of previous NO_3^- fractionation during phytoplankton assimilation.

Natural phytoplankton communities growing on ammonium have been found to discriminate only 6.5 to 9 ‰ against $^{15}NH_4^+$ which is considerably lower than observed in laboratory studies (Cifuentes et al. 1989, Montoya et al. 1991). E.g. mixed phytoplankton samples from Chesapeake Bay (USA) were 6.5 to 8 ‰ depleted in $\delta^{15}N$ compared to the $\delta^{15}N$ of the surrounding ammonium (Montoya et al. 1991). $\delta^{15}NH_4^+$ values ranged from 10 to 20 ‰ and particulate organic matter dominated by phytoplankton had $\delta^{15}N$ values of 4.8 to 10.5 ‰ while ammonium concentrations ranged from 3.2 to 21.7 µmol L^{-1}.

Natural samples of *Trichodesmium thiebautii* and *T. erythraeum* from the East China Sea had $\delta^{15}N$ values of -0.8 and -2.0 ‰, respectively (Minagawa and Wada 1986) and are similar

to *Trichodesmium* spp. samples from the SW Sargasso and NW Caribbean Sea which had δ^{15}N values of 0.7 to 0.25 ‰ (Carpenter et al. 1997). Field samples therefore have δ^{15}N values that are almost identical to the δ^{15}N values observed in cultures.

The utilization of different N-sources for primary production in the Vietnamese upwelling area has been investigated in chapters 3.2 and 3.3.

Nitrogen from algae is transferred to higher trophic levels via consumption by herbivores or omnivores. Whereas diatom or dinoflagellate blooms are often controlled by grazers, only few species directly feed on *Trichodesmium* spp. (Sellner 1997). This may be due to a low content of polyunsaturated fatty acids in cyanobacteria compared to dinoflagellates and diatoms as found by Shamsudin (1998). Direct grazing of unicellular or diatom-associated cyanobacteria has not been reported from marine areas yet. However, Montoya et al. (2004) suggested that the pathways by which recently fixed nitrogen enters higher trophic levels might also be distinct for these different groups of marine diazotrophs, e.g. direct grazing on diatom associated symbionts whereas fixed nitrogen from unicellular cyanobacteria may be passed on to higher trophic levels as dissolved organic nitrogen (DON). Besides direct grazing it has been proposed that the remineralization of decaying cyanobacteria and the diazotroph production of ammonium is the most important pathway by which atmospheric nitrogen is made available for other primary producers (Sellner 1997). Another pathway may be via dissolved organic nitrogen since different authors found that 25 to 50 % of recently fixed N was released as amino acids and other dissolved organic nitrogen forms (Capone et al. 1994, Glibert and Bronk 1994). However this has not been studied in detail so far.

Any feeding process leads to an isotopic enrichment of up to 5.5 ‰ in the consumer compared to the diet (Peterson and Fry 1987). Therefore if zooplankton feed on algae that have a δ^{15}N of 5 ‰ the animals may have a δ^{15}N value between 6.3 to 10.5 ‰. Laboratory and field studies by Macko et al. (1982) with *Amphithoe valida* showed that in both approaches the amphipod was 0.4 ‰ enriched compared to the food algae *Ulva* spp. and *Gelidium* spp. A second amphipod *Parhyale hawaiensis* was 2.4 ‰ enriched compared to the same food source in both laboratory and field samples. Field studies from Minagawa and Wada (1984) showed that decapods and copepods were 2.1 and 5.3 ‰ enriched compared to their diet. Isotopic enrichment in zooplankton is attributed to the preferential excretion of ^{14}NH$_4^+$ during food ingestion and protein metabolism (Checkley and Miller 1989). Checkley and Miller (1989) incubated copepodite V stages of *Neocalanus* spp. as well as a diverse assemblage of copepods and doliolids. They found that the δ^{15}N of whole body tissues of the animals were linearly related to the δ^{15}N in the excreted NH$_4^+$. δ^{15}N values in ammonium

ranged from -2 to +4 ‰ and were always 2.7 ‰ depleted compared to the animal tissue. This depletion generally is attributed to the deamination of food during digestion by which "light" $^{14}NH_4^+$ is produced and excreted, leaving the animal enriched in ^{15}N due to isotope mass balance (Minagawa and Wada 1984). Minagawa and Wada (1984) stated that the scatter in isotopic fractionation during excretion found in different animals may be due to variable food sources or due to differences of the internal nitrogen balance that depends on environmental and biochemical conditions. The transfer of the different N-sources for primary production into higher trophic levels in the Vietnamese upwelling area has been investigated in chapter 3.3.

In a new approach the internal nitrogen balance of zooplankton has been tested by comparing nitrogen stable isotopes in amino acids from plankton within and outside the upwelling area. The results of this study are discussed in chapter 3.4.

1.3.   Carbon Supply in Plankton

Pelagic food webs can be analysed more differentially by the additional determination of stable carbon isotopes in the organisms. Stable carbon isotopes behave more conservative than nitrogen isotopes once the carbon is assimilated by phytoplankton. Consumers are only 1 ‰ enriched in $\delta^{13}C$ compared to the diet and therefore may help to identify the principle food source for zooplankton if more than one is available (Peterson and Fry 1987). Differences in the isotope signature of carbon are attributed to the uptake mechanisms of the carbon by algae. Marine microalgae are generally considered C3 plants (Burns and Beardall 1987), therefore C-fixation is catalyzed by ribulose-1,5-bisphosphate carboxylase oxydase (acronym Rubisco). Rubisco catalyses the reaction:

Ribuslos-1.5-bis-phosphate + CO_2 +H_2O→ 2 Phosphoglycerate + $2H^+$ (1.1)

Marine microalgae can use either CO_2 or HCO_3^- as C-source. CO_2 diffuses passively into the cell, whereas for HCO_3^- primary and secondary active transport mechanisms through the cell membrane exist (Kohl and Nicklisch 1987). HCO_3^- is the more abundant DIC-species in seawater and algae contain high concentrations of the enzyme carbonic anhydrase (CA) to dehyrize HCO_3^- to CO_2 that is the substrate for Rubisco (Burns and Beardall 1987). DIC is also fixed by the β-carboxylation which is the carboxylation of phosphoenolpyruvat (PEP) or pyruvat by the enzymes phosphoenolpyruvate-carboxykinase (PEPCK), phosphoenolpyruvate -carboxylase (PEPC), or pyruvate carboxylase (PYRC). The substrate for PEPCK is CO_2, for PEPC and PYRC is HCO_3^- (Cooper and Wood 1971). Descolas-Gros and Fortugne (1985)

and Descolas-Gros and Oriol (1992) found that diatoms contain PEPCK, dinoflagellates contain PEPCK, PEPC, and PYRC and cyanobacteria contain PEPC. McCarthy and Goldman (1979) observed in laboratory studies high rates of β-carboxylation transiently in nitrogen-starved algal cultures that had been enriched with NH_4^+. Although it is assumed that β-carboxylases provide only 4.5 to 25 % of the cellular carbon demand McCarthy and Goldman (1979) hypothesized that they may be important for the intermittent assimilation of ammonium pulses in microalgae. This was confirmed by different studies showing that under these conditions β-carboxylation serves to replenish carbon skeletons for the GS/GOGAT catalyzed NH_4^+ assimilation (Guy et al. 1989, Vandlerberghe et al. 1990, Huppe and Turpin 1994).

Carbon isotope distribution in marine microalgae vary considerably approximately between -30 ‰ to -10 ‰ (Goericke et al. 1994). The $\delta^{13}C$-DIC in seawater is principally determined by bicarbonate (HCO_3^-), because the balance reaction favours HCO_3^- in seawater at a pH < 8.5 while only 1 % of DIC is available as CO_2. The $\delta^{13}C$ of HCO_3^- in the upper 1000 m of the global ocean generally is 1.5 ‰, although biological and air-mixing processes may cause some variability (Kroopnick 1985). Depending on the temperature, the $\delta^{13}C$ of CO_2 is e.g. at 25 °C 8.5 ‰ lighter than the $\delta^{13}C$ of HCO_3^-. Therefore at 25 °C if $\delta^{13}C$- HCO_3^- = 1.5 ‰ $\delta^{13}C$-CO_2 would be -7 ‰, at 30 °C -6.9 ‰ or 0 °C -10.5 ‰ (*see* dehydration of HCO_3^- in Tab. 1.1). The isotopic equilibrium however is not achieved in the ocean due to the slow reaction kinetics of HCO_3^- and CO_2. Different to nitrogen, carbon is supposed to be not limiting in the ocean. Therefore maximum discrimination against ^{13}C-DIC compared to ^{12}C-DIC is developed in algae.

Diatoms may be more enriched in $\delta^{13}C$ than dinoflagellates or cyanobacteria as indicated by laboratory studies by Falkowski (1991). He showed that the isotopic composition in marine phytoplankton species grown at 15 °C was lowest in the dinoflagellates *Amphidinium carterae* and *Cachonina niei* and that the diatoms *Skeletonema costatum*, *Melosira nummuloides*, *Thalassiosira pseudonana* were significantly enriched in ^{13}C compared the dinoflagellates. $\delta^{13}C$ values in the diatoms ranged from -9.5 ‰ to -16.4 ‰ and in the dinoflagellates from -15.2 to -29.7 ‰. $\delta^{13}C$ in two cyanobacteria was -17.4 ‰ for *Phormidium luridum* grown at 15°C and -28.8 ‰ for *Phormidium persicinum* grown at 20 °C. Also natural diatoms samples were enriched in $\delta^{13}C$ compared to other plankton as shown in a study by Fry and Wainright (1991). Differences in the $\delta^{13}C$ between algal species have been attributed to the carbon fixation by β-carboxylases (Descolas and Fortugne 1985). Descolas and Fortugne (1985) measured Rubisco, PEPCK and PEPC activity together with $\delta^{13}C$ values

in the diatoms *Fragilariopsis kerguelensis*, and *Skeletonema costatum* and in the dinoflagellate *Prorocentrum micans*. They found that low $\delta^{13}C$ values were related to high Rubisco activity and high $\delta^{13}C$ values in the algae that were related to high PEPCK and PEPC activities. Rubisco discriminates against $^{13}CO_2$ by 20-29 ‰, PEPCK similarly by 20-40 ‰, whereas PEPC discriminates against HCO_3^- only by 2 ‰ (Goericke et al. 1994).

Rau et al. (1990) found size specific differences in the $\delta^{13}C$ signatures of plankton ranging from < 3 µm to > 150 µm (Fig. 1.6). They measured $\delta^{13}C$ in plankton size fractions of < 3 µm, 3-8 µm, 8-20 µm, 20-150 µm and > 150 µm during four seasons in the Mediterranean Sea. In April and Juli $\delta^{13}C$ decreased with increasing plankton size from -25 ‰ to -22.5 ‰ (April) and -20 ‰ (July), respectively. $\delta^{13}C$ decreased with increasing plankton size from -24 ‰ to -20 ‰ in September and to -22.5 ‰ in December, respectively. In size fraction 8-20 µm diatoms, naked oligotrichous ciliates, dinoflagellates, and tintinids were found. In contrast, these organisms were absent in size fraction 3 - 8 µm.
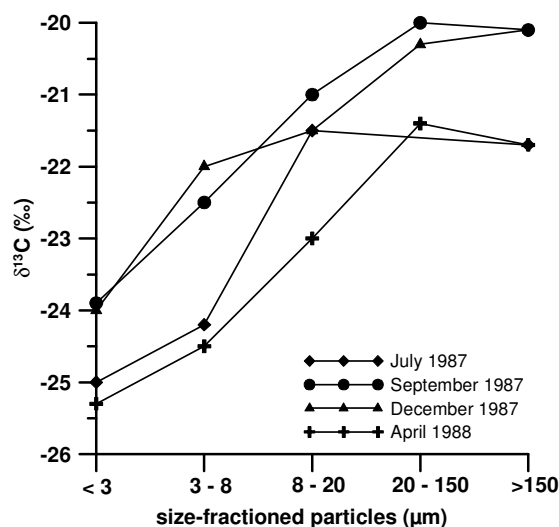
Fig. 1.6: $\delta^{13}C$ values in different plankton size fractions ranging from < 3 µm to > 150 µm from the Mediterranean Sea from four seasons. Source: Rau et al. (1990).

Rau et al. (1990) interpreted these findings as an effective separation of certain biotic groups belonging to four different trophic levels. Their interpretation was strongly supported by minicell recapture predator-prey and model results from Wikner and Hagström (1988). Wikner and Hagström (1988) identified and characterized four trophic levels in plankton ranging from 1 - 12 µm from waters near the sampling site from the study by Rau et al. (1990). The first trophic level was found in size fraction 1-5 µm and contained of pico- and small nanoflagellates (e.g. *Ochromonas* sp., and *Bodo* sp.), the second trophic level was found in size fraction 5-8 µm and contained of nanoflagellates (e.g. *Chryptomonas* sp. and

Monas sp.), the third trophic level was found in size fraction 8-10 µm and contained nanoflagellates (e.g. *Chromulina* sp.), and the fourth trophic level was found in size fraction 10-12 µm and contained ciliates and flagellates (e.g. *Cyclidium* sp.). Differences in $\delta^{13}C > 1$ ‰ - indicating the separation of different trophic levels - have been also been found in different plankton size fractions from the Vietnamese upwelling area. The results of this study and their implications are discussed in chapter 3.3.

1.4.   Isotope Theory

The following chapter unless otherwise noted is based on the book Stable Isotope Ecology from Brian Fry (in press). The stable isotopes ^{15}N and ^{13}C are natural tracers for nitrogen and carbon cycling in an ecosystem. Carbon and nitrogen occur in two stable isotopes, ^{14}N and ^{15}N for nitrogen which have 7 and 8 neutrons in their nucleus, and ^{12}C and ^{13}C for carbon which have 6 and 7 neutrons in their nucleus. Although an extra neutron does not change the chemical behaviour, they cause small differences in the atomic masses that entail a slightly selective uptake of the lighter isotopes e.g. by algae or microorganisms. This discrimination against the heavy isotopes causes patchy distributions of isotope ratios in different compounds compared to big N and C pools like the ocean and the atmosphere that can be detected.

The difference in ^{15}N:^{14}N or ^{13}C:^{12}C in these compounds are measured precisely relative to the ratio of the isotopes in universal reference standards by mass spectrometry. The heavier isotopes are much rarer than their lighter twins and are therefore measured in ratios rather than in absolute numbers. The standard for N isotopes is N_2 and for C isotopes is Pee Dee Belemnite (PDB). The difference between a sample and the standards is expressed in δ-notation in units of per mil (‰) in which $\delta^{15}N$-N_2 and $\delta^{13}C$-PDB are set to 0 ‰ (Equation 1.2):

$$\delta^{15}N_{sample}(‰) = \left(\frac{(^{15}N/^{14}N)_{sample}}{(^{15}N/^{14}N)_{N_2}} - 1 \right) \times 1000 . \qquad (1.2)$$

The selective uptake of light isotopes is called fractionation. Mixing of the fractionated nitrogen and/or carbon compounds counteracts the effect of fractionation, because it recombines separated heavy and light isotopes, thus erasing the effects of fractionation. The reason why fractionation occurs is that there is a time-dependent or kinetic discrimination of the heavy compared to the light e.g. nitrogen isotope in the reaction A→B as shown in the reactions 1.3, 1.4, and 1.5:

$$A \xrightarrow{k_{14_N}} B \qquad (1.3)$$

$$A \xrightarrow{\ k_{15_N}\ } B \tag{1.4}$$
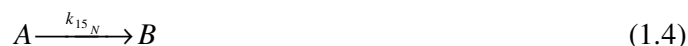
$$k_{14_N} \neq k_{15_N} \tag{1.5}$$

k_{14_N} is the reaction rate constant for the ^{14}N compound, k_{15_N} is the reaction rate constant for the ^{15}N compound. These constants are slightly different, because the ^{14}N compound is taken up a little bit faster than the ^{15}N compound. The ratio of these reaction rate constants (k_{14N}:k_{15N}) is called "isotopic discrimination factor α" or "isotopic enrichment factor ε", which is the transversion of the dimensionless α into a per mil illustration as shown in equation 1.6:

$$\varepsilon(\text{\textperthousand}) = 1000 \times (\alpha - 1) \tag{1.6}$$

Fractionation occurs at the atom level and may be separated into physical and chemical fractionation. Diffusion is an important physical fractionation, where the extra neutron difference in the nucleus means a slower reaction rate. Chemical fractionation occurs during the making and breaking of bonds. Table 1.1 shows the ε-values of some important carbon and nitrogen transformation processes. The averaging effects of atom level fractionation lead to distinct isotope patterns of a composite sample like a whole organism or bulk sample size fractions.

Table 1.1: Dominant processes associated with ^{15}N and ^{13}C fractionation in microalgae. Compiled from reviews by Sigman and Casciotti (2001) and Goericke et al. (1994). Question marks indicate where uncertainties exist concerning the fractionation factor of the respective process.

Reaction	Substrate	ε
NO_3^- assimilation	NO_3^-	4 - 6 ‰
N_2 fixation	N_2	0-2 ‰
NH_4^+-assimilation	NH_4^+	6.5 – 8.0 ‰
Nitrification	NH_4^+	15 ‰
Denitrification	NO_3^-	20-30 ‰
CO_2 diffusion	CO_2, HCO_3^-	< 0.7 ‰
dehydration of HCO_3^-	HCO_3^-	8-12 ‰
passive DIC uptake	CO_2	< 0.7 ‰, ?
active DIC uptake	CO_2, HCO_3^-	small, ?
backdiffusion of CO_2	CO_2	< 0.7 ‰, ?
Rubisco carboxylation	CO_2	20-29 ‰
β-carboxylation PEPC	HCO_3^-	2 ‰
β-carboxylation PEPCK	CO_2	20-40 ‰

Fractionation reactions proceed differently depending on whether the substrate concentration that is added once and then used up over time, or whether it enters and exits continuously. A system in which the substrate is not renewed and used up over time is called closed system, whereas a system with concentrations remaining the same over time is called opens system. Examples for closed systems are closed-bottle batch cultures in the laboratory or plankton blooms in the sea that use up nutrients in a few days. Examples for open systems are flow-through cultures or carbon acquisition by a leaf where CO_2 concentrations are reduced from the internal leaf air spaces due to fixation by photosynthetic enzymes. CO_2 can also leak back out to the atmosphere, so that in all there are two exit fluxes from the CO_2 inside the leaf. It is sometimes difficult to consider whether a system is open or closed and some caution has to be taken e.g. when a closed system may not be truly closed.

The fractionation reactions for closed and open systems follow distinct equations in which the fraction reacted "f" is key to understanding isotopic compositions (Mariotti et al. 1981). Fractionation therefore is not a random process, but is determined by a few enzymes that are involved in nitrogen and carbon uptake as shown in the two previous chapters. This leads together with the nitrogen and carbon source pools and ecological stoichiometry to characteristic patterns of isotope values in an ecosystem like the ocean (Fig. 1.7).
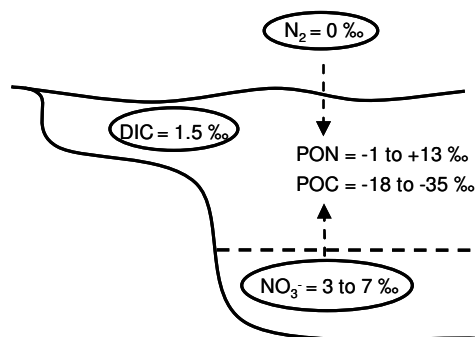
Fig. 1.7: Simplified schematic of $\delta^{15}N$ and $\delta^{13}C$ values of the principal N- and C- pools (encircled) for marine biological production and isotope ranges of particulate organic nitrogen (PON) and carbon (POC), respectively, assimilated from them. Continental inputs are excluded due to their extreme variable or often negligible influence in marine areas. Compiled from Kroopnick 1985 (DIC), Goericke and Fry 1994 (POC), Liu and Kaplan 1989 & Liu et al. 1996 (NO_3^-), Sigman and Casciotti 2001 (N_2), Montoya et al. 2002 & Altabet and Francois 1994 (PON).

Natural abundance distribution of stable nitrogen and carbon isotopes in few selected inorganic and organic compounds like nitrate and different plankton size fractions allow a straightforward characterization and differentiated understanding of elemental flow through a planktonic food web (Michener and Schell 1994).

1.5.   Aim of the Study

The aim of the study was to investigate the primary nitrogen sources for primary and secondary production during upwelling and non-upwelling season off southern central Vietnam. This study is based on data from three cruises from southwest monsoon 2003, spring intermonsoon 2004 and southwest monsoon 2004. The major focus of this PhD-thesis was set on the quantification of the transfer of nitrogen from nitrogen fixation and subthermocline nitrate into primary producers and subsequently into higher trophic levels of the planktonic food web. Furthermore N-limitation in higher trophic levels was examined.

Prior to the food web-focused analysis a detailed analysis of the physico-chemical conditions during upwelling season 2003 was performed to evaluate the influence of upwelling and intrusions of the Mekong River on dissolved inorganic nitrogen distribution as shown in chapter 3.1.

The amount of N_2 as N-source for primary production was quantified by N_2-fixation rate measurements from summer monsoon seasons 2003, 2004 and intermonsoon season 2004 as shown in chapter 3.2.

The roles of NO_3^-, N_2 and NH_4^+ as N-sources for primary and secondary production and the disclosure of some of the pelagic food web structure were identified and quantified from both southwest monsoon seasons and the spring intermonsoon season via the stable isotope approach as shown in chapter 3.3.

Based on nutrient and Chl. *a* distribution it is hypothesized that zooplankton was nitrogen limited outside the upwelling area. To test this, the $\delta^{15}N$ of six different amino acids in net-plankton size fractions were compared from stations within to stations outside the upwelling area as shown in chapter 3.4.

This PhD has been part of an interdisciplinary project in which the results of different scientists intertwine. Full comprehension of the results of this thesis can only be achieved with respect to the results from other project members. Therefore the results and discussion in chapter 3 are presented within the context of designated external results in a manuscript-like structure. In order to avoid repetition, material and method descriptions were pre-drawn into chapter 2 with cross references to the respective studies. In chapter 4 the results of this thesis are related to global marine nitrogen cycling and implications for future research are drawn.

2.   Material and Methods

2.1.   Study area and sampling

The study area off southern central Vietnam was sampled on different station grids during three cruises on board of RV *Nghien Cuu Bien* during southwest monsoon (SWM) 2003, spring intermonsoon (SpIM) 2004 and SWM 2004 (Fig. 2.1). Not all transects were sampled during the different cruises due to logistic and changing weather conditions and the station grids as well as some sampled parameters differed between cruises. Fig. 2.1 shows the station grid of each cruise.
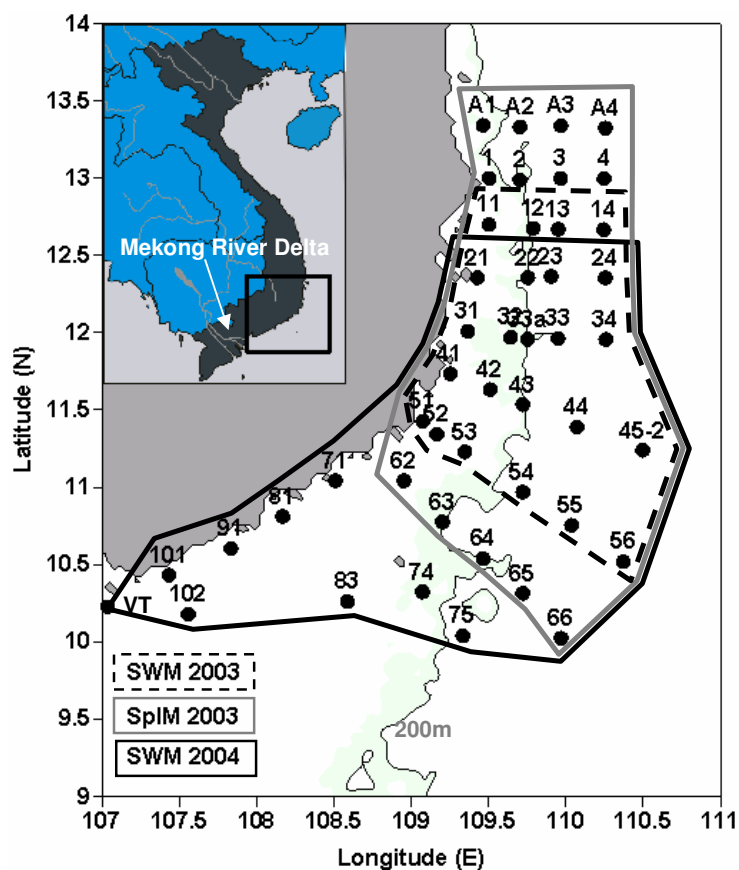
Fig.2.1: Station map during the three sampling periods in southwest monsoon (SWM) and spring intermonsoon seasons.

Stations were sampled with a Seabird CTD rosette system and different plankton nets. Table 2.1 comprises the different parameters collected during each cruise. The studies described in chapters 3.1 to 3.4 are based on different parameters and rely on data from different cruises as will be described in the respective material and method section of each study.

Table 2.1: Parameters collected during the three cruises onboard of RV *Nghien Cuu Bien*.

SWM 2003	SpIM 2004	SWM 2004	parameter	sampling and/or measurement device
✓	✓	✓	wind speed (ms^{-1}) and direction (deg)	Aanderaa system
✓	✓	✓	air temperature (°C)	Aanderaa system
✓			relative humidity (%)	Aanderaa system
✓	✓	✓	air pressure (hPa)	Aanderaa system
✓	✓	✓	cloudiness (okta)	Aanderaa system
✓	✓	✓	precipitation (mm)	Aanderaa system
✓	✓	✓	solar radiation (Wm^{-2})	Aanderaa system
✓	✓	✓	water depth (m)	Aanderaa system
✓		✓	current speed (ms^{-1}) and direction (deg)	ADCP NOBSKA MAVS 2
✓	✓	✓	secchi depth (m)	Secchi disc
✓	✓	✓	water temperature (°C)	Seabird CTD
✓	✓	✓	water salinity	Seabird CTD
✓	✓	✓	sampling depth (m)	Seabird CTD
✓	✓	✓	fluorescence (mg m^{-3})	Seabird CTD
✓			DIC (µmol L^{-1})	water sample CTD rosette
✓	✓	✓	Chl. *a* (mg m^{-3})	water sample CTD rosette, spectrophotometer
✓	✓	✓	nutrients NO_3^-, NO_2^-, PO_4^{3-}, SiO_4 (µmol L^{-1})	water sample CTD rosette
✓	✓	✓	oxygen (mg L^{-1})	water sample CTD rosette, DOA
✓	✓	✓	PON, POC (µmol L^{-1})	water sample CTD rosette
✓	✓	✓	nano-/picoplankton taxonomy and abundance (species level, cells mL^{-1})	water sample CTD rosette
✓	✓	✓	ichthyoplankton taxonomy and abundance (species level, cells mL^{-1})	JUDAY net 500 µm
✓	✓	✓	mesoplankton taxonomy and abundance (species level, cells mL^{-1})	JUDAY net 200 µm
✓	✓	✓	microplankton taxonomy and abundance (species level, cells mL^{-1})	JUDAY net 45 µm
✓	✓	✓	δ^{15}N-POM, δ^{13}C-POM (‰)	water sample CTD rosette, Thermo Finnigan Delta S or Delta Plus IRMS
✓	✓	✓	δ^{15}N-NO_3^- (‰)	water sample CTD rosette, Thermo Finnigan Delta S or Delta Plus IRMS
✓	✓	✓	$^{15}N_2$/ $^{13}CO_3^{2-}$-fixation rates (nmol L^{-1} hr^{-1})	water sample CTD rosette, simulated *in-situ* incubations, Thermo Finnigan Delta S or Delta Plus IRMS

(continued next page)

Tab. 2.1: *Continued from the previous page.*

SWM 2003	SpIM 2004	SWM 2004	parameter	sampling and/or measurement device
✓		✓	$^{15}NO_3^-$-fixation rates (nmol L^{-1} hr^{-1})	water sample CTD rosette, simulated *in-situ* incubations, Thermo Finnigan Delta S or Delta Plus IRMS
✓	✓	✓	$\delta^{15}N$-/$\delta^{13}C$ mesoplankton (‰)	JUDAY net 200 µm, Thermo Finnigan Delta S or Delta Plus IRMS
✓	✓	✓	$\delta^{15}N$-/$\delta^{13}C$ microplankton (‰)	JUDAY net 45 µm, Thermo Finnigan Delta S or Delta Plus IRMS
✓		✓	$\delta^{15}N$-/$\delta^{13}C$ amino acids microplankton (‰)	JUDAY net 200 µm, Hewlett Packard 58590 – MAT 252 GC-C-IRMS
✓		✓	$\delta^{15}N$-/$\delta^{13}C$ amino acids mesoplankton (‰)	JUDAY net 45 µm, Hewlett Packard 58590 – MAT 252 GC-C-IRMS

The cumulative and manuscript-like structures of the chapters 3.1 to 3.4 cause restating of some information. To diminish repetitions later on a detailed material and method section for each chapter was pre-drawn into this chapter. Instead chapters 3.1 to 3.4 include references to the respective material and method comprised here to ensure easy comprehension of the handled data in each study.

2.2.   Monsoon Induced Upwelling

During the southwest monsoon from July 8 to 28, 2003, an interdisciplinary cruise took place in the central area of Vietnamese upwelling with RV *Ngien Cuu Bien*. In the first part of the cruise, observations on a fixed station grid were carried out from July 10 to 16 (Fig. 2.2). The grid size was designed to resolve the internal radius of deformation. For logistic reasons, we had to interrupt the cruise for two days. From July 19 to 22, during the passage of typhoon no. 3 and rough weather conditions, we sampled near coastal stations southwards until Vung Tau, close to the river mouth of River Mekong (Fig. 2.2). From July 24 to 26, after the passage of the typhoon, we deployed a lagrangian sediment trap in the center of the upwelling area and followed the drifter. In this paper only the observations on the grid stations will be presented. At each station CTD-observations, using a Seabird system, were made for temperature (T), salinity (S), depth (D), and fluorescence down to a maximum depth of 300 m. At oceanographic standard depths water samples were taken which were analysed on board for nutrients (Nitrate, nitrite, phosphate, and silicate), oxygen, pH, alkalinity, and dissolved inorganic carbon (DIC) and chlorophyll *a*. Immediately after sampling, water samples were

measured by standard methods for DIC, nitrate, nitrite, and silicate after Grasshoff et al. (1999), for phosphate after Murphy and Riley (1962) and for oxygen after Culberson (1991) with a Dissolved Oxygen Analyser by SIS. For chlorophyll *a* determination 1 to 3 liter of water was filtered through Whatman GF/F filters and frozen (-20 °C) before further spectrometrical processing after Jeffrey and Humphrey (1975).
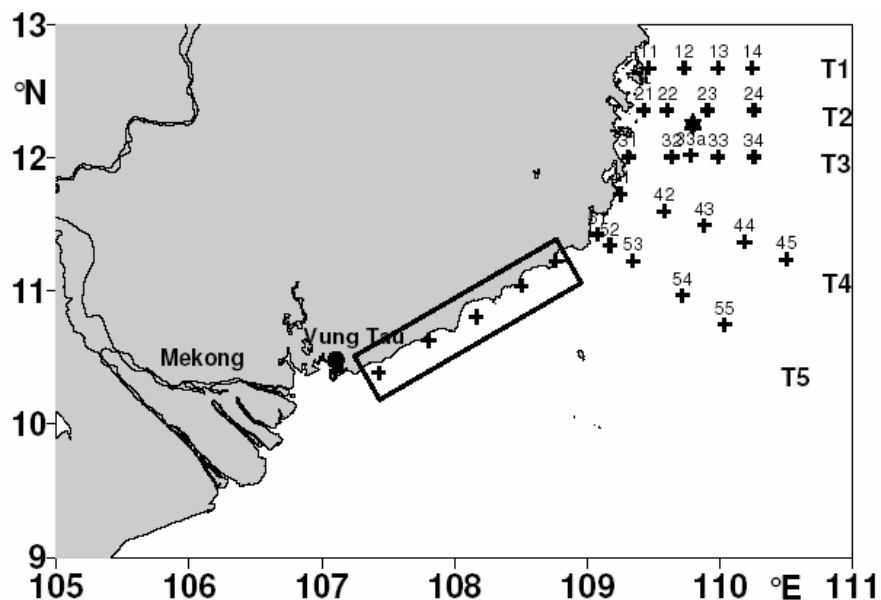
Fig. 2.2: Station map of the Vietnamese upwelling experiment. Crosses mark the CTD-stations, the rectangle marks the area of near coastal experiments, and the asterisk north of station 33a marks the area of the drifter experiment with a lagranian sediment trap. The numbers mark the transect T1-T5 referred to in the text.

At selected stations, water samples were taken for incubation experiments with respect to primary production, nitrogen fixation and new production. Vertical hauls of phytoplankton, zooplankton and Ichthyoplankton has been taken with different mesh sizes. During daylight, secchi depths were observed. At all stations vertical profiles were measured down to a water depth of 130 m using an ADCP (NOBSKA, MAVS 2) with a sampling frequency of 1.42 Hz. Meterological observations on board were recorded automatically every 10 min with an Aanderaa system. These observations were used by J.W. Dippner to compute a heat flux budget (attachment 1).

2.3.   Nitrogen Fixation off Vietnam

Three Vietnamese-German (VG) cruises on board of RV *Nghien Cuu Bien* were carried out in the SCS (Figure 2.1): VG3 from July 18 to 28, 2003, VG4 from April 21 to May 2004, and VG7 from July 8 to 26, 2004. In 2003 we encountered a post-ENSO year with weaker upwelling than normal, but in 2004 we had typical upwelling compared to the climatological mean (Dippner et al. subm.). Altogether 101 stations were sampled with a Seabird CTD ro-

sette system, 28 stations were sampled for nutrient analysis and nitrogen fixation assays. Standard depth, representing 100 % (0m), 75 % (5 m), 50 % (10 m), 23 % (20 m), 13 % (30-40 m) and 6 % (40-80 m) of the surface irradiance, were sampled each morning before sunrise; but not all light depths were sampled each morning. Nutrients (NO_3^-, NO_2^-, PO_4^{3-}) were analysed after Grasshoff et al. (1983). Nitrogen fixation was measured in duplicates after the method described by Montoya et al. (1996) in 2.3 L polycarbonate bottles sealed with Teflon coated butyl-rubber septa. We added 460 µl of a 0.1 molar ^{13}C labelled bicarbonate solution (99 % $H^{13}CO_3^{2-}$) and 2.5 ml of $^{15}N_2$ enriched gas (98 % Campro Scientific) to each sample, which was incubated for six hours under simulated in-situ conditions on deck using neutral density screening and running surface sea water for cooling. The incubations were ended by gentle filtration through precombusted Whatman GF/F filters. Filters were immediately dried for 48 hrs at 60° C in a drying oven and stored at room temperature. In the lab the filters were fumed for 2 hrs with HCL and dried again. Isotopic measurements of the filters were done with a delta S (Thermo) isotope ratio mass spectrometer connected to an elemental analyser CE1108 via an open split interface. Calibration for tracer measurements was done with enriched IAEA standards, 310 for nitrogen (50 ‰ and 200 ‰) and 309 for carbon (100 ‰ and 550 ‰). Calibration for C and N was done with acetanilide at the start of each sample run that comprised app. 20 filter measurements. After each fifth sample an internal standard, a protein solution (Peptone, Merck Chemicals), was measured. The precision is < ±0.2 ‰ for both elements. The integration of concentrations and rate measurements (Table 3.2.1) was done assuming 12 hrs of N_2-fixation activity and integrated from surface to 40 m depth after the trapezoidal rule. Mixed layer depths were estimated from the maximum in the buoyancy frequency of the water column.

2.4.   Pelagic Nitrogen Dynamics

The Vietnamese upwelling area was sampled during three cruises on board of RV *Nghien Cuu Bien* during southwest monsoon 2003 (18th to 28th of July), spring intermonsoon 2004 (21st of April to 2nd of May), and southwest monsoon 2004 (8th to 26th of July, Fig. 2.1). Altogether 46 stations were sampled with a seabird CTD system with attached 10 l water bottles. 45 stations were analysed for nutrients, 43 for particulate organic matter (POM), and 33 for $\delta^{15}N$-nitrate from 5-6 depth during the three sampling periods. Additionally 41 stations were sampled for net-plankton, separated into six size fractions.

Samples for POM and nutrients were taken from standard depths covering surface waters (0 or 5 m), 20 m, 40 m, 50 m, 70 m, 100 m, and 150 m depth. Additionally samples were taken from the chlorophyll maximum and from maximum 800 m depth at few stations. Nitrate

was analysed after Grasshoff et al. (1983) with a precision of $\pm$ 0.1 µmol L^{-1}. GF/F-filtered seawater for isotopic analysis of nitrate was collected when nitrate concentration exceeded 1.5 µmol L^{-1}. Samples were transferred to polyethylene bottles and preserved with concentrated HCl to a final pH of 1 to 2. Nitrate was collected for isotopic analysis by reduction to ammonia, which was then extracted from solution by diffusion and trapping on an acified GF/F-filter (Sigman et al. 1997).

POM was collected by vacuum filtration (< 400 mm Hg vacuum) of 1 to 5 litres of seawater through precombusted (450 °C for 2 h) 25 mm GF/F-filters. Visible organisms on the filters were removed. Filters were dried at 60 °C and stored dry for analysis in the laboratory onshore.

Net-plankton was collected with a 45 µm and a 200 µm mesh size JUDAY-net (opening diameter 0.37 m) through the upper 100 m or the entire water column in the case of shallow stations. Plankton from the 45 µm net was separated into two size fractions by passing it through 166 µm and 55 µm Nitex sieves. Plankton caught with the 200 µm net was separated into four size fractions by passing it through 2500 µm, 1500 µm, 1000 µm, and 330 µm Nitex sieves. Prior to drying at 60 °C and storage in aluminium foil, all plankton size fractions were qualitatively inspected under a stereo microscope (50 x magnification). At some stations not enough material for isotopic analysis in all plankton size fractions could be sampled.

In the following the terms net-plankton size fractions will be used for plankton from the net-hauls, whereas POM will be used for plankton filtered on GF/ F filters.

For isotope analysis, dry acified POM and nitrate filters were transferred to a tin capsule; net-plankton size fractions were ground to fine powder and weighed in tin capsules. All natural abundance measurements were made by continuous-flow isotope mass spectrometer (Finnigan Delta S or Delta Plus) via a Conflow II open split interface. Calibration for the total carbon and nitrogen determination was done daily with an acetanilide standard. All isotope abundances are expresses in δ notation as follows: δX (‰) = [(R$_{sample}$/R$_{standard}$) - 1)] * 10^3, where X is ^{13}C or ^{15}N, and R is the ^{13}C:^{12}C or ^{15}N:^{14}N ratio. IAEA-N3 (KNO$_3$) and IAEA-CH-6 (sucrose sugar) were used as the standards for carbon and nitrogen, respectively. A laboratory internal standard (Peptone, Merck) was run for every 6th sample for net-plankton and every 4th sample for POM filters. The peptone standard indicated an analytical error associated with the isotope measurements of less than 0.2 ‰ for both isotopes. Two replicates were analysed from each sample of net-plankton.

For the comparability of POM and net-plankton values, the vertical integrated concentration weighed δ^{15}N-PON was calculated for the upper 100 m or the entire water column in the case of shallow stations according to Equation 2.1 after Montoya et al. (1992).

$$\overline{\delta^{15}\text{PON}}_{0\text{-max.}100\,\text{m}} = \frac{\sum \Delta Z_i \delta^{15}PON_i [PON]_i}{\sum \Delta Z_i [PON]_i}, \tag{2.1}$$

where Δ Z is the thickness of the individual layers between sampled depths, i denotes the depth layers between the surface and 100 m depth or the entire water column in the case of a shallow station, [PON] is the concentration in µM and δ^{15}N-PON is the isotope ratio in ‰. The same was done for the δ^{13}C-POC.

Vertically integrated concentration weighted δ^{15}N from nitrate$_{sub}$ was also calculated according to Equation 2.1 for the depths range between the mixed layer and maximum 150 m. This depth interval includes the starting horizon of the upwelling velocity at approximately 125 m depth (Vo 1997). The mixed layer depths were estimated from the maximum in the buoyancy frequency of the water column.

2.5.   Nitrogen Limitation in Zooplankton

During southwest monsoon 2003 and 2004, observations on a fixed station grid with RV *Nghien Cuu Bien* took place in the Vietnamese upwelling area at 11° to 12.7 ° N and 109° to 110.5° E from July 10th to 16th 2003 and from 8th to 26th of July 2004 (Fig. 2.1). Net-plankton was collected in vertical tows with JUDAY-nets (45 µm and 200 µm mesh, respectively, diameter 0.37 m) through the upper 100 m of the water column. Plankton was separated into size fractions by passing it through 166 µm and 55 µm 2500 µm, 1500 µm, 1000 µm, 330 µm by passing them through graded series of Nitex sieves. Samples were rinsed plenteously during the separation process to break up and remove any Trichodesmium colonies caught in the sieves. Prior to drying at 60 °C and storage in aluminium foil, all size fractions were qualitatively inspected under a microscope.

2.5.1   Plankton sample selection for GC-C-IRMS analysis

Four sets of size fractioned plankton samples were chosen for stable nitrogen amino acid analysis based on the position of the sampling stations within or outside the upwelling area (Fig. 2.3). Stations within the upwelling area included stations 11 and 12 (2003) and station 21 (2004). We pooled the plankton size fractions from stations 11 and 12 to get enough material for the amino acid analysis (Fig. 2.4). Pooling criteria were a similar hydrography at the stations, as will be shown later on, and similar bulk δ^{15}N values (Fig. 2.4).
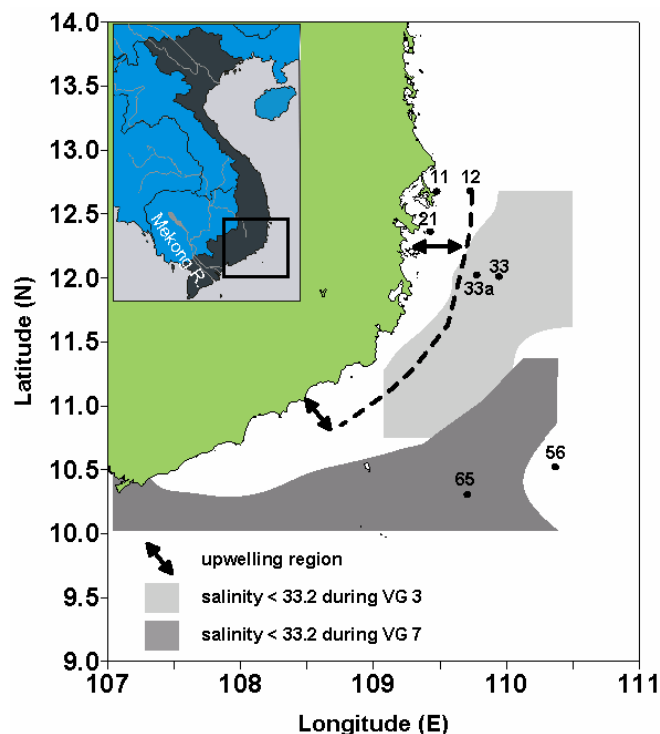
Fig. 2.3: Positions of the stations chosen for amino acid analysis in- and outside the upwelling area as indicated by the dotted line after Dippner et al. (subm.). Stations 11, 12, 33a, and 33 were sampled during SWM 2003, stations 21, 56, and 65 during SWM 2004. Also included are the sea surface salinities < 33.2 indicative for the influence of modified Mekong waters (Voss et al. 2006).

Stations outside the upwelling area included stations 33a and 33 (2003) and stations 56 and 65 (2004). We pooled the plankton size fractions from stations 33a and 33 and added size fraction 166 – 330 from station 56 to better cover the size spectrum, of which especially size fraction 55-166 µm was poorly covered due to lack of plankton material as shown in Fig. 2.4. All δ^{15}N-bulk measurements were made by continuous-flow isotope mass spectrometer (Finnigan Delta Plus) via a Conflow II open split interface. Calibration for the total carbon and nitrogen determination was done daily with an acetanilide standard. IAEA-N3 (KNO_3) was used as the standard for nitrogen. A laboratory internal standard (Peptone, Merck) was run for every 6th sample. The peptone standard indicated an analytical error associated with the isotope measurements of less than 0.2 ‰ for nitrogen stable isotopes. Two replicates were analysed from each sample. A detailed description of bulk plankton δ^{15}N analysis has been given in the previous chapter 2.4. Here we will describe only the additional steps for GC-C-IRMS analysis.

2.5.2   Sample preparation and GC-C-IRMS analysis

Analysis of stable nitrogen isotopes in individual amino acids was done for twenty samples as shown in Fig. 2.4. Samples were prepared for Gas Chromatography-Combustion-Isotope Ratio Mass Spectrometry (GC-C-IRMS) analysis of amino acids by acid hydrolysis followed by derivatization to triflur-acetylated-amino acid esters (TFA) (Hofmann et al. 2003). In brief, between 10 to 50 mg of dried sample was placed in a 16 x 150 mm glass tube with a

28

polytetrafluoroethylene (PTFE)-lined cap and hydrolyzed with ultra pure 6 µM hydrochloric acid at 110 °C for 24 hours.
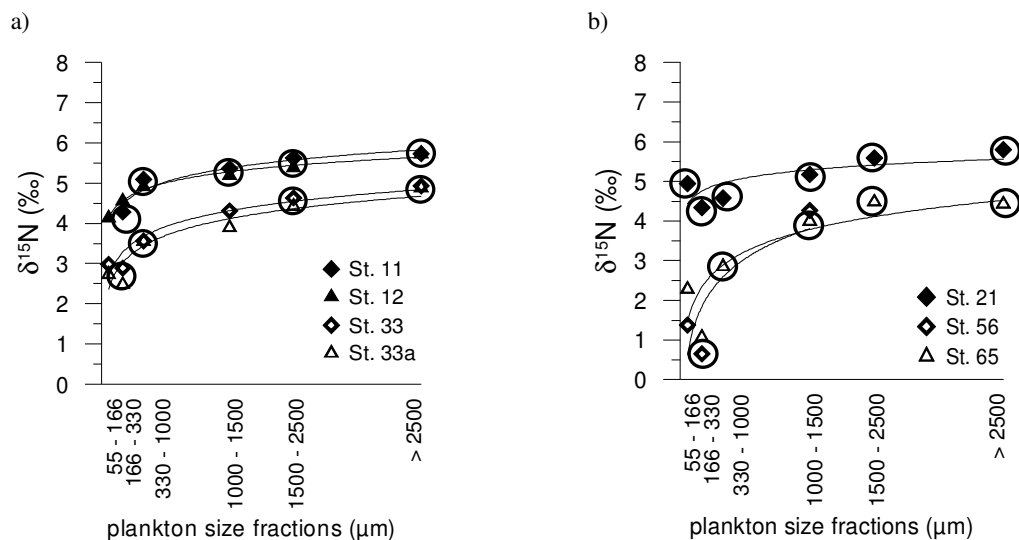
Fig. 2.4: $\delta^{15}N$ bulk values from July 2003 (a) and 2004 (b) from stations inside (black symbols) and outside (open symbols) the upwelling area. Encycled are the samples used or pooled for analysis of $\delta^{15}N$ in individual amino acids.

The hydrolysate was filtered through 0.2 µm sterile glasfiber filters and evaporated to dryness with a rotary evaporator. Iso-propanol and acetylchloride (4:1) were added to the dried samples and esterification reaction took place at 110 °C for one hour. After evaporation to dryness under a gentle stream of N_2-gas, 500 µl dichlormethane (DCM, ultrasterile, $H_2O < 0.001$ %) and 500 µl trifluor-aceticacid-anhydrid were added (exotherm reaction). Acetylation reaction took place over night at room temperature (20 °C). The remaining liquid was dried under a stream of N_2-gas. Derivatised amino acids were solved in 500 µl of DCM and stored at 4 °C before GC-C-IRMS analysis within the next seven days.

This preparation scheme allows the analysis of thirteen common amino acids plus Trans-4-(aminomethyl)-cyclohexanecarboxylic acid (internal standard). In the acidic milieu the $\delta^{15}N$ values of asparagine and glutamine are only measured in mixture from the acids and the accompanying amides and could not be separated. To simplify matters we will uniformly term them aspartic acid (asp) and glutamic acid (glu) in the following. Separation problems with the esterification/TFA derivatization method may occur for phenylalanine, lysine, and tyrosine. Here, peaks clearly were separated for tyrosine but not for phenylalanine and lysine. The advantage of this derivatization method compared e.g. to the esterification/acetylation method is that a relatively simple, rapid reaction set-up is possible for a two-step reaction without additional cleaning of the derivates (Hofmann et al. 2003).

The stable isotopic composition of nitrogen in TFA-derivates of amino acids were analyzed by GC-C-IRMS (GC: HP 58590 series II, Hewlett Packard, USA;-C: Combustion Interface, -IRMS: MAT252). Mixes of amino acid derivatives from samples were injected into the GC, separated on a BPX5 (SGE) capillary column (50 m x 0.32 mm inner diameter, 0.5 µm film thickness; SGE, Australia), combusted, reduced, and finally passed through the cold trap to remove water and CO_2 before introduction to the mass spectrometer. Nitrogen isotope ratios for each amino acid in a mix were measured sequentially. Injections were done 2 to 5 times per sample splitless or in dilution of 15:1, 10:1, 5:1, 3:1 or 2:1 at 250 °C and contained 1 to 5 µL of sample to optimize peak separation and shape. The GC temperature program for each run was as follows: Initially 50°C, held for 1 min; increased at steps of 10 °C min^{-1} to 80 °C, the temperature was held for 5 min; increased from 80 to 210 °C at 3 °C min^{-1}, held for 5 min; increased from 210 to 280 °C at 15 °C min^{-1}, held at 280 °C for 5 min.

Standard mixtures of amino acids were run after every 10th sample through the entire analytical procedure to confirm the reproducibility of isotope measurements. Analytical error associated with isotope measurements of mixtures of purified amino acids through our derivatization were < 1 ‰ for external standards. As check on our sample processing, we added an internal standard (Trans-4-(aminomethyl)-cyclohexanecarboxylic acid) to each sample before the hydrolysis step. Analytical error associated with our derivatization and analytical protocols were < 0.3 ‰ for these internal standards. All natural samples were injected and analysed two to five times depending on the quantity of the sample. Satisfactory analysis of natural samples were accomplished for seven amino acids including alanine, glycine, leucine, proline, aspartic acid, glutamic acid, and tyrosine with standard deviations < 1.5 ‰.

3.   Results and Discussion

3.1   Monsoon Induced Upwelling off the Vietnamese Coast

The results from this thesis are part of the interdisciplinary manuscript "Monsoon Induced Upwelling off the Vietnamese Coast" by J. W. Dippner, K. V. Nguyen, H. Hein, T. Ohde and N. Loick. This manuscript has been submitted to Ocean Dynamics. My own share in this manuscript constitutes 40 % which includes the physico-chemical analysis of the different water masses, discussion of the results and participation in the writing of the manuscript.

3.1.1   Introduction

The South China Sea (SCS) is the largest marginal sea in the tropics with a maximum depth reaching more than 5000 m (Fig. 1.1). It covers an area from the equator to 23 °N and from 99 °E to 121 °E. The deep central basin is bordered by two broad shelf regions with water depth less than 100 m. The northern shelf, including the area south of China and the Gulf of Tonkin, extends from Taiwan south westward to 15 °N. The southern shelf consists of the Gulf of Thailand and the Sunda Shelf between the Malay Peninsula and Kalimantan. In the south, the Sunda Shelf is connected to the Java Sea and the Indian Ocean through the Strait of Malacca. In the east, the Philippines and Palawan Islands separate SCS from the Pacific Ocean. Here the continental slope is steepest with practically no continental shelf. Four openings at the eastern boundary exist: in the north, the Taiwan Strait and the Luzon Strait (elsewhere called Bashi Strait, Hu et al. 2000) connect SCS with the East China Sea and the Pacific Ocean. Two narrow and shallow passages to the north and to the south of the Palawan Islands connect SCS with the Sulu Sea and the Pacific Ocean in the south east. The water mass exchange between the SCS and the Sulu Sea through these two passages as well as the exchange between SCS and the Java Sea through the Strait of Malacca are relatively unimportant. The main exchange with the East China Sea and the Pacific Ocean is through the Strait of Taiwan and the Strait of Luzon where a strong inflow of the Kuroshio occurs during NE monsoon.

Climatic variations in the atmosphere and in the upper ocean of the SCS are primarily controlled by the East-Asian monsoon, which follows closely the climatic variations in the equatorial central Pacific. The southwest (summer) monsoon lasts from June to September. The stronger northeast (winter) monsoon appears from November to March and is known to vary with the Southern Oscillation Index (Liu et al. 2002). The annual cycle of wind stress fields (Hellerman and Rosenstein 1983) shows that northeasterly winds prevail over the whole region with an averaged magnitude of 9 m s^{-1} in winter. In contrast, during summer weaker

southeasterly winds of about 6 m s^{-1} dominate over most parts of the SCS. The seasonal circulation in the SCS and its adjacent seas were investigated by many authors (e.g. Dale 1956, Wyrtki 1961, Pohlmann 1987, Shaw and Chao 1994, Metzger and Hurlburt 1996, Wu et al. 1998, Hwang and Chen 2000, Morimoto et al. 2000, Qu 2000, Isobe and Namba 2001, Fang et al. 2002, Yang et al. 2002). Most of them are summarized in a review (Hu et al. 2000). During winter monsoon, the circulation in the SCS is forced by the north easterly wind stress itself, whereas in summer during the southwest monsoon, the circulation is driven by the curl of the wind stress (Chao et al. 1996). In general, the seasonal circulation pattern can be separated into a northern and a southern circulation in the SCS. The circulation in the southern SCS is driven by the monsoon only, forming a cyclonic gyre during winter monsoon and an anticyclonic gyre during summer monsoon. In the northern part of the SCS the circulation is forced by the monsoon and the inflow through the Strait of Taiwan and the Strait of Luzon (Hu et al. 2000). During winter a cyclonic gyre is formed which merges with the southern cyclonic gyre to a basin wide cyclonic circulation pattern. In summer also a cyclonic gyre exists which interacts with the anticyclonic gyre in the south, forms a dipole circulation cell and is, therefore, associated with an eastward offshore current off the coast of Vietnam at ca. 12 °N (Wu et al. 1998). Yang and Liu (1998) concluded that solar radiation, the monsoon wind and the SCS topography, consisting of steep gradients and a lot of seamounts, could be considered as the main influencing factors for the SCS circulation.

Between the shelf in the Gulf of Tonkin and the Sunda Shelf the continental shelf is extremely small at the Vietnamese coast between 11 °N and 16 °N. This area is the centre of monsoon induced Vietnamese upwelling during summer monsoon. The upwelling is manifested by a drop of more than 1 °C in the long-term mean of sea surface temperature (Levitus 1984). This upwelling area is the subject of our interest. Upwelling on eastern boundaries of the ocean is a research subject since the 1960s (Smith 1968, Hagen 2001). The California Current, the Humboldt Current off Peru, the northwest African upwelling or the Benguela Current were subject of many interdisciplinary investigations (Mittelstaedt 1976, 1991, Margalef 1978, Brink 1983, Wefer and Fischer 1993, John et al. 2000, 2004, Mohrholz et al. 2001). The general theoretical background has been provided by Yoshida and Mao (1957) and by Yoshida (1967) which can be summarized in terms of the vorticity equation as: a negative wind stress curl at the sea surface (in the upper layer) is connected with upwelling via Ekman suction and the released upward (vertical) movement is related to net poleward transport in the lower layer by the β-effect. Although this mechanism is independent from the existence of a coast, it considers the balance of local forcing and is, therefore, only partially

applicable to the Vietnamese upwelling. Such a situation has been observed e.g. in the Mozambique Channel (Schemainda and Hagen 1983).

The interannual variability of the monsoon is strongly controlled by the ENSO (Zhang 2000). Investigations of large scale structures by Zhang (2000) show a teleconnection between the western tropical Pacific and the East Asian region which has significant impact on the East Asian summer climate. Chao et al. (1996) describe the influences of the 1982-1983 El Niño on the dynamics of SCS. The authors compare the mean climatology from the Comprehensive Ocean Atmosphere Data Set (COADS) for the period 1980-1992 with the ENSO period 1982-1983. The El Niño event in SCS began with increased evaporative cooling in late 1982, followed by a weak northeast monsoon in the winter 1982-1983 and a weak southwest monsoon in the following summer. The surface water showed persistently higher than normal heat content from late 1982 to late 1983. The increase in heat content could not be explained by a decrease in latent heat fluxes. Instead, the surface circulation, which was weaker than normal, played a major role in the increased surface temperature. The strength of upwelling and downwelling were reduced, resulting in weaker vertical advection of heat and warming of surface waters (Chao et al. 1996).

In monsoon driven areas such as the Indian Ocean mainly the Somalia Current and the western Arabian Sea has been subject of interest (Schott and McCreary 2001). Detailed studies of the Vietnamese upwelling do not exist and unlike the Arabian Sea the SCS has received relatively little attention in the biogeochemical research (Liu et al. 2002).

In this chapter physical, nutrient and phytoplankton observations are presented and upwelling will be analysed with respect to local forcing, regional forcing and far field forcing; nutrient distributions will be discussed with respect to different water masses.

3.1.2 Results

The results of this chapter are based on the material and methods described in detail in chapter 2.2.

Meteorology and Heat Fluxes

Figure 3.1.1 shows the meteorological conditions during the cruise measured on board. The sea level air pressure shows a pronounced semidiurnal atmospheric tide (Lindzen 1979). The air temperature had a range from 25 to 31 °C with daily amplitude of ca. 4 °C. During the grid stations the wind speed observed on the ship was 4 m/s from southwest which was also influenced by local gust effects. The relative humidity varied strongly with a mean value of 43 %. During the whole measuring campaign (grid stations) no precipitation occurred.
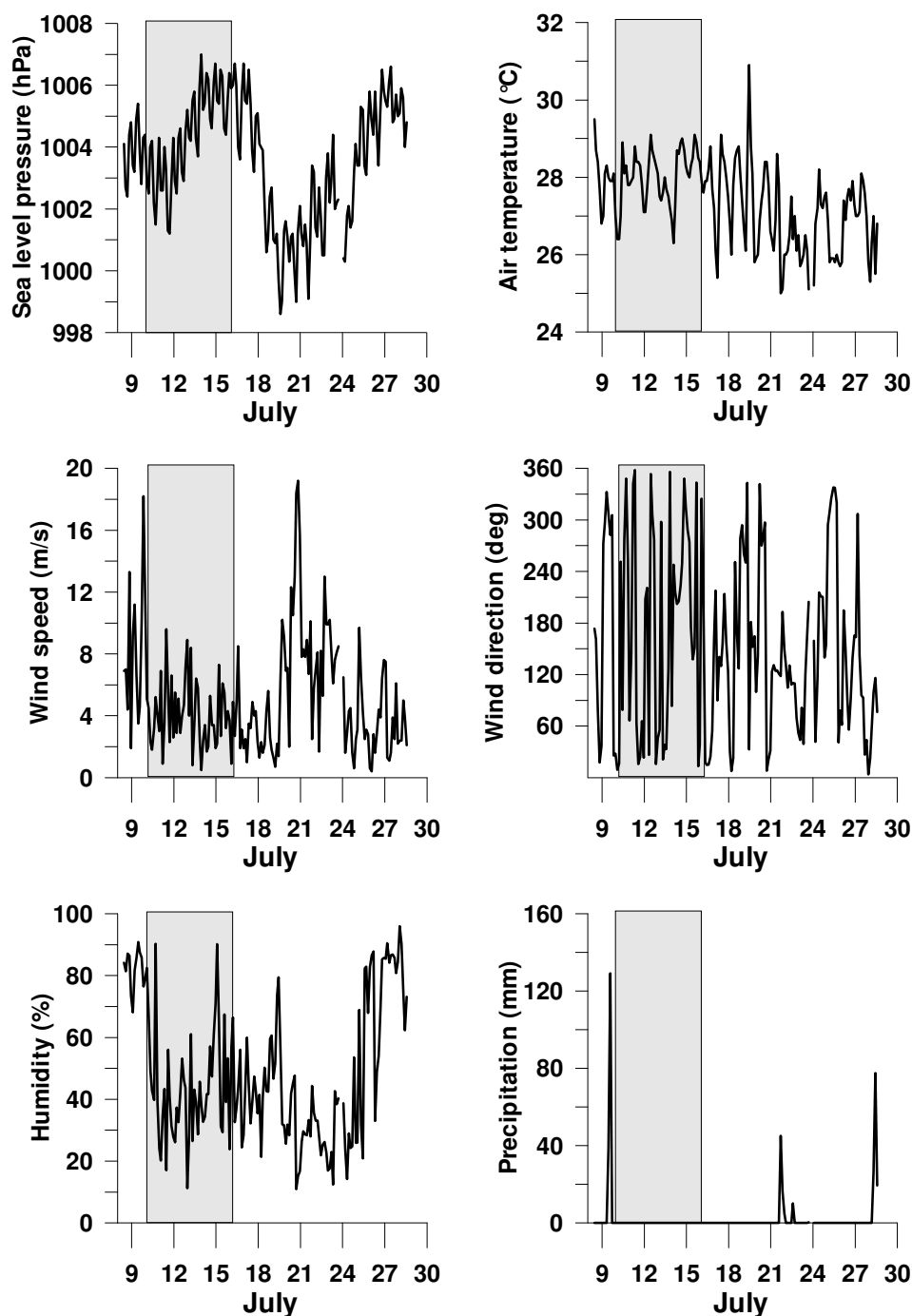
Fig. 3.1.1: Meteorological observations measured with an Aanderaa system on board of RV *Nghien Cuu Bien*. The grey area marks the period of investigation during the cruise.

Figure 3.1.2 shows the observed incoming short wave solar radiation, the computed sensible and latent heat flux and the corresponding long wave radiation. These atmospheric observations are compared with the climatic means of the Comprehensive Ocean Atmosphere Data Set (COADS) for the period 1950-1992 (Slutz et al. 1985, Woodruff et al. 1987). The computed heat fluxes from the observations are also compared with the computed heat fluxes from COADS (Oberhuber 1988, Table 3.1.1).
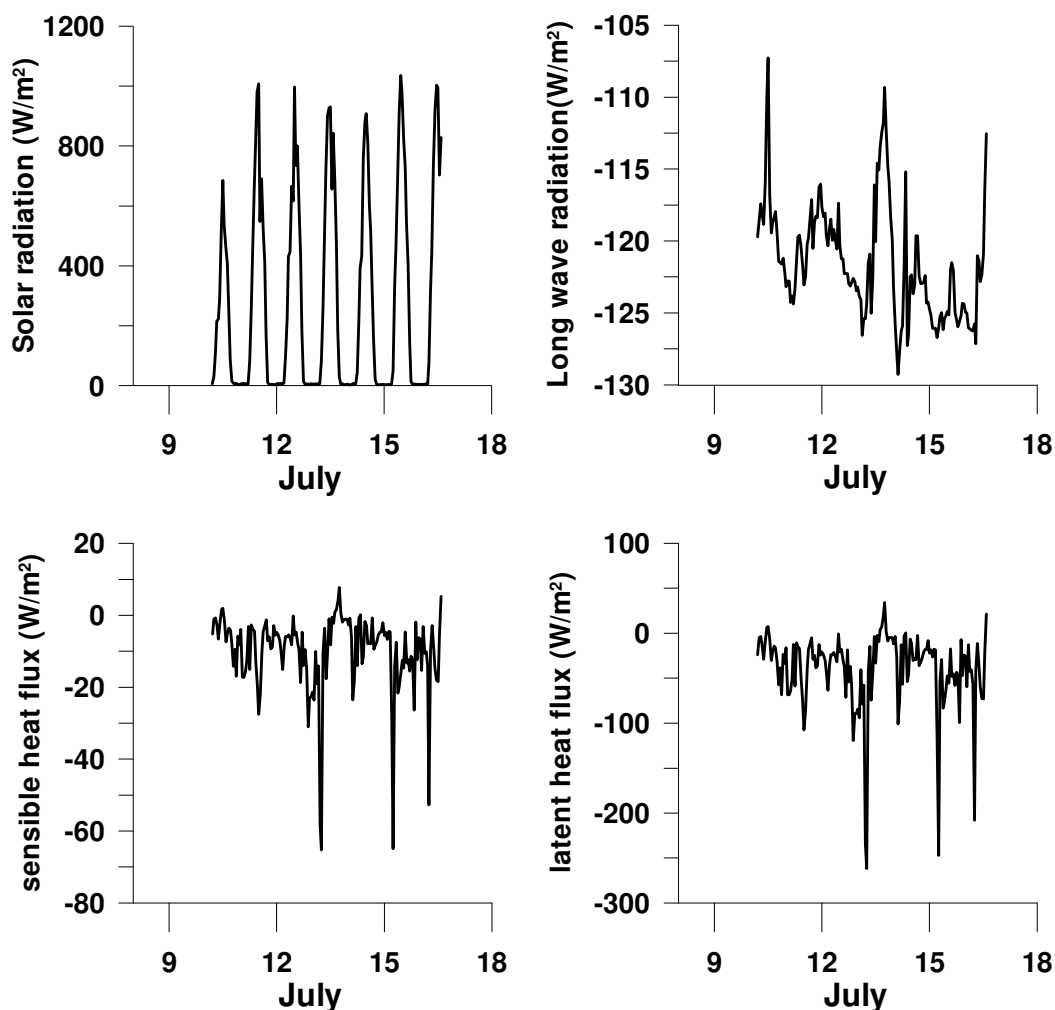
Fig. 3.1.2: Observed short wave solar radiation and computed heat fluxes after Oberhuber (1988) for the period of observations.

Table 3.1.1: Comparison of climatologic mean atmospheric values from COADS (Slutz et al. 1985, Woodruff et al. 1987) for the period 1950-1992 and the computed values from the atlas of global heat flux balance (Oberhuber 1988) with the observations in July 2003.

	COADS	July 2003
sea level pressure (hPa)	1004	1004.5 ± 1.6
atmospheric temperature (°C)	28	28.05 ± 0.7
sea surface temperature (°C)	28	29.2 ± 0.8
wind speed (m s^{-1})	6	4.0 ± 2.1
humidity (%)	83	43 ± 21.7
sensible heat flux (W m^{-2})	-10	-9.98 ± 10.9
latent heat flux (W m^{-2})	-125	-39.4 ± 42.9
long wave back radiation (W m^{-2})	-45	-121.5 ± 3.9

July 2003 had a higher than normal sea surface temperature, a lower wind speed and less humidity compared to the climatologic mean July. The sensible heat flux is in the same order as the computation of Oberhuber (1988), however, the latent heat flux is in the order of

ca. -40 W m^{-2} which is less than the climatologic mean of -125 W m^{-2} due to the reduced wind speed. In contrast, the long wave back radiation with ca. -120 W m^{-2} is much larger than the climatologically value of -45 W m^{-2} due to the larger difference between the SST and the atmospheric temperature (Table 3.1.1).

HorizontalDistributions

Figures 3.1.3-3.1.5 show the horizontal distribution of salinity, temperature, and nitrate at selected depth. The salinity distribution (Fig. 3.1.3) shows isolines parallel to the coastline with a pronounced minimum in the upper 20 m indicating the water masses from the River Mekong and the Gulf of Thailand.
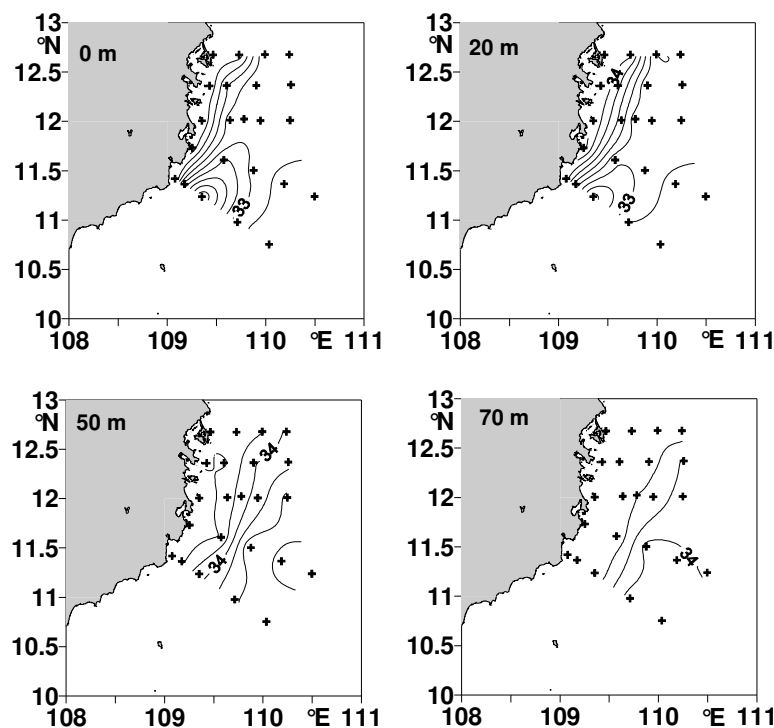
Fig. 3.1.3: Horizontal salinity distribution in different depth. Contour interval (CI) = 0.2.

The temperature distribution (Fig. 3.1.4) shows a very warm surface layer with a temperature between 28 °C and 30 °C. Near coastal upwelling could not be detected in the upper layer. Below 20 m water depth, intermediate upwelling occurred close to the coast with a local maximum between 11.5 °N and 12 °N. The nitrate distribution (Fig. 3.1.5) shows a nutrient depleted surface layer and local maxima below 50 m water depth within the upwelling water between 11.5 °N and 12 °N. According to Hansell et al. (2004), excess nitrate (DIN$_{xs}$) is computed from the data where DIN$_{xs}$ = N – 16 P, N is the concentration of nitrate plus nitrite and P the concentration of soluble reactive phosphate. DIN$_{xs}$ is the excess in nitrate concentration relative to that expected from Redfield et al. (1963) stoichiometry.
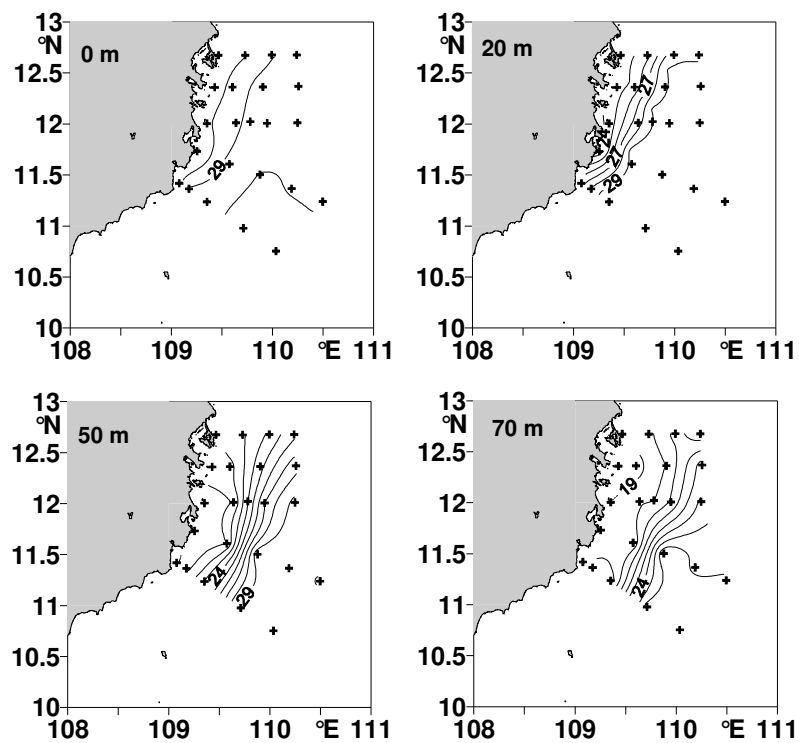
Fig. 3.1.4: Horizontal temperature distribution in different depth. CI = 1°C.
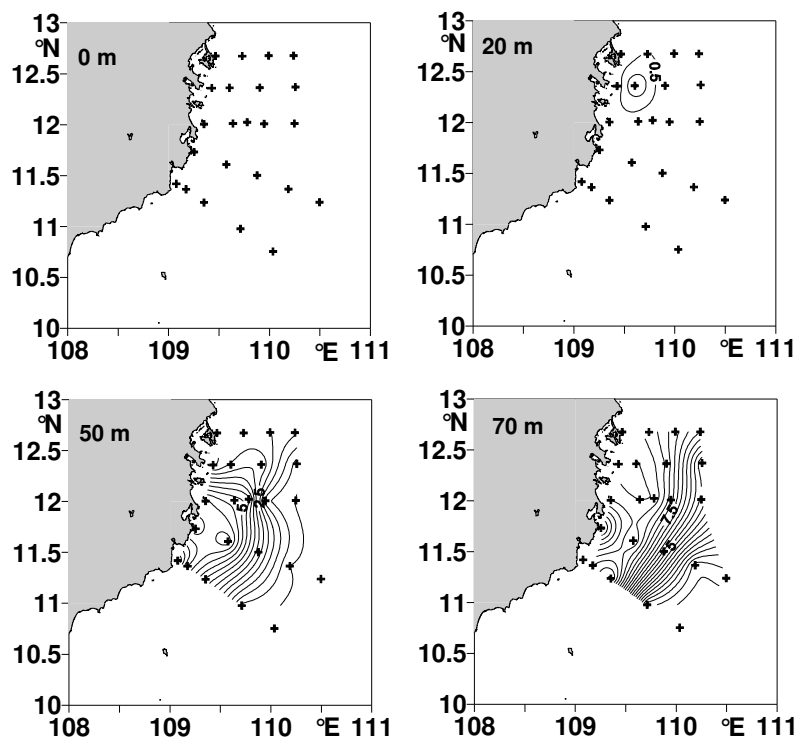
Fig. 3.1.5: Horizontal nitrate distribution in different depth. CI = 0.5 μmol L^{-1}.

The excess nitrate DIN$_{xs}$ (not shown) has negative values in the upper 50 m indicating nitrogen limitation of the system and in deeper parts below 50m water depth some patches with positive DIN$_{xs}$ values indicating phosphate limitation. Negative DIN$_{xs}$ values in the

upper layer may favour blooms of diazotrophic cyanobacteria (Montoya, pers. comm.). However, no strong bloom of *Trichodesmium* spp. or other diazotrophic species could be detected. *Trichodesmium* spp. was present in the phytoplankton nets, but, in low concentrations. Figure 3.1.6 shows the depth of the thermocline. The isolines are parallel to the coast with a pronounced onshore slope indicating upwelling. Using the density profiles, the buoyancy frequency $N^2 = -(g/\rho)\,(\partial\rho/\partial z)$ and the first baroclinic mode of the internal radius of deformation $R = NH/f$ can be computed. The scale height H is in this case the depth of the thermocline. The averaged radius of deformation is 42 km in the Vietnamese upwelling area. The thick line in Fig. 3.1.6 marks the distance of the radius of deformation from the coast. This line separates the near coastal upwelling area from the offshore area.
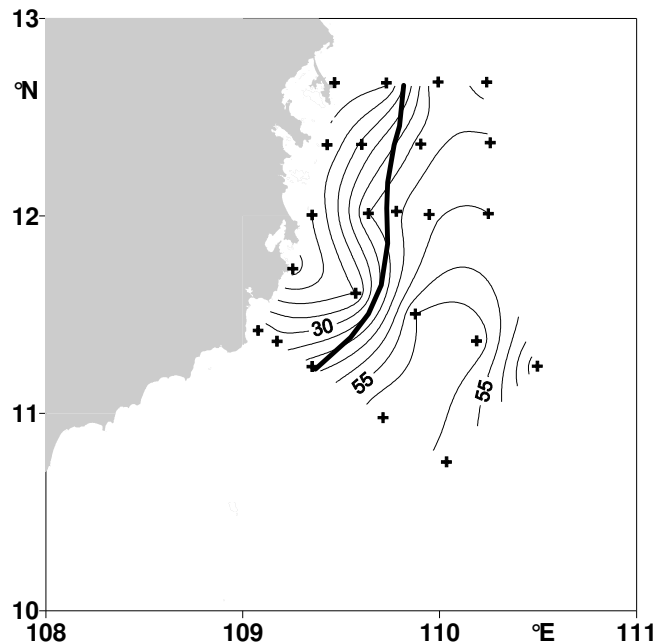
Fig. 3.1.6: Horizontal distribution of the depth of the thermocline. The thick line marks the distance of the radius of deformation from the coast. CI = 5 m.

Fig. 3.1.7 displays the chlorophyll *a* concentration integrated over the upper 40 m. The highest chlorophyll *a* concentrations up to 36 mg m^{-2} occur close to the coast in the upwelling area which is offshore limited by the radius of deformation. In the identified offshore area the chlorophyll *a* concentration is much lower. In the northern part on transect 1 the chlorophyll *a* maximum of 28 mg m^{-2} separates from the coast. This can be explained by an inspection of the velocity field.

The ADCP data were vertically integrated over the upper 130 m from the maximum salinity water to the surface and a stream function Ψ is constructed, which is defined as $\Psi = \int V\,dx$ where V is the northward transport component on transect 1 to 3 and the transport component normal to the coast at transect 4 and 5.
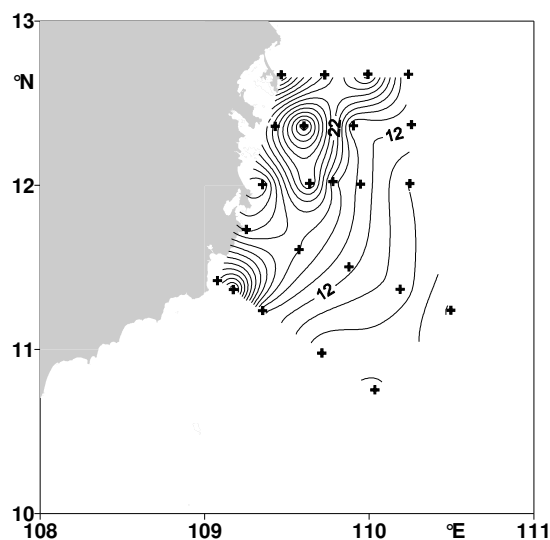
Fig. 3.1.7: Horizontal distribution of chlorophyll *a* integrated over the upper 40 m. CI = 2 mg m^{-2}.
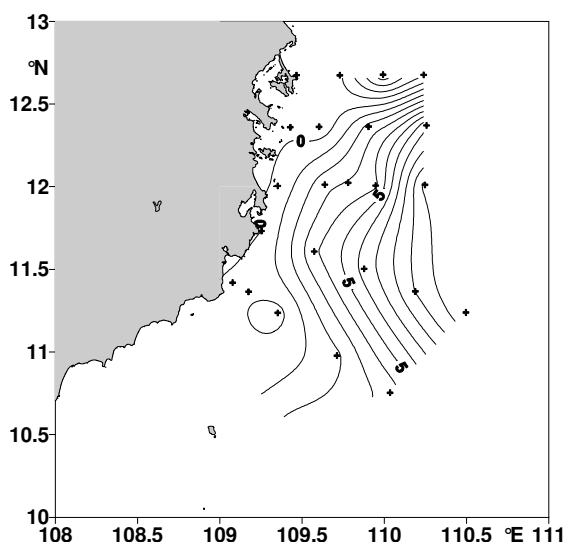
Fig. 3.1.8: Surface stream function, defined as $\Psi = \int V$ dx, for the upper 130 m. CI = 1 Sv (10^6 m^3 s^{-1})

Figure 3.1.8 shows the stream function which indicates a flow field parallel to the coast up to 12 °N. Here the flow field, influenced by the southward counter current, turns to the east between 12 °N and 12.5 °N and propagates eastwards into the central SCS and towards the Strait of Luzon. In the vicinity of the counter current also a local chlorophyll *a* maximum exists at Station 13. The chlorophyll *a* maxima in the northward current meets the chlorophyll *a* in the southward counter current and the offshore transport causes advection of deep chlorophyll into the central basin.

Vertical Distributions

Figure 3.1.9 shows the vertical distribution of the velocity at transects 1 to 3. At transect 1 except at station 14 the flow field points to the south with a core of strong velocity of 1.4 m s^{-1} between 70 – 100 m at station 13. This strong counter current was recently detected by Vo and Dang (2002). At transect 2 close to the coast a weak counter current exists at Station 21 and 22. At transect 3 the whole flow field points towards the north and a near coastal jet appears between 40 and 80 m water depth. Transects 4 and 5 (not shown) have a similar structure as transect 3 with northwards flow and the appearance of a near coastal jet. Figure 3.1.10 shows the vertical chlorophyll *a* distribution along the transects T1, T2 and T3. The transects 4 and 5 (not shown) are very similar to transect 3. The chlorophyll *a* distribution (Fig. 3.1.10) shows a patch distribution with peaks between 20 and 40 m water depths near the thermocline and in the vicinity of the strong under current.

a)

a)

b)

b)

c)

c)
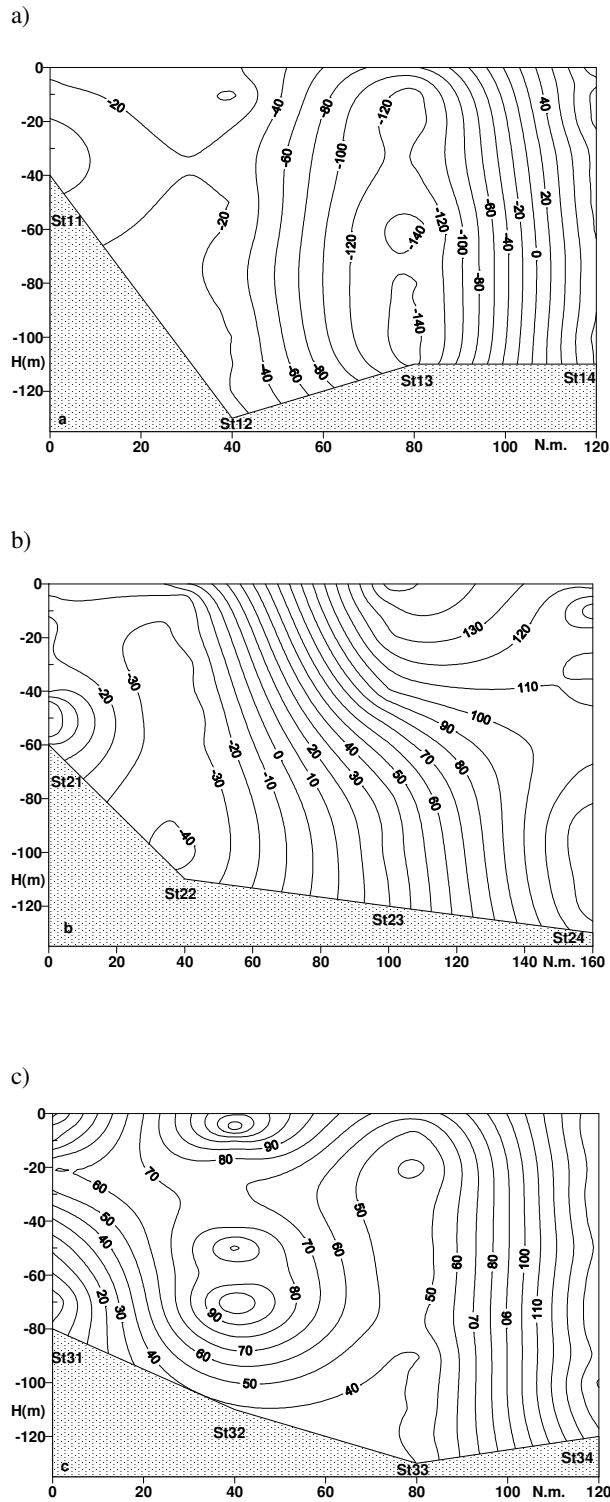
Fig. 3.1.9: Meridional component of the velocity field at the transects a) T1, b) T2, and c) T3. St xx mark the position of stations. Positive values indicate northward, negative values southward currents. CI = 20 cm s⁻¹.
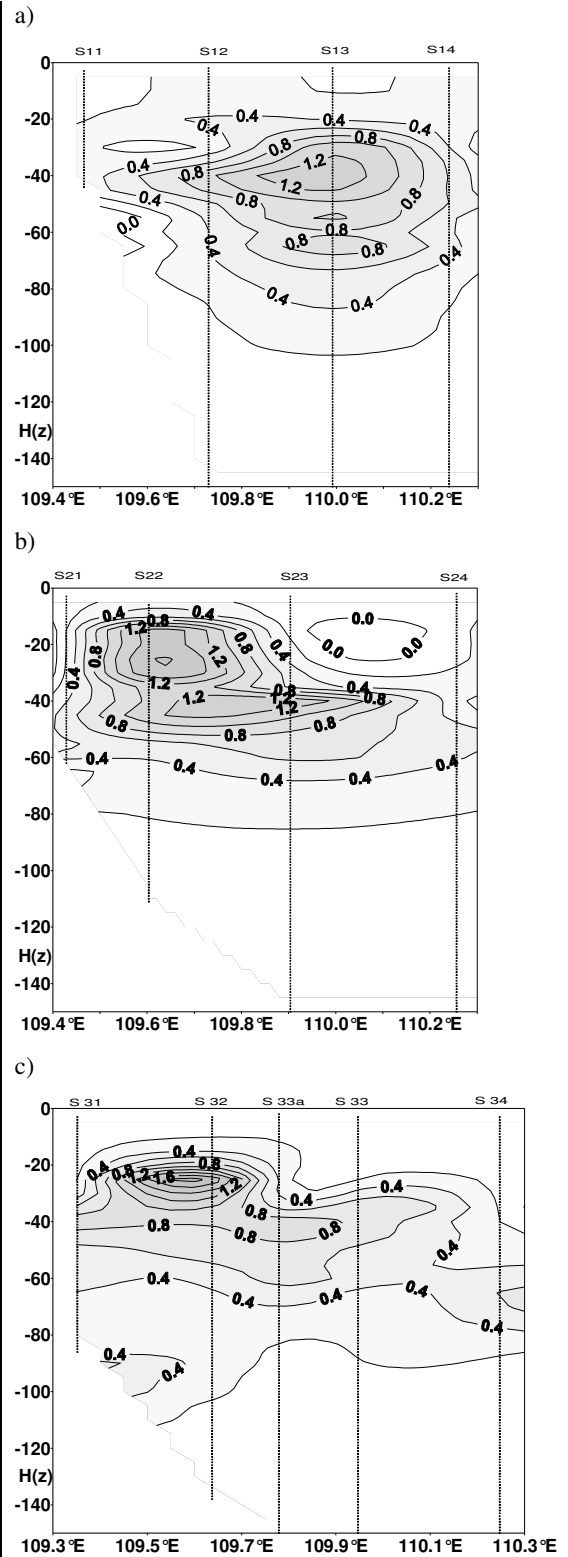
Fig. 3.1.10: Vertical distribution of chlorophyll *a* at the transect a) T1, b) T2, and T3. CI = 0.2 mg m⁻³.

Figure 3.1.11 shows the zonal component of the velocity at ca. 110 °E. At 12 °N the general circulation leaves the coast as flow with a maximum speed of 1.2 m s^{-1} eastwards into the central SCS and towards the Strait of Luzon.
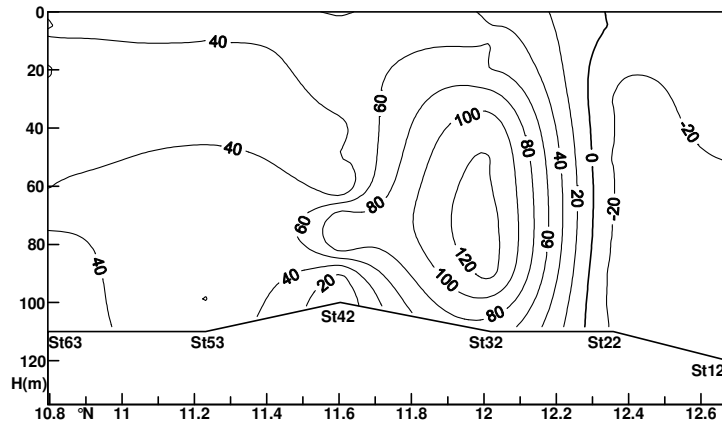
Fig. 3.1.11: Zonal component of the velocity field at ~ 110 °E. Stxx mark the position of the stations. Positive values indicate eastward currents, negative values westward currents. CI = 20 cm s^{-1}.

Water Masses

All CTD profiles are used for plotting an overall TS-diagram (Fig. 3.1.12) to identify specific water masses which serves as "end member" for mixing between water masses. Figure 3.1.12 shows four different water masses.
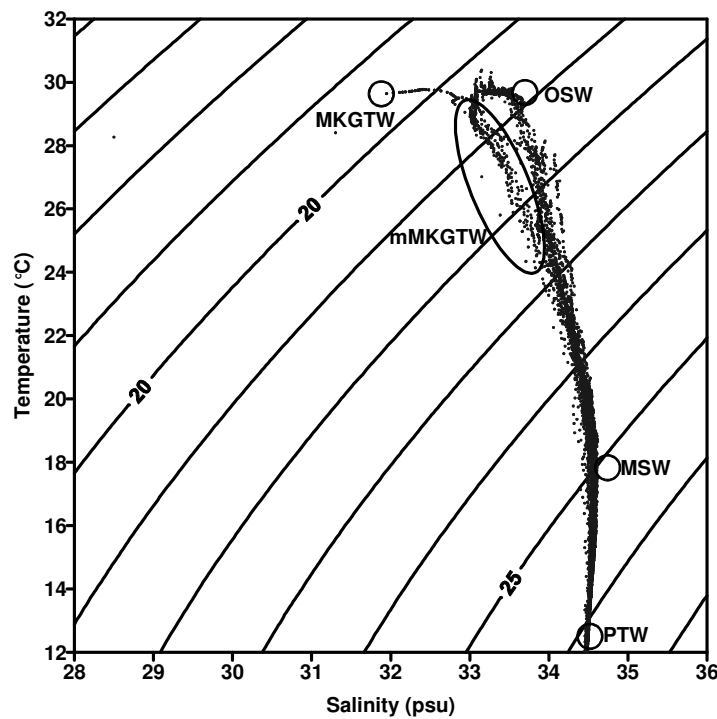
Fig. 3.1.12: Temperature vs salinity diagram of all CTD-measurements in the upper 350 m. Dots show the observation in a field of σ_t isolines. Circles mark the four "end members" of water masses PTW, MSW, OSW, and MKGTW which contribute to mixing processes. The ellipse marks the mMKGTW which is mixing water between MSW, OSW and MKGTW.

The water mass characteristics are summarized in Table 3.1.2. According to Rojana-anawat et al. (2001), three of these water masses can be identified as Open Sea Water (OSW),

41

Maximum Salinity Water (MSW) and Permanent Thermocline Water (PTW). The fourth water mass was Mekong and Gulf of Thailand Water (MKGTW), which has been described by Nguyen (1990) to enter the SCS with a salinity above 32 psu. The TS-diagram shows a bifurcation between the 20.5 and 23 σ_t isopycnal line. This bifurcation identifies two different mixing processes. The right branch of the scatter plot marks mixing water between OSW and MSW, the left branch represents the modified River Mekong and the Gulf of Thailand Water (mMKGTW) which is marked with an ellipse in Figure 3.1.12.

Table 3.1.2: Water mass characteristics of the five different water bodies: Permanent Thermocline Water (PTW), Maximum Salinity Water (MSW), Open Sea Water (OSW), Mekong and Gulf of Thailand Water (MKGTW) and the modified Mekong and Gulf of Thailand Water (mMKGTW). Subscripts in brackets are the numbers of measurements.

water mass	mMKGTW	MKGTW	OSW	MSW	PTW
depth (m)	0 – 40	0 – 20	0 – 70	50 – 175	150 – 285
temperature (°C)	$26 - 28.5_{(10)}$	$\geq 29.4_{(3)}$	$\geq 26_{(24)}$	$15 - 20_{(34)}$	$< 15_{(4)}$
salinity (psu)	$33.3 - 33.85_{(10)}$	$\leq 32.9_{(3)}$	$33.4 - 33.7_{(24)}$	$\geq 34.5_{(34)}$	$34.5 - 34.6_{(4)}$
oxygen (mg L^{-1})	$3.7 - 4.6_{(7)}$	$4.5 - 4.7_{(3)}$	$4.5 - 4.9_{(19)}$	$2.7 - 4.6_{(28)}$	$2.8 - 3.2_{(3)}$
NO$_3^-$ (µmol L^{-1})	$0.3 - 2.1_{(7)}$	$0 - 0.1_{(3)}$	$0 - 0.7_{(19)}$	$7 - 17_{(28)}$	$14 - 20_{(3)}$
PO$_4^{3-}$ (µmol L^{-1})	$0.1 - 0.3_{(7)}$	$0 - 0.1_{(3)}$	$0 - 0.2_{(18)}$	$0 - 1.3_{(28)}$	$0.6 - 1.4_{(3)}$
SiO$_2$ ((µmol L^{-1})	$2.0 - 6.0_{(7)}$	$0 - 4.1_{(3)}$	$0 - 5.9_{(19)}$	$0.4 - 24.7_{(28)}$	$9.8 - 22.6_{(3)}$
NO$_2^-$ (µmol L^{-1})	$0.0 - 0.4_{(7)}$	$0.0_{(3)}$	$0.0 - 0.1_{(19)}$	$0.0 - 0.4_{(28)}$	$0.0_{(3)}$
Chl. *a* (mg m^{-3})	$0.3 - 1.5_{(10)}$	$0.2 - 0.3_{(2)}$	$0.1 - 0.8_{(22)}$	$0.0 - 0.6_{(31)}$	$0.0 - 0.1_{(2)}$

This water mass is a mixed water body consisting of MKGTW, OSW and MSW. mMKGTW can be separated from OSW only by very narrow subdivisions of the TS domains (*see* Tab. 3.1.2). Oxygen, nutrient, and chlorophyll *a* distributions were assigned to the different water masses for their further characterization. Table 3.1.2 summarizes the parameter ranges that occurred in the different water masses. Oxygen concentrations were highest in the near surface water bodies of OSW, MKGTW and mMKGTW, whereas lower values were observed in the deeper parts of the water column in PTW and MSW, respectively. In PTW and MSW increased nutrient values were found for nitrate, phosphate and silicate. The three shallower water masses were much more depleted in nutrients due to the biological production. mMKGTW still contained low nitrate, phosphate and silicate concentrations. OSW and MKGTW were completely depleted in nitrate and phosphate and showed low silicate concentrations. Nitrite concentrations were generally low in all water masses. Maximum chlorophyll *a* concentrations were found in mMKGTW (0.3 – 1.5 mg m^{-3}) and

relatively high values appear in OSW (0.1 – 0.8 mg m^{-3}) and MKGTW (0.2 – 0.3 mg m^{-3}) due to the high production. Despite high nutrient values, PTW and MSW contained very low chlorophyll *a* concentrations.

3.1.3   Discussion

Was 2003 a Typical Year?

Due to the fact that the meteorological observations and the heat fluxes are different to the climatologic means and no upwelling could be detected on the sea surface, the question arises whether 2003 was a typical year or not. An inspection of climatologic time series helps to bring light into the situation. Figure 3.1.13 shows the standardized weekly SST anomaly in the NINO3 area and the monthly values of Southern Oscillation Index (SOI, difference in standardized monthly sea level pressure anomalies of Durban minus Tahiti). The data source is: www.cpc.ncep.noaa.gov.
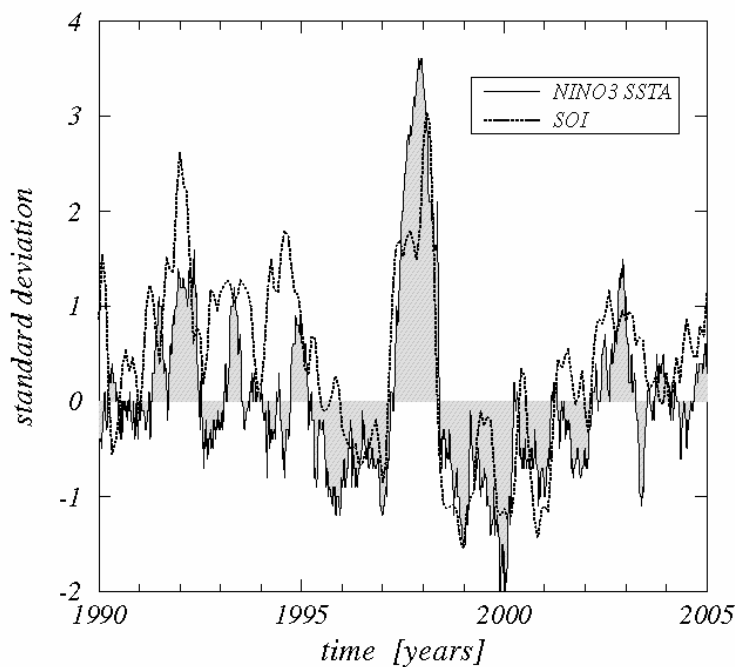
Fig. 3.1.13: Standardized weekly SST anomaly in the NINO3 area (full line with grey filling) and monthly values of Southern Oscillation Index (SOI, difference in standarddized monthly sea level pressure anomalies of Durban minus Tahiti, dotted line). Data source: www. cpc.ncep.noaa.gov.

The Figure shows the big 1997 El Niño, but also a signal at the end of 2002 with a positive sea level pressure anomaly in the SOI of 1.4 standard deviation. The temperature anomaly in the NINO3 area was 1.6 standard deviation and in the NINO34 area 1.9 standard deviation. This signal is accompanied by a negative anomaly in the outgoing long wave radiation at the equator in the area of 160 °E – 160 °W of –1.6 standard deviation (www.cpc.ncep.noaa.gov). All signals indicate a weak ENSO which modulates the Vietnamese upwelling. The mean sea surface temperature was 1.2 °C warmer than the climatologic mean due to the impact of the

weak 2002-2003 El Niño. The same response in SST occurred 1998 after the extreme strong 1997-1998 El Niño. Figure 3.1.14 shows a sequence of satellite images (TMI-TRMM-Microwave Imager) of the averaged SST in July for the period 1998 to 2003. In the post El Niño years of 1998 and 2003, SST is much higher than normal whereas under climatologic normal conditions a clear upwelling structure can be observed at the coast of Vietnam from 1999 to 2002. The offshore advection of upwelled water is visible in the period 1999 to 2002 and can be attributed to the general circulation in the SCS.

a) 1998   b) 1999   c) 2000

d) 2001   e) 2002   f) 2003
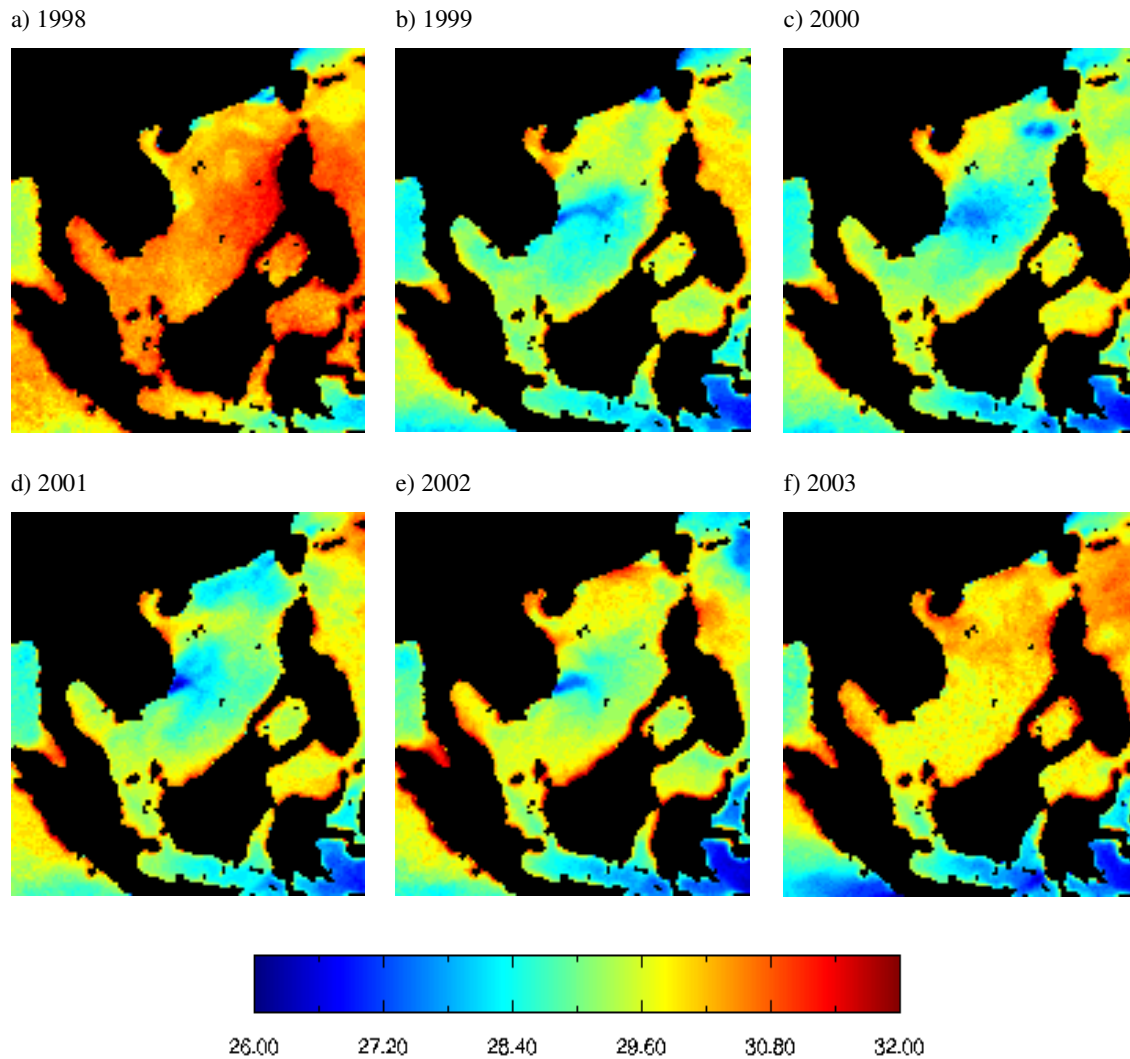
Fig. 3.1.14: July averaged sea surface temperature in °C in the SCS for the period 1998 - 2003. Data source: www.remss.com/tmi/tmi_description.html.

An inspection of daily SST satellite pictures shows that the offshore advection is a persistent structure during the SW monsoon. The cold upwelling water is transported into the central SCS. Chao et al. (1996) mentioned that the increase in heat content could not be explained by a decrease in latent heat fluxes. In contrast we observed a reduced latent heat flux of

-39.4 W m^{-2} which is much less that the climatologic mean of -125 W m^{-2} (Oberhuber 1988). However, in a complete heat balance the deficit in latent heat due to weak wind speed is compensated by the long wave back radiation due to the higher difference in SST and air temperature and nearly no cloudiness. A summation of all outgoing heat fluxes from the sea is nearly equal to the corresponding climatologic value. A higher insolation due to less cloudiness at the sea surface and a weaker than normal wind speed which prevents deeper mixing of heat into the water column are the reasons for higher than normal water temperatures. In the post El Niño years 1998 and 2003 wind speed of SW monsoon was very weak in the order of 2-3 m s^{-1} in the NCEP data (www.cpc.ncep.noaa.gov) whereas the climatologic mean wind speed is 6 m s^{-1} during SW monsoon (Hellermann and Rosenstein 1983). We observed on board an averaged wind speed of 4 ± 2.1 m s^{-1} which is less than the climatologic mean, but higher than the observed NCEP wind. A possible explanation might be local wind effects at the coast which result in higher values than the NCEP data. The coastal upwelling is reduced due to weaker wind speed. Nevertheless, upwelling occurred which is visible in the salinity and temperature distributions (Figs. 3.1.3 and 3.1.4). The conclusion from this result is that in a post El Niño year the wind induced upwelling is strongly reduced and the ENSO is modulating the upwelling intensity. The fact that in 2003 upwelling is not visible on the SST satellite images does not necessarily mean that no upwelling occurred. The depth of thermocline (Fig. 3.1.6) clearly shows an onshore slope which is connected with weak upwelling.

Upwelling Intensity

Following the theory of Yoshida and Mao (1957), in the classical understanding upwelling can be separated into a wind induced part (the so-called Ekman upwelling) and a dynamic part due to the rotation of the northward undercurrent. Using equation 2.8 from the attachment, the wind induced Ekman upwelling can be computed from the wind observations, using the computed radius of deformation of 14 – 56 km. The resulting Ekman upwelling velocity varies between 1.35 x 10^{-5} to 5.26 x 10^{-5} m s^{-1}. Using the averaged radius of deformation of 42 km the upwelling velocity is 1.82 x 10^{-5} m s^{-1}. Assuming the climatologic mean wind speed of 6 m s^{-1} (Hellermann and Rosenstein 1983), the theoretical Ekman velocity would result in 6.7 x 10^{-5} to 2.6 x 10^{-4} m s^{-1} with an averaged value of 9 x 10^{-5} m s^{-1}. The northward jet and the dynamical upwelling were analysed using the vorticity equation. Equation 2.12 from the attachment is used for the analyses. All production terms are computed from the observations. The largest contribution to anticyclonic vorticity production is the solenoid term with a local maximum in the northward jet of 9 x 10^{-7} s^{-2} followed by the divergence term

with a local maximum of 3×10^{-7} s^{-2}, whereas the contribution of Coriolis term is small and the tilting term operates against the production. Figure 3.1.15 shows the vertical pattern of the vorticity production (right hand side of Eq. 2.12) and the pattern of the dominant solenoid term between transects T2 and T3.
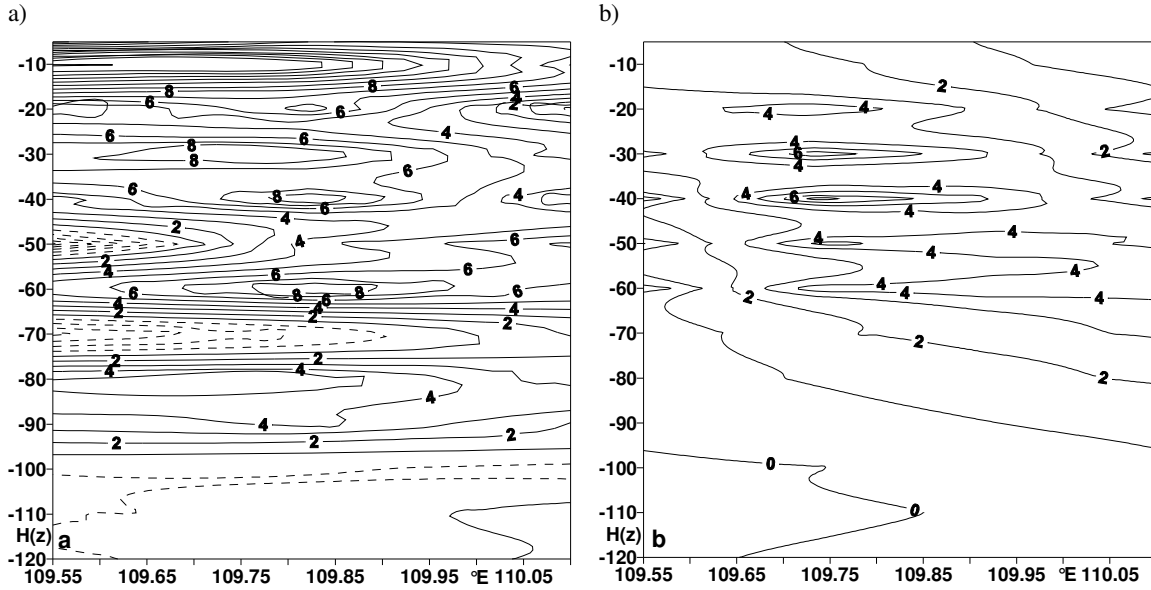
Fig. 3.1.15: Zonal section of vorticity between T2 and T3: a) total production (right hand side of Equation 12 in the material and method section 2.2, CI = 10^{-7} s^{-2}; b) the solenoid term, CI = 10^{-7} s^{-2}.

Fig. 3.1.15a shows beside a strong vorticity production in the upper 10 m local maxima in 30 m and 40 m water depth which are pronounced signal in the solenoid term (Fig. 3.1.15b). Equation 2.13 from the attachment is used for the computation of the dynamical upwelling velocity. The upwelling velocity is in the order of $1.8 \ 10^{-5}$ to $1.2 \ 10^{-3}$ m s^{-1} with an averaged value of $6.3 \ 10^{-4}$ m s^{-1}. In the vicinity of the northward jet a local maximum of upwelling velocity of $2.8 \ 10^{-3}$ m s^{-1} appears. The peculiarity of the Vietnamese upwelling is caused by stretching deformation. The spatial heterogeneity of the wind stress during SW monsoon results in a cyclonic gyre in the northern part of SCS and an anticyclonic gyre in the southern SCS (Chao et al. 1996). This circulation pattern forms a dipole and is associated with an eastward offshore current off the coast of Vietnam at ca. 12 °N (Wu et al. 1998). The northward undercurrent with a local maximum of 1 m s^{-1} in 70 m water depth (Fig. 3.1.9c) meets the southward current with a maximum speed of 1.4 m s^{-1} between 70 – 100 m at ca. 12 °N resulting in the mentioned offshore jet (Fig. 3.1.11) with a maximum speed of 1.2 m s^{-1} eastwards. This regional circulation pattern causes a stretching deformation close to the coast.

To estimate the stretching deformation induced upwelling, the equation of incompressibility in a vertically integrated form is used:

$$w_s = w_i - \frac{\partial U}{\partial x} - \frac{\partial V}{\partial y} \qquad\qquad (3.1.1)$$

where w_s is the vertical velocity at surface, w_i the vertical velocity at the interface (130 m) and U and V the vertically integrated zonal and meridional transport. W_i is estimated from the mean Ekman upwelling velocity. According to Equation 3.1.1, the local maxima in upwelling occurred between the transects T1 and T3 with velocities of $1.9 \ 10^{-4} - 3.7 \ 10^{-4}$ m s^{-1} and a maximum of $2.1 \ 10^{-3}$ m s^{-1}, which is one order of magnitude higher than the estimated Ekman upwelling during normal conditions. The stretching deformation of the flow field is responsible for asymmetry of coastal upwelling and the formation of the local maximum in upwelling at ca. 12 °N. With these values a ranking of upwelling intensities is possible: the strongest contribution to Vietnamese upwelling is the dynamical upwelling due to the clockwise rotation of the northward undercurrent, followed by the stretching deformation induced upwelling due to the general circulation pattern in the SCS. The weakest contribution is the wind induced upwelling because its intensity is weakened. This holds for the post ENSO year 2003, however in a "normal" year the wind induced upwelling is one order of magnitude higher.

Water Mass Analysis

Rojana-anawat et al. (2001) have identified six different water bodies in the whole SCS. These are the Permanent Thermocline Water (PTW), the Maximum Salinity Water (MSW), the Open Sea Water (OSW), the Seasonal Thermocline Water (STW), Continental Shelf Water (CSW) and Deep Water (DW). However, in the Vietnamese upwelling area we only found PTW, MSW and OSW. Rojana-anawat et al. (2001) made their observations during inter-monsoon in April when the runoff of River Mekong is weak (*see* Table 3.1.3). They call the Gulf of Thailand water the southern CSW. During SW monsoon however, both, water from the Gulf of Thailand and water from the River Mekong with a runoff of 17300 m^3 s^{-1} are transported into the upwelling area off Vietnam. We call this water mass MKGTW. Rojana-anawat et al. (2001) gave a salinity range of the Gulf of Thailand Water of 27–33 psu whereas Nguyen (1990) describes MKGTW as a water mass with salinity above 32 psu. However, it is impossible to separate these two water masses from temperature and salinity only. The reason is the extreme long tidal excursion of the River Mekong of 390 km. Because the first weir

after the river mouth is located in Cambodia a strong tidal mixing occurs in the River Mekong (Nguyen 1990) which results in high salinity at the river mouth during runoff.

Table 3.1.3: Long-term monthly mean runoff of the River Mekong in $m^3 s^{-1}$ after Nguyen (1990).

Month	runoff	Month	runoff	Month	runoff
January	7040	May	3690	September	31000
February	4190	June	10400	October	29900
March	3020	July	17300	November	20500
April	2680	August	26000	December	12100
		annual mean 13900			

A separation of the water masses from nutrient concentrations seems rather impossible due to the fact that we know no measurements of nutrients from the Gulf of Thailand and due to the completely depleted nutrient concentrations in the River Mekong caused by the mangrove forests. Waters that would fit into the STW-characteristics were clearly part of the mixing waters of MSW and OSW. During our sampling period, mMKGTW lay band-like off the southern Vietnamese coast outside the upwelling zone. Vertical nutrient concentrations lay within the range described by Pham et al. (2002) for May/June 2000. They reported depleted surface waters and steady increasing nutrient concentrations between 100 m and 500 m depths with nitrate, phosphate and silicate values of 6 µmol L^{-1}, 1.13 µmol L^{-1} and 7.0 µmol L^{-1} in 100 m depths and of 17.9 µmol L^{-1}, 1.6 µmol L^{-1}, 35.7 µmol L^{-1} in 300 m depths, respectively.

The observation of the subthermocline chlorophyll maxima were in the same range as the observations during spring and summer 1999 (Nguyen and Hoang 2001, Deetae and Wisespongpand 2001). Liu et al. (2002) argue that the outflow of the River Mekong and the Gulf of Thailand can be observed on SeaWiFS images showing a band of high chlorophyll concentration on a width of 100 km and a length of 600 km extending north-eastward from the mouth of River Mekong during summer monsoon. In our data set the river plume was well identified by salinity (Fig. 3.1.3). The Mekong delivers annually, and especially during the SW-Monsoon, about 160 Mt of suspended sediment, and around 5.0, 0.1 and 0.6 Mt of dissolved silica, phosphate and nitrate, respectively, to the coastal zone of Vietnam (Meybeck and Carbonnel 1975, Milliman 1991, Nguyen and Vo 1999). However, during our measurements the river plume was strongly depleted in nutrients probably due to the

mangrove forests along the river and included only very few chlorophyll *a* when it entered our investigation area ca. 200 km northeast of the Mekong river mouth. Most chlorophyll *a* peaks higher 1 mg m^{-3} were measured in the MSW influenced water body mMKGTW and at the boundary between OSW and MSW. Figure 3.1.10 shows the vertical chlorophyll *a* distribution along the transects T1, T2 and T3. The distribution shows a strong similarity to the meridional component of the velocity fields (Fig. 3.1.9). The maximum of chlorophyll *a* lays above the clockwise rotating northward undercurrent which brings on the near coastal side of the jet nutrients into the euphotic zone and transports on the offshore side subthermocline chlorophyll *a* in the transition zone between mMKGTW and MSW. We therefore conclude that phytoplankton growth in this area was fertilized by nutrient rich upwelling water (MSW) due to dynamical upwelling rather than by nutrient poor riverine water (MKGTW). This finding is in contrast to the recent investigation of Tang et al. (2004) who argued from the analysis of satellite images that the high phytoplankton biomass in front of the Vietnamese coast is initiated by river discharge of the River Mekong.

The position of the chlorophyll *a* maxima, the current field and the separation of water masses allows us to construct a schematic sketch of the relative vertical positions of water masses (Fig. 3.1.16). In the upwelling area which is limited offshore by the internal radius of deformation, the surface water is characterized by OSW which is influenced by upwelled MSW. MSW itself lays above PTW. Offshore – outside of the upwelling area – the surface water is mMKGTW, a mixture of MKGTW, OSW and MSW, which lays above MSW and above PTW. Inside the upwelling zone, all upwelling mechanisms transport nitrate from MSW into the upper layer. Here the new production is based on nitrate. In contrast, offshore the nutrient composition shows a deflection from Redfield ratio. Here the new production is additionally based on nitrogen fixation besides the production based on nitrate entering the upper layer via diffusion from MSW. A recent paper by Voss et al. (2006) supports this. Deflection from the Redfield ratio in the C:N ratio and negative DIN_{xs} identifies the region as nitrogen limited. This is consistent with findings by Pham et al. (2002) for the same area and with findings from the SCS off Taiwan (Chen et al. 2004, and references therein). Nitrogen limitation may favour cyanobacteria blooms, due to their nitrogen fixing potential. Blooms of the cyanobacteria *Trichodesmium* were reported from the northern part of the South China Sea off Taiwan by different authors (Wu et al. 2003, Chen et al. 2003, 2004). In the waters off southern Vietnam *Trichodesmium* blooms were reported from inter-monsoon periods in April and May with abundances between 107 to 109 cells m^{-3} (Nguyen and Doan 1996, Nguyen and Vu 2001).
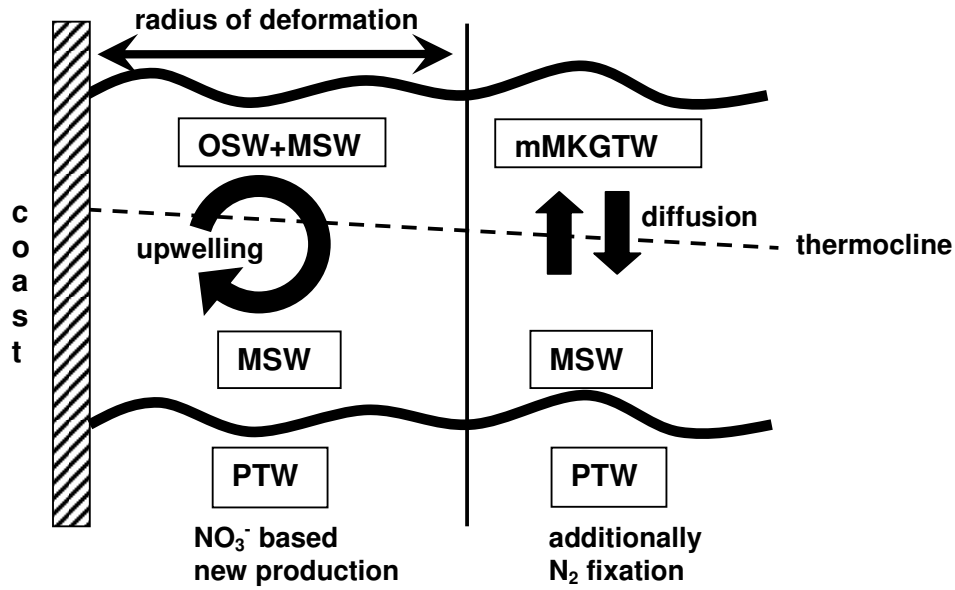
Fig. **3.1.16**: Schematic sketch of vertical water mass distribution in the Vietnamese upwelling area during SWM.

Further investigations e.g. of stable nitrogen isotope distribution will help to clarify the potential role of cyanophyceae in the pelagic nitrogen cycle off southern central Vietnam (Loick et al. 2006, Voss et al. 2006).

3.2   Riverine Influence on Nitrogen Fixation in the Upwelling Region off Vietnam, South China Sea

The results of this chapter are part of the manuscript "Riverine Influence on Nitrogen Fixation in the Upwelling Region off Vietnam, South China Sea" by M. Voss, D. Bombar, N. Loick and J. Dippner. This article is published in Geophysical Research Letters 2006, Vol. 33, L07604, doi: 10.1029/2005GL025569. My own share in this paper constitutes 30 % which includes practical work on board like rate measurements (HCO_3^-, N_2 and NO_3^- -fixation), stable isotope analysis of the samples and discussion of the results.

3.2.1   Introduction

Estimates of nitrogen fixation have increased over the past years, and regions not traditionally regarded as sites favourable for fixation, seem to be important as well (Capone et al. 2005); these sites include river plumes (Carpenter et al. 1999) and upwelling regions (Voss et al. 2004, Walsh 1996). In the upwelling region off Vietnam primary production is mainly driven by nutrients from below the thermocline (Tang et al. 2004). Some of the upwelled nitrate is lost through denitrification, either in the suboxic zone of the water column or in the sediments leading to NO_3^- PO_4^{3-} ratios <16 (Chen et al. 2001). This may foster the growth of cyanobacteria relying on a phosphate surplus (Nguyen and Doan 1996). Nitrogen fixation has not yet been studied in great detail in the South China Sea (SCS) and published fixation rates are based on cell counts of *Trichodesmium* sp. that have been extrapolated based on single trichom fixation rates from the literature (Wu et al. 2003). Such estimates only come from the northern part of the SCS and are relatively low between 0.007 and 0.05 nmol N_2 L^{-1} hr^{-1}. The cyanobacteria are suggested to be limited by dissolved iron (Wu et al. 2003).

Another potentially important nitrogen source in the SCS is the Mekong River, whose plume flows southward in winter and turns northward in summer (Hu et al. 2000). The river, however, carries relatively low concentrations of nutrients compared to other tropical rivers of around 35 µmol L^{-1} NO_3^- and 3 µmol L^{-1} PO_4^{3-} (www.gemstat.org/). Nevertheless, high phytoplankton concentrations of harmful algae blooms have been indicated by SeaWiFS satellite data and confirmed by cell counts (Nguyen 1999, Tang et al. 2004).

Upwelling off Vietnam occurs during the summer SW-monsoon (SWM, July through September) when a cyclonic circulation cell in the northern and an anticyclonic gyre in the southern SCS are initiated by the spatial asymmetry in the wind field (Wu et al. 1998). Besides the dynamical and Ekman upwelling, a stretching deformation of the flow pattern of the gyres forms an offshore jet at 12° N that causes locally an enhancement of the upwelling

(Dippner et al. subm.). The offshore width of the coastal upwelling area can be defined by the size of the deformation radius which is in the order of 40–50 km (Figure 3.2.1). In the intermonsoon (IM) period from March to June oligotrophic conditions prevail.

The high productivity off Vietnam is determined by upwelling during the monsoon seasons and potentially enhanced by nitrogen fixation and river input. To evaluate the different N-sources and their roles for zooplankton nutrition a three years project with several cruises to the SCS was launched in 2003.
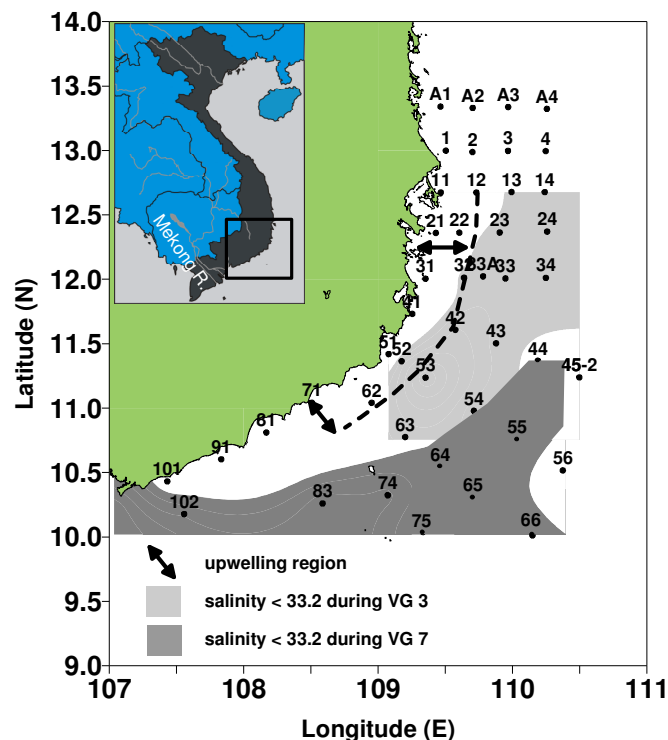
Fig. 3.2.1: Map of the South China Sea off Vietnam with all CTD stations, the insert shows SE Asia. (N_2-fixation was measured at the 32 stations). Stations A1 to A4 and 1 to 4 were only visited during VG4, stations 62 to 65 only during VG4 and VG7. The shaded area denotes Mekong river influence and the line the extension of the upwelling region from the coast.

We measured nitrogen fixation rates in July 2003 and 2004 and in April 2004 along with the hydrological and chemical variables. In our study area, the competition of nitrogen fixers with nitrate consuming phytoplankton is potentially large. Few new production data (7 stations, 3 depths) measured in July 2003 were between 200 and 2000 µmol N m^{-2} d^{-1} and are app. 10 times larger than the nitrogen fixation rates encountered. Here we compare the N_2-fixation rates within and outside the upwelling region, and between seasons to evaluate the importance of this process under different environmental settings.

3.2.2   Results and Discussion

The results of this chapter are based on the material and methods described in detail in chapter 2.3.

Seasonal Differences of N₂-Fixation Rates

Seasonal Differences of N_2-Fixation Rates

Nitrogen fixation rates in the SCS off Vietnam are in the lower range of those reported from the tropical North Atlantic Ocean (Capone et al. 2005) and in a similar range of those measured at station ALOHA in the Pacific (66 µmol N m^{-2} d^{-1}, Montoya et al. 2004) or the Arabian Sea (129 ± 23 µmol N m^{-2} d^{-1}, Capone et al. 1998). The N_2-fixation rates off Vietnam are considerably higher during the SWM in June/July (21.4 to 190.6 µmol N m^{-2} d^{-1}) than in the IM period of April/May (1.9 to 36.0 µmol m^{-2} d^{-1}; Figure 3.2.2). Measured rates would cover 0.1–8.2 % (VG 3), 0.2–2.9 % (VG 4), and 0.1–4.2 % (VG 7), of the N demand of the primary producers using a C/N ratio of 6.6, thus fall in the range of values (<3 %) reported by (Chen et al. 2004) for the northern part of the SCS, or 6 % from the Arabian Sea (Capone et al. 1998).
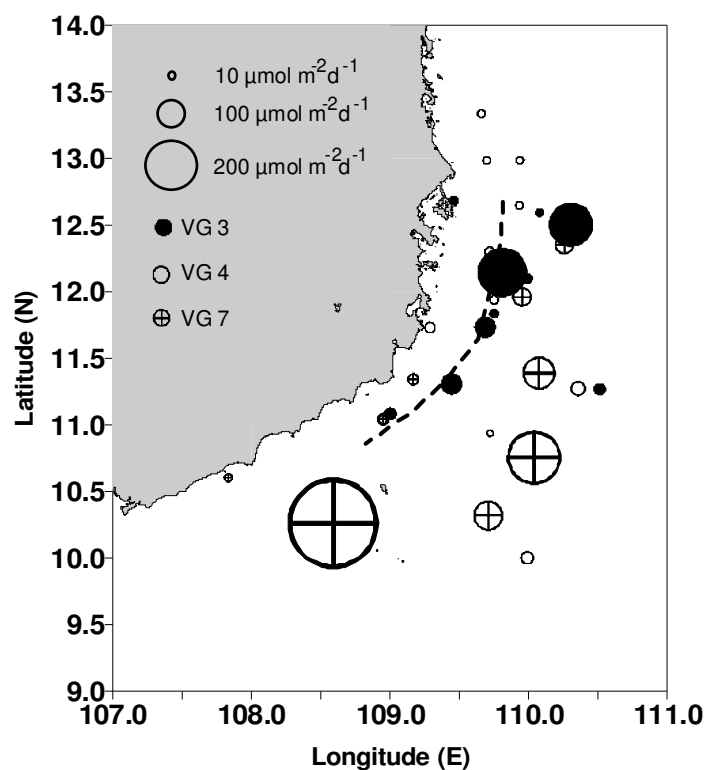
Fig. 3.2.2: N_2-fixation rates, symbols are scaled linearly proportional to the measured values. The dashed line visualises the offshore limitation of the upwelling area.

With rates up to 1.2 nmol L^{-1} hr^{-1} we measured significantly higher values than the maximal of 0.05 nmol L^{-1} h^{-1} found for July 2001 (Wu et al. 2003). The station Wu et al. (2003) sampled, was located in the northern SCS app. 5° north of our investigation area and is not affected by upwelling. Wu et al. (2003) consider N_2-fixation by *Trichodesmium* sp. only and suggest that the fraction <3mm - contributing 80 % of the phytoplankton biomass - and *Richelia intracellularis* could significantly contribute as well. Up to now all evidence of nitrogen fixation in upwelling regions is only indirectly inferred from the depletion ratios of

dissolved inorganic carbon (DIC) and NO_3^- off Venezuela and Peru (Walsh 1996). Off West Africa, close to the Mauritanian upwelling region, high rates were mainly attributed to unicellular and/or heterotrophic diazotrophs since they were found throughout the whole euphotic zone and in the nutricline (Voss et al. 2004). Enhanced nutrient concentrations will not have affected our rates since highest values were usually encountered near the surface (Figure 3.2.3) where nutrients were depleted (Figure 3.2.4). Of our 28 nitrogen fixation profiles only three from far offshore (St. 24 VG 3, St 55 and 83 VG 7) had elevated rates below the surface (Figure 3.2.3).
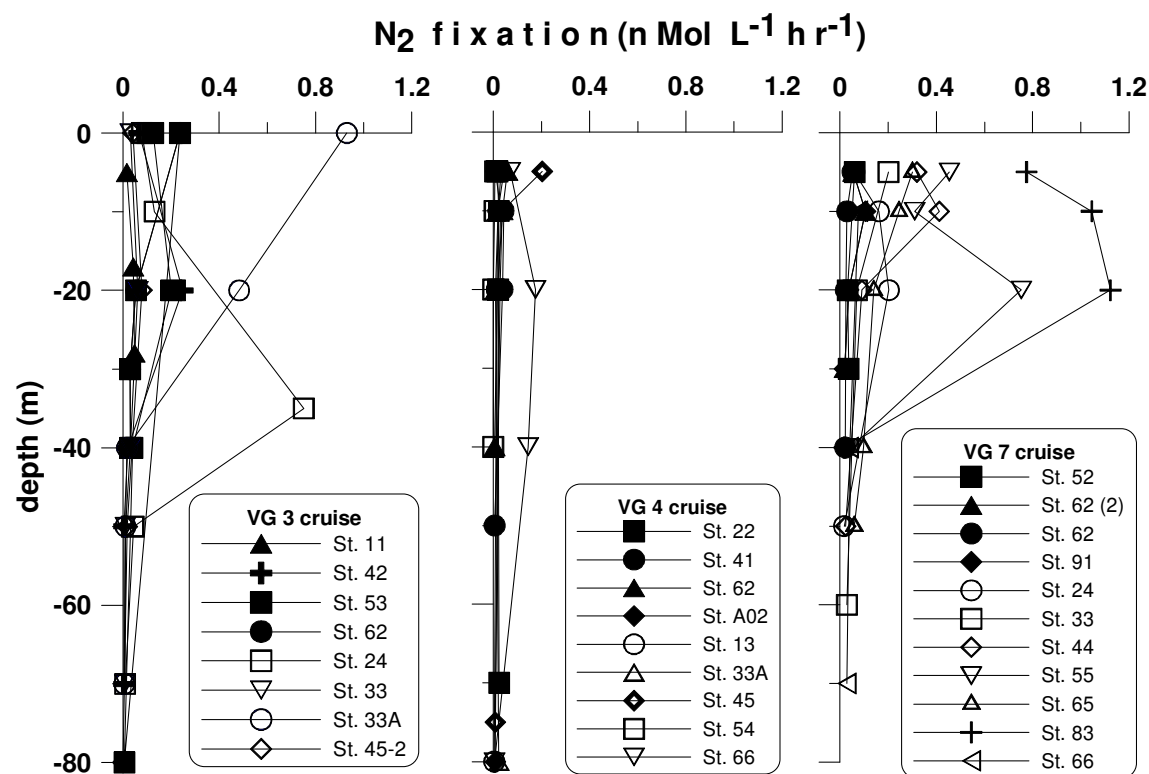
Fig. 3.2.3: Nitrogen fixation rates over depth for all stations and cruises, VG 3 and 7 (SWM) and VG 4 (IM). Closed symbols depict the coastal near stations, open symbols the stations offshore, which were partly under influence of the Mekong River plume.

It is therefore improbable that the same group of unicellular diazotrophs is responsible for the N_2-fixation in the SCS as off West Africa. The temperature in our investigation area was always within the optimal growth temperature of Trichodesmium (Carpenter and Romans 1991) with >20 °C and usually >25 °C (Table 3.2.1). Only during the SWM in 2004 the upwelling region had 22.6 °C. The upwelling along the coast was less intense in the post ENSO year of 2003 than in 2004, and the primary production was considerably lower (Table 3.2.1). The weak upwelling may have had an effect on the overall productivity and on the contribution of nitrogen fixation to the primary production (Table 3.2.1). However, coastal

near chlorophyll concentrations were higher during both monsoon cruises compared to the IM. Temperature differences in the upwelling strip of almost 3 °C between both years were found. Difficult to explain is a higher mixed layer depth in 2003 when less wind was observed. It may be a consequence of the weak upwelling.

Table 3.2.1: Summary of means and standard variations of variables for the three cruises[a].

	VG 3 - SWM	VG 4 - IM	VG 7 - SWM
N_2-fix. (μmol N m^{-2} d^{-1}) - upwelling	41.6 ± 37.0	16.3 ± 6.0	19.1 ± 9.9
N_2-fix. (μmol N m^{-2} d^{-1}) - offshore	84.5 ± 76.3	14.1 ± 12.0	115.0 ± 112.8
Prim. Prod. (mmol C m^{-2} d^{-1}) - upwelling	18.5 ± 8.0	9.7 ± 5.6	117.5 ± 66.8
Prim. Prod. (mmol C m^{-2} d^{-1}) - offshore	19.7 ± 17.0	6.4 ± 3.4	36.8 ± 35.8
% N_2-fix. of N demand - upwelling	1.3 ± 0.7	0.9 ± 0.8	1.7 ± 1.7
% N_2-fix. of N demand - offshore	4.1 ± 3.1	0.8 ± 0.8	1.5 ± 1.5
mixed layer depth (m) - upwelling	31	10	17
mixed layer depth (m) - offshore	56	24	32
temperature (°C) - upwelling	25.4 ± 0.8	26.4 ± 0.8	22.6 ± 1.8
temperature (°C) - offshore	29.2 ± 0.7	28.0 ± 1.2	25.0 ± 1.9
salinity - upwelling	34.0 ± 0.3	34.0 ± 0.1	33.1 ± 2.1
salinity - offshore	33.4 ± 0.6	33.9 ± 0.1	31.0 ± 0.5
NO_3^-/PO_4^{3-} (mol/mol) diffusing through the thermocline - upwelling	14.8	17.0	16.8
NO_3^-/PO_4^{3-} (mol/mol) diffusing through the thermocline - offshore	12.5	22.7	15.1

[a]The mixed layer depth was calculated by means of the maximum in the buoyancy frequency. During VG4 we encountered an intermonsoon (IM).

In the upwelling region we encountered a shallow mixed layer depth of 10 - 31 m (Table 3.2.1) compared to the oligotrophic offshore region where it was between 24 and 56 m depth. We found steep vertical gradients in NO_3^- concentrations, during VG 7 with a coastal near nutricline at 30 m depth and 193 km off the coast at 70 m depth (Figure 3.2.4a) but no negative relationship between single N_2-fixation measurements and areal NO_3^- concentrations. Furthermore, our calculation of the nutrient ratios potentially diffusing through the thermocline indicate slightly lower values during the SWM than during the IM thus suggesting a PO_4^{3-} surplus (Table 3.2.1). This supports dinitrogen fixers while the combined N may not affect dinitrogen uptake at concentrations < 1 μmol L^{-1} (Mulholland et al. 2001).

Riverine Influence on Nitrogen Fixation Rates

All of our highest N_2-fixation rates were found at stations situated in the river plume (Figures 3.2.1 and 3.2.2). The plume of the Mekong River cuts through the upwelling area only in the monsoon season while it flows toward the south during the rest of the year (Hu et al. 2000).
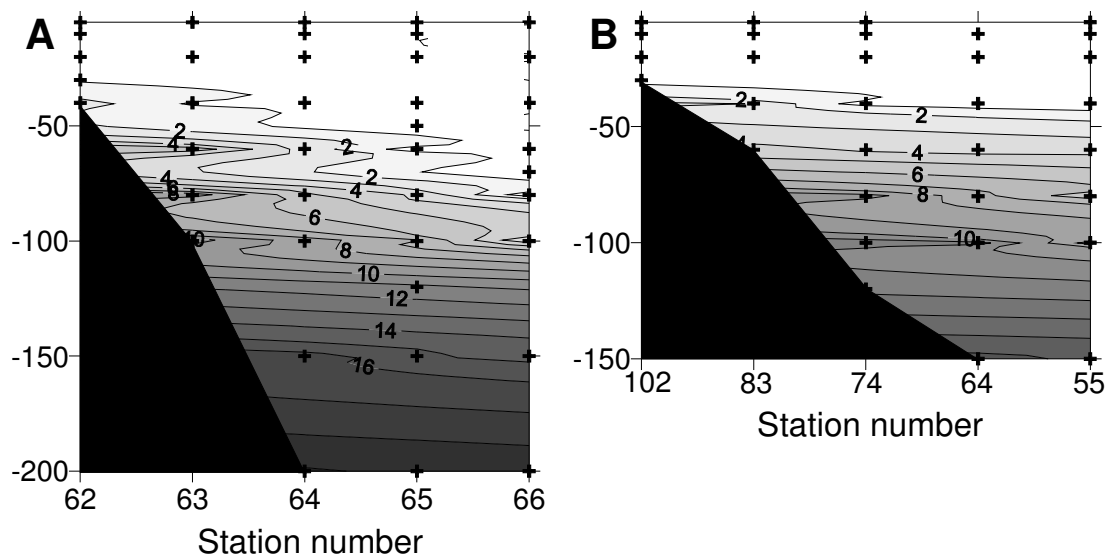
Fig. 3.2.4: Nitrate concentration in µmol L^{-1} (a) along transect 6 (stations 62 to 66) and (b) along the Mekong River outflow.

This finding supports the notion that the river plume may be responsible for the higher nitrogen fixation rates. Although we find no correlation between salinity, nitrate, and N_2-fixation we see that only at salinity values < 33.5 N_2-fixation rates are above 0.2 nmol N_2 L^{-1} h^{-1} (Figure 3.2.5a).
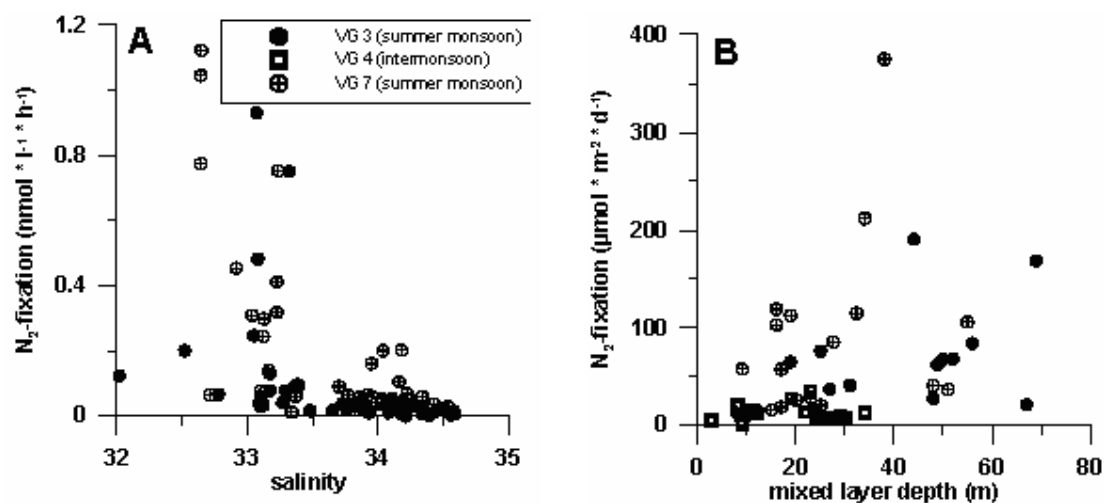
Fig. 3.2.5: (a) Nitrogen fixation rates versus salinity, all data from the cruises VG 3, VG 4 and VG 7. (b) Depth integrated nitrogen fixation rates over mixed layer depth from VG 3, VG 4, and VG 7.

The Mekong River water may increase the stability of the water column and support the positively buoyant cells to keep them at the surface, although no significant correlation exists (Figure 3.2.5b). The river water may also contain high sediment and trace metal loads, a typical feature of tropical rivers (Nitterouer et al. 1995), and especially Si-rich river water may support the growth of diatoms that potentially contain the symbiontic cyanobacteria, *Richelia* sp. (Carpenter et al. 1999). The latter phenomenon has been observed in the western tropical Atlantic in the Amazon River plume. Results from 10 °N, 52 °W describe a pronounced CO_2 drawdown (Körtzinger 2003) due to the riverine nutrient load and high productivity. The phytoplankton composition in the Amazon plume revealed symbiontic N_2-fixing species *Richelia intracellularis* living within the diatom *Hemiaulus hauckii* as dominant phytoplankton species (Carpenter et al. 1999). In our study nitrate (and silica) concentrations were depleted in the surface waters from the river mouth toward the sea (Figure 3.2.4b) but may have initiated the biomass build-up closer to the coast. The presence of *Hemiaulus hauckii* was confirmed for the VG 3 cruise while the analysis of the symbionts and the regional distribution of the species are still under investigation (H. Doan-Nhu, personal communication). The Mekong River has a Si:N ratio (www.gemstat.org/) favourable for diatom growth of around 3, but concentrations are low compared to the global estimates of mean riverine dissolved silicate concentrations (Conley 1997). Thus, further studies concentrating on the plume as such are necessary to support the data presented here.

3.3   Pelagic Nitrogen Dynamics in the Vietnamese Upwelling Area According to Stable Nitrogen and Carbon Isotope Data

The results of this chapter are part of the interdisciplinary manuscript "Pelagic Nitrogen Dynamics in the Vietnamese Upwelling Area According to Stable Nitrogen and Carbon Isotope data" by N. Loick, J. Dippner, H. N. Doan, I. Liskow, and M. Voss. This manuscript has been submitted to Deep-Sea Research I. My share in this manuscript constitutes 90 % and includes the plankton sampling and the isotope analysis in the lab, the discussion of results as well as the writing of the manuscript.

3.3.1. Introduction

The upwelling area off southern central Vietnam is the most productive one of three areas in the South China Sea (Liu et al. 2002). However, it is also the least well studied one with most biogeochemical work relying on remote sensing data without ground truth validation (Liu et al. 2002). During summer monsoon from June to September upwelling events regularly fertilize the otherwise nitrogen limited area within a 40 km long strip along the coast (Dippner et al. subm., Pham et al. 2002). Upwelling events last between 2 to 9 days (Vo 1997). This results in chlorophyll *a* values of up to 0.9 mg m^{-3} according to CZCS-Sea WiFS data (Liu et al. 2002). Besides upwelling, the Mekong river influences the sea area off southern central Vietnam. The river plume turns northward in summer due to the anticyclonic gyre in the southern basin of the South China Sea (SCS) and brings in less saline waters (Hu et al. 2000). However, no additional nitrate or phosphate is carried further offshore into the sea area off southern central Vietnam, where the riverine influence is still detectable by salinities below approximately 33.2 psu (Dippner et al. subm.).

High nutrient concentrations along the coast allow the occurrence of diatom blooms of the species *Pseudonitzschia* spp., *Chaetoceros* spp., *Rhizosolenia* spp., and *Coscinodiscus* spp., while further offshore in nutrient exhausted waters cyanobacteria of the species *Trichodesmium erythraeum* and *T. thiebautii* occur (Nguyen 1996, Nguyen and Doan 1996). These findings are supported by a recent study that showed high nitrogen fixation rates in the low salinity waters (Voss et al. 2006). It is hypothesized that the stability of the water column, micronutrients and/or trace metals in the Mekong river plume may be responsible for enhanced cyanobacteria growth (Voss et al. 2006).

The trophic transfer of nitrogen has not yet been studied in this region, although different phytoplankton communities are expected to support different heterotrophs e. g. only few species directly feed on cyanobacteria (Sellner 1997). Indirect transfer of fixed nitrogen via

the microbial loop has also been considered and may support heterotrophs offshore of the actual upwelling region (Montoya et al. 2002). In this study we evaluated the roles of the different N-sources for zooplankton nutrition by means of stable nitrogen isotopes in subthermocline nitrate (nitrate$_{sub}$) and by carbon and nitrogen stable isotopes in particulate organic matter (POM) and six net-plankton size fractions.

δ^{15}N in nitrate$_{sub}$ will be used as tracer for nitrogen fixation, because only nitrogen fixation causes a lowering of the δ^{15}N values in nitrate$_{sub}$ below the global mean value of 4.5 to 6 ‰ (Liu and Kaplan 1989). In the upper water column fractionation processes have to be considered to correctly interpret stable nitrogen isotope data. Variations in δ^{15}N of near-surface ocean nitrate can occur, if not all nitrate is completely consumed by phytoplankton. This leads to an isotopic fractionation of up to 12 ‰ during uptake and is expressed as low δ^{15}N for plankton and increased δ^{15}N for nitrate as function of its degree of utilization (Needoba et al. 2003, Altabet 1996). Furthermore, the preferentially release of ^{14}N-ammonium, the end product of heterotrophic metabolism, leads to a lowering in surface water δ^{15}N (Sigman and Casciotti 2001, Checkley and Miller 1989). The excretion of light ammonium seems to be the principal cause for enrichment in the δ^{15}N of consumers by 2 to 3.5 ‰ compared to the diet (Peterson and Fry 1987). This fact is widely used as trophic level indicator in ecological studies (Peterson and Fry 1987). Incomplete bacterial remineralization alternates the δ^{15}N of decaying organic material because preferential recycling of ^{14}N leaves increased δ^{15}N in the residual organic material (Montoya 1992). However, nitrate assimilation, ammonium recycling or remineralization processes cannot change the average δ^{15}N of the system because they neither add nor remove nitrogen from the system. δ^{13}C can be used as food source indicator, because diet and consumers in marine systems generally differ by less than 1 ‰ (Peterson and Fry 1987).

Combined measurements of stable nitrogen and carbon isotopes in nitrate$_{sub}$, POM and the different plankton size fractions therefore can serve as indicators of the food web structure and the ultimate N and C - sources for secondary production. A two source mixing equation will be used to estimate the fraction of N in nitrate and plankton derived from nitrogen fixation during non-upwelling spring intermonsoon (SpIM) and upwelling southwest monsoon (SWM) seasons.

3.3.2. Results

The results of this chapter are based on the material and methods described in detail in chapter 2.4.

Sea Surface Temperature and Sea Surface Salinity

During SWM 2003 a weak gradient in sea surface temperature (SST) off the coast of Vietnam was observed (Fig. 3.3.1). This reflected the weak upwelling conditions for the post-ENSO year 2003 as described in detail by Dippner et al. (subm.). Compared to 2003, SST was 2 °C cooler during SWM 2004 and reflected a stronger upwelling intensity. During SpIM no SST gradient was found, therefore no coastal near upwelling occurred. Similar to temperature, sea surface salinity (SSS) showed strong coastal gradients during both SWM periods (Fig. 3.3.1). No gradient was found during SpIM. During both SWM periods low salinity waters of less than 33.2 psu entered the study area from the south.
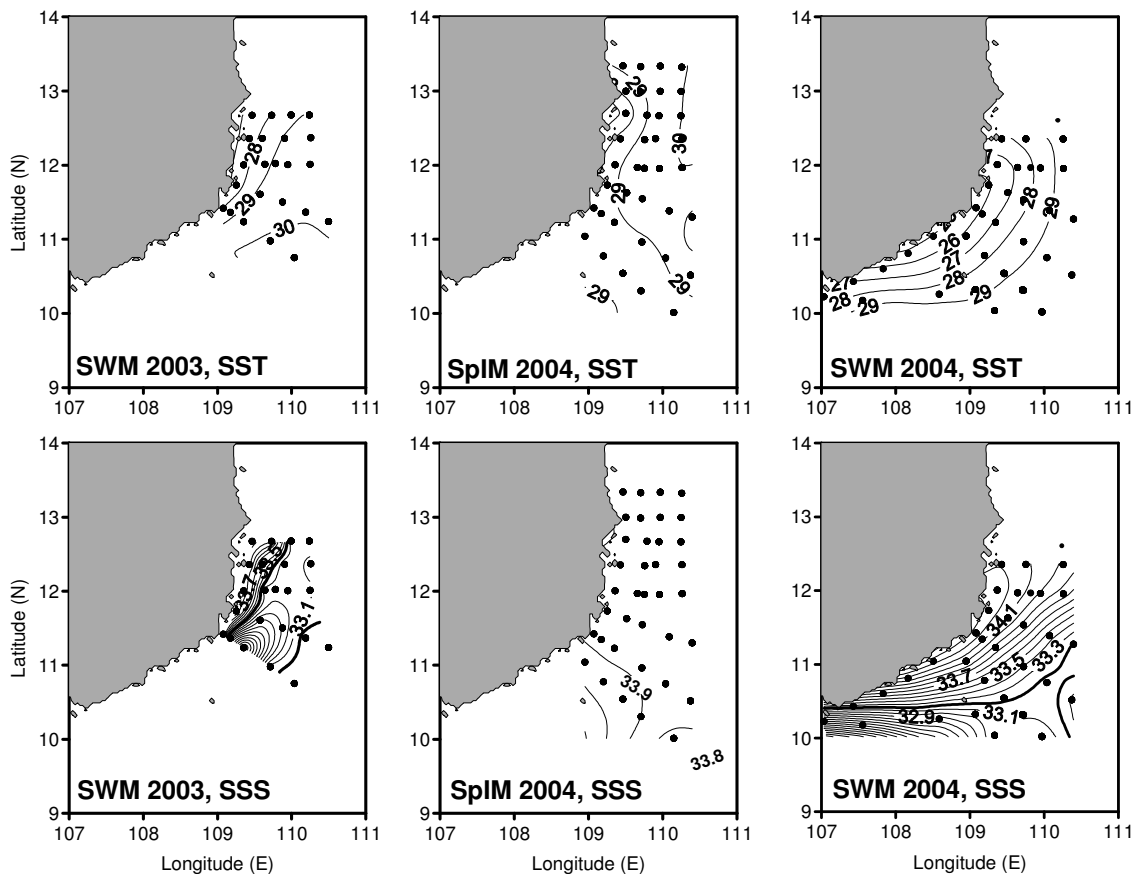
Fig. 3.3.1: Sea surface temperature (SST) in °C (upper panel) and sea surface salinity (SSS) in psu (lower panel) during southwest monsoon (SWM) and spring intermonsoon (SpIM) seasons. Black dots mark the sampling stations. The thick 33.2 psu isoline indicates low salinity waters influenced by the Mekong plume after Dippner et al. (subm.). $CI_{SST} = 1$°C; $CI_{SSS} = 0.1$ psu.

These waters have been described as an extension of the Mekong river plume that turns northwards during SWM by Dippner et al. (subm.). During SpIM no low salinity waters were found and SSS was evenly high between 33.9 to 34.0 psu.

Nitrate concentrations

Coastal near upwelling of nitrate was indicated during the SWM, when nitrate concentrations increased from zero at the surface to 4 and 8 µmol l^{-1} in 40 m depth (Fig. 3.3.2). The nutricline was situated at approximately 20 m within the upwelling area and at 40 to 60 m offshore during SWM. Upwelling nitrate reached surface waters only at station 22 during SWM 2003 (Fig. 3.3.2a) and at station 52 during SWM 2004 (Fig. 3.3.2c). During SpIM the nutricline generally was found in 60 m depth, whereas no horizontal gradient was apparent.
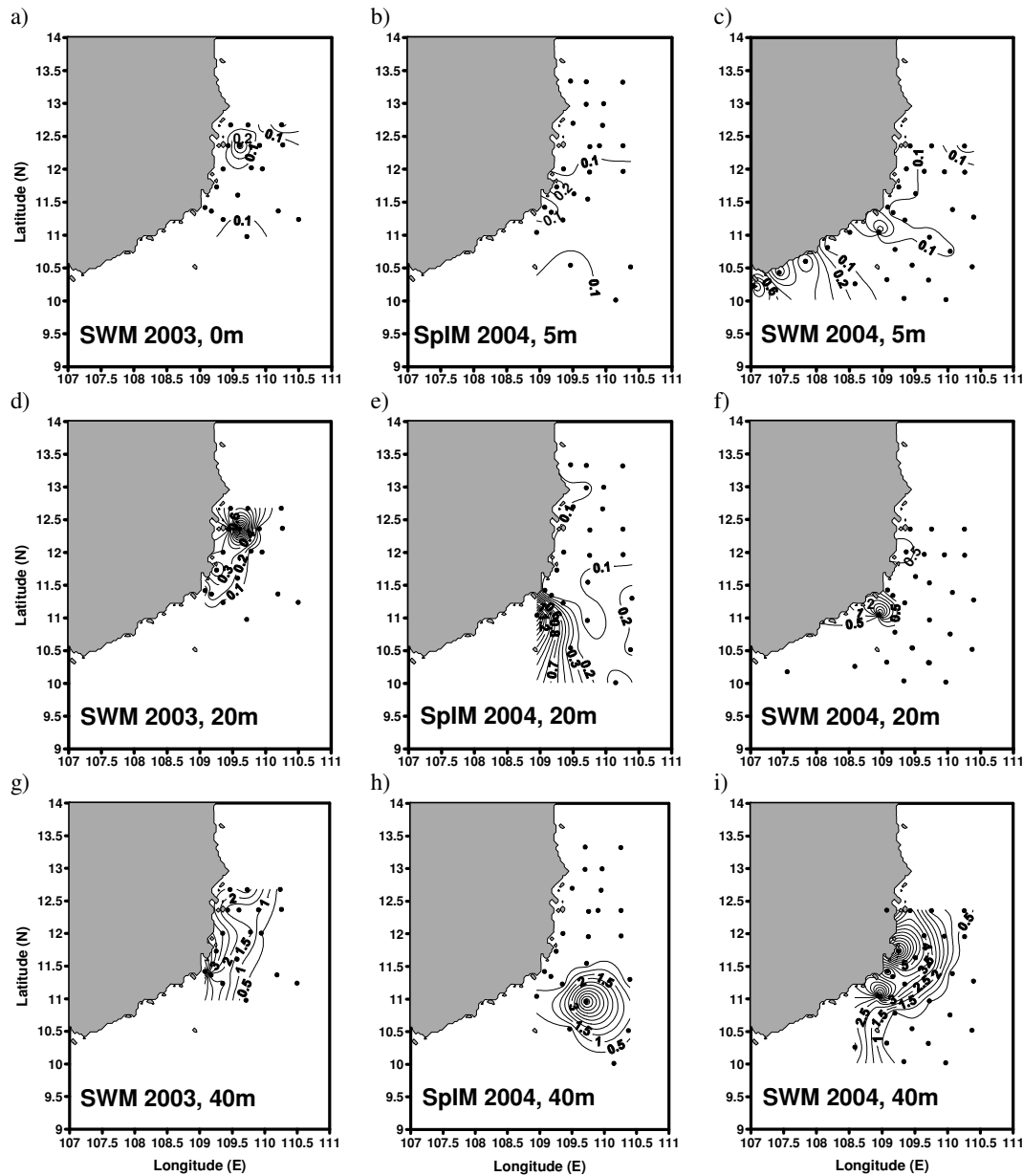
Fig. 3.3.2: Horizontal nitrate concentrations in µmol L^{-1} from surface waters (0 or 5 m), 20 m, and 40 m depth during southwest monsoon (SWM) and spring intermonsoon (SpIM) seasons. Black dots mark the sampling stations. Note: CI differ between plots as follows: a-e, 0.1 µmol L^{-1}; f-i, 0.5 µmol L^{-1}.

61

Furthermore enhanced surface concentrations of up to 0.9 µmol L^{-1} were found at the southernmost coastal stations during SWM 2004 (Fig. 3.3.2c) and of up to 1.6 µmol L^{-1} in 20 m depth during SpIM 2004 (Fig. 3.3.2e). Nitrate concentrations in the water column were similar to previously reported values by Pham et al. (2002) and Dippner et al. (subm.).

Stable isotope data

δ^{15}N values in nitrate were most variable in the upper 150 m (Fig. 3.3.3). In SWM 2003 values ranged from 2.6 to 4.9 ‰, in SpIM from 0.8 to 5.3 ‰, and in SWM 2004 from 2.2 to 7.2 ‰. Below 150 m to maximum 800 m δ^{15}N-nitrate was similar between seasons with an average value of 4.0 ± 0.6 ‰ (n = 15). Vertical profiles of δ^{15}N in nitrate were rather similar in- and outside the upwelling area during SWM seasons (Fig. 3.3.3). Only during SpIM lower values were found at coastal near stations compared to stations > 42 km offshore. The concentration weighed average values of nitrate$_{sub}$ were 3.5 ± 0.3 (n=11 stations, SWM 2003), 2.9 ± 0.9 (n = 19 stations, SpIM 2004), and 3.7 ‰ ± 0.6 (n = 15 stations, SWM 2004, Fig. 3.3.4). During SWM 2003 and SpIM 2004 surface δ^{15}N in particulate organic matter (POM) varied around   2 ‰ whereas during SWM 2004 values were ca. 2 ‰ enriched (Fig. 3.3.3). δ^{15}N-POM increased with depth by 2 to 4 ‰, a distribution generally attributed to isotopic fractionation in the course of remineralization of POM (Montoya et al. 1992). The vertical profiles were similar between stations in- and outside the upwelling area during all sampled seasons (Fig. 3.3.3). The integrated values $\overline{\delta^{15}N_{PON_{0-\max.100m}}}$ for the upper water column to a maximum of 100 m showed no difference in the in-offshore distribution of the δ^{15}N values like the net-plankton (Fig. 3.3.4). Average values were 2.9 ‰ (± 0.5, n = 9) during SWM 2003, 2.8 ‰ (± 1.0, n = 24) during SpIM 2004, and 4.2 ‰ (± 0.8, n = 40) during SWM 2004. Average $\overline{\delta^{13}C_{POC_{0-\max.100m}}}$ values were -24.1 ‰ (± 0.3, n = 9) during SWM 2003, -23.5 ‰ (± 0.3, n = 24) during SpIM 2004, and -23.1 ‰ (± 0.8, n = 40) during SWM 2004, Fig. 3.3.5).

POM was in 81 % of all cases enriched over the nitrate isotopic signature by 2.1 ± 1.2 ‰ (n = 69) and only in 16 samples depleted by 1.7 ± 1.5 ‰ during SWM seasons. During SpIM season POM is less (65 % of all samples), enriched by 2.2 ± 1.4 ‰ (n = 30) compared to nitrate and in 16 cases depleted by 2.4 ± 1.9 ‰.

The δ^{15}N values in the six net-plankton size fractions generally increased from the smallest (55-166 µm) to the largest (> 2500 µm) size fraction (Fig. 3.3.4).
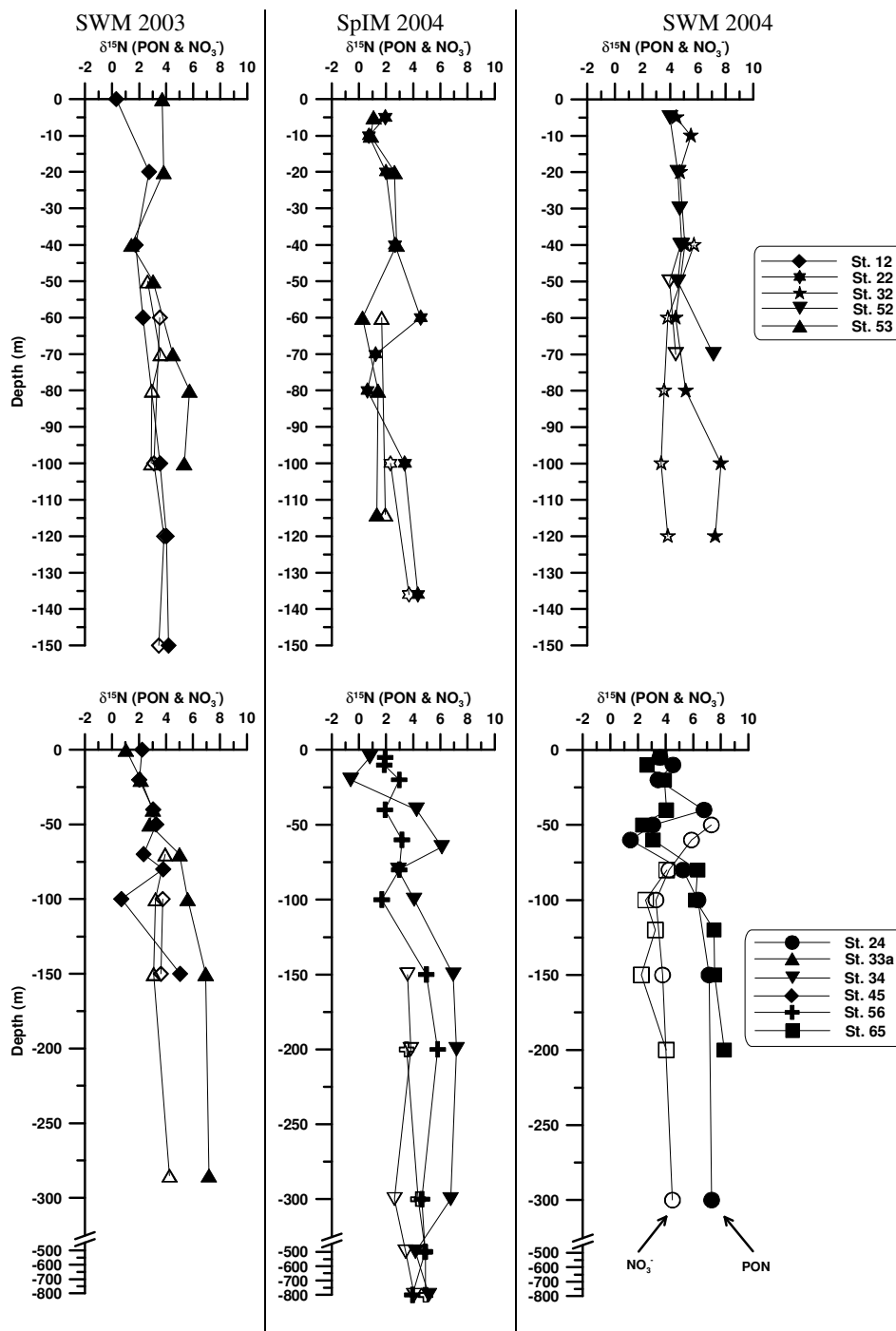
Fig. 3.3.3: $\delta^{15}N$ values of NO_3^- (open symbols) and PON (closed symbols) from inshore sites, shown on the upper panel, and offshore sites, shown on the lower panel including one northern and one southern station during southwest monsoon (SWM) and spring-inter monsoon (SpIM) seasons. Note the larger depth scales in the lower panels.

Lowest $\delta^{15}N$ values of 1.4 and 0.6 ‰ were found during SWM 2003 and 2004, respectively. Highest $\delta^{15}N$ values were also found during SWM seasons (8.0 and 7.8 ‰ in 2003 and 2004, respectively). During SpIM 2004 values ranged from 3.0 to 6.8 ‰ and no spatial differences were found between in- and offshore stations, the latter means > 40 km offshore (Fig. 3.3.4).
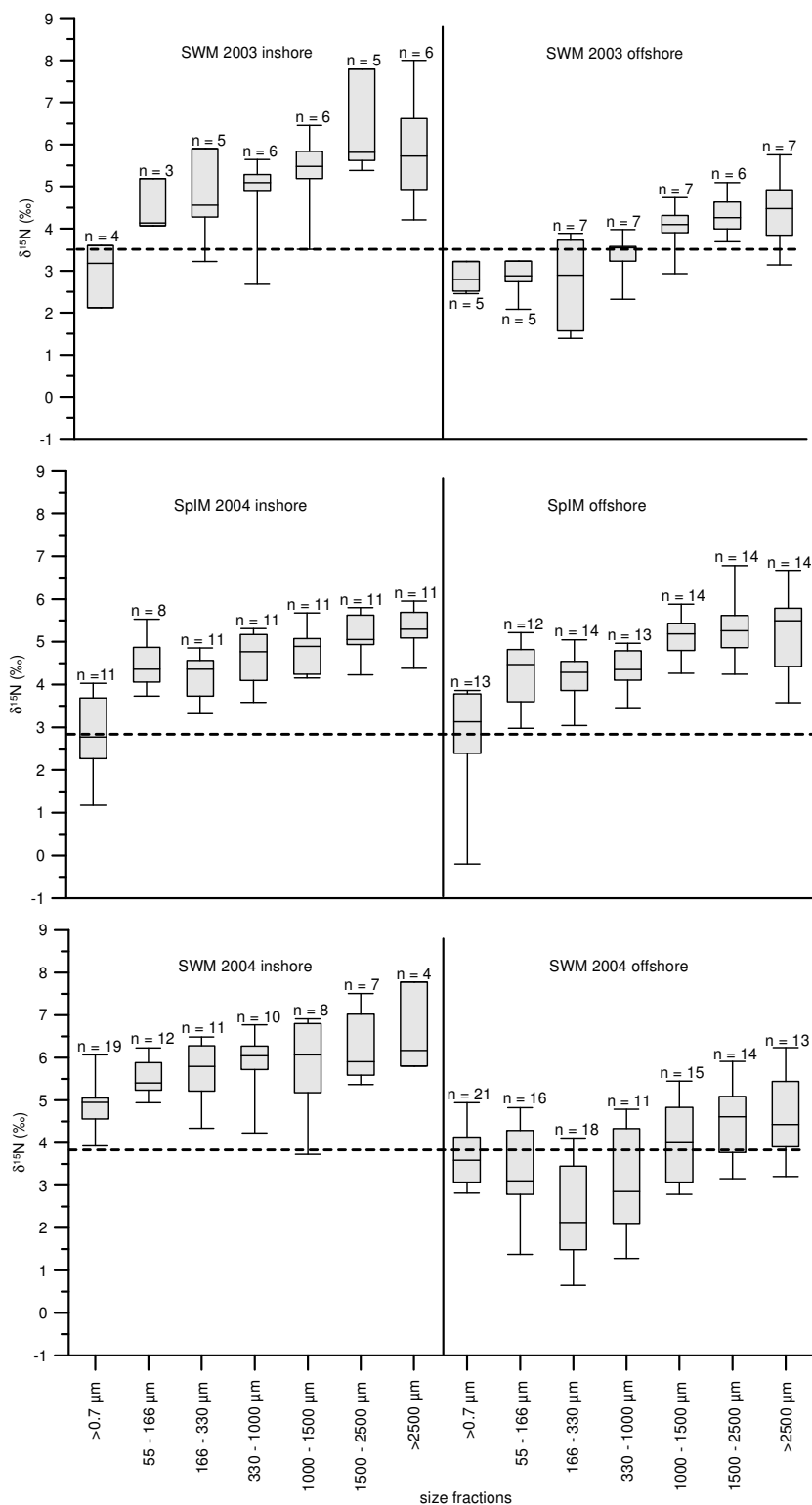
Fig. 3.3.4: $\delta^{15}N$ patterns of particulate organic matter (POM > 0.7 µm) and six net-plankton size fractions (55 - > 2500 µm) from the upper 100 m during (a) southwest monsoon 2003, (b) spring intermonsoon 2004, and (c) southwest monsoon 2004. The full lines separate inshore (< 42 km off the coast) and offshore (> 42 km off the coast) stations. Dashed lines give the integrated concentration weighed $\delta^{15}N$ value of subthermocline nitrate for each season. Note: Inshore during SWM seasons means within the upwelling area.

During monsoon season δ^{15}N values in all net-plankton size fractions were in average 1.6 ‰ (SWM 2003) and 2.3 ‰ (SWM 2004) depleted outside compared to inside the upwelling area.
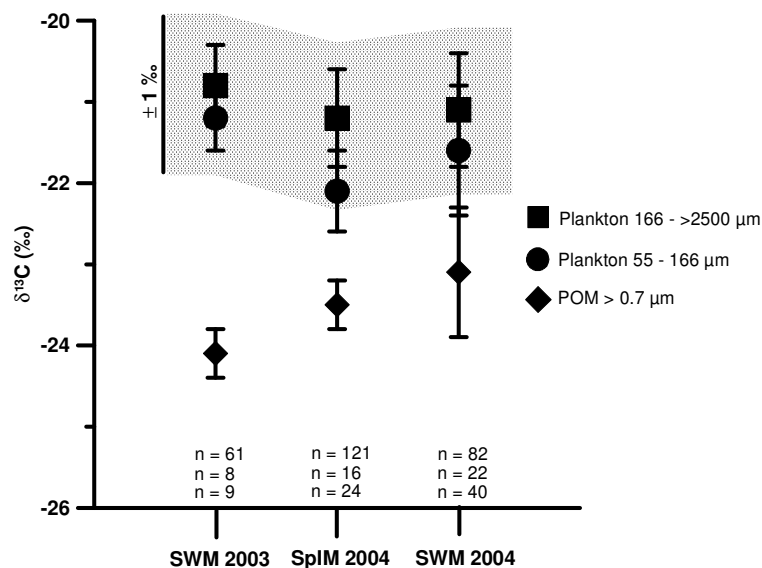
Fig. 3.3.5: Average δ^{13}C values of POM, net-plankton size fraction 55-166 µm, and net-plankton size fraction 166 - >2500 µm. Number of samples are given above the x-axis for each respective season and plankton size fraction for size fraction 166 - >2500 µm (top), size fraction 55-166 µm (middle), and POM (bottom). Dotted area indicates the ± 1 ‰ interval for potential food source of plankton in size fractions 166 - >2500 µm according to Peterson and Fry (1987).

The δ^{13}C values in the six net-plankton size fractions were statistically not different and had mean values of -20.9 (± 0.5, n = 69, SWM 2003), -21.3 (± 0.6, n = 137, SpIM 2004), and -21.2 (± 0.8, n = 104, SWM 2004, Fig. 3.3.5).

3.3.3. Discussion

Differences between POM and net-plankton

Stable carbon isotope data in POM of -23.3 ‰ (± 0.7, n = 73) were significantly depleted compared to δ^{13}C values of -21.2 ‰ (± 0.7, n = 315) in net-plankton (Fig. 3.3.5). This suggests that POM was dominated by a plankton community, which is different from the plankton caught by the net-hauls. The only study that systematically analyzed δ^{13}C values in plankton size classes covering the size range of pico-, nano-, micro- and mesoplankton was published by Rau et al. (1990). The terminology pico-(0.2-2 µm), nano-(2-20 µm), micro-(20-200 µm) and mesoplankton (200-2000 µm) was chosen according to Sieburth (1979). Rau et al. (1990) fractionated 140 l of seawater from the Mediterranean Sea into < 3µm, 3-8 µm, 8-20 µm, 20-150 µm, and > 150 µm size fractions during four seasons. Their results showed

that $\delta^{13}C$ in these size fractions increased with size from -24.6 ‰ ($\pm$ 0.7, < 3µm) to -23.3 ‰ ($\pm$ 0.1, 3-8 µm), to -21.6 ‰ ($\pm$ 0.8, 8-20 µm), to -20.5 ‰ ($\pm$ 0.8, 20-150 µm), and to -21 ‰ ($\pm$ 0.1, > 150 µm). The size classes included different species, e.g. the 8 to 20 µm fraction was dominated by diatoms, naked oligotrichous ciliates, dinoflagellates, and tintinids, which were absent in the 3 to 8 µm fraction, and size fraction < 3 µm was dominated by nanoflagellates. Rau et al. (1990) proposed that the activity of different phytoplankton species could cause isotopic differences in the size classes. If we compare our results to those from Rau et al. (1990), $\delta^{13}C$ values in our POM samples are similar to the $\delta^{13}C$ values of pico- and nanoplankton covering a size range of < 3 to 20 µm from the Mediterranean Sea. In contrast $\delta^{13}C$ values from our net-plankton are more similar to the micro-and mesoplankton values from Rau et al. (1990) that covered a size range of 20 to > 150 µm. This may indicate a dominance of small nano- and picoplankton on our POM filters even though the sampling strategy for POM collection ensures the quantitative sampling of plankton up to a size of 200 µm (Bé 1968). Opposed to that, net-plankton may have been dominated by micro-and mesoplankton. Carbon cycling in marine planktonic food webs is generally separated in two different pathways, the microbial and the herbivore pathway (Legendre and Le Févre 1991, Pesant et al. 2000). The difference in $\delta^{13}C$ of 2 to 3 ‰ between POM and net-plankton (Fig. 3.3.5) indicate that nano-and picoplankton may have been too small to be eaten by zooplankton of 166 to > 2500µm. Size fraction 55-166 µm probably was dominated by phytoplankton, which is suggested by an average C:N ratio of 7.4 ($\pm$ 0.8, n = 44) and microscopic inspection on board. Typically diatoms like *Rhizosolenia* spp., *Chaetoceros* spp., *Coscinodiscus* spp., *Thalassiosira* spp., *Thalasionema* spp., *Hemiaulus* spp., *Pseudonizschia* spp. or *Stephanopyxis* spp., cyanobacteria like *Trichodesmium* spp., and dinoflagellates like *Protoperidinium* spp., *Ceratium* spp., *Amphisolenia* spp., or *Pyrocystis* spp. were found in this size fraction. $\delta^{13}C$ values in this size fraction generally differed by less than 1 ‰ from the other size fractions, indicating a close trophic interaction between them (Fig. 3.3.5). The results from the $\delta^{13}C$ analysis imply a decoupling of the plankton community caught on the filters and in the net hauls. The exchange between both communities is limited. This interpretation is in consensus with observed co-existences of pico-and nanoplankton populations and larger-sized phytoplankton supporting micro- and mesozooplankton populations in the oceans as reviewed by Kiørboe (1993).

$\delta^{15}N$-POM showed no seasonal or spatial trend as found in $\delta^{15}N$ of the net-plankton size fractions (Fig. 3.3.4). That means the factors controlling the $\delta^{15}N$ patterns in net-plankton may not apply for the $\delta^{15}N$ distribution in POM. Low $\delta^{15}N$ values of surface particles may be due

to N_2-fixation or ammonium recycling (Sigman and Casciotti 2001). In order to separate both processes we think it is important to consider the phytoplankton size. Regenerated ammonium is an important nitrogen source for phytoplankton; however, it may be restricted especially to the small nano-and picoplankton (Wafar et al. 2004). Larger phytoplankton cells are considered to be depending on alternative N sources, especially on nitrate when it is available in high concentrations, due to a strong diffusion limitation for ammonium (Stolte et al. 1994). Differences in $\delta^{15}N$ in POM compared to net-plankton, therefore, may be due to the utilization of recycled ammonium as preferred N source in nano- and picophytoplankton.

$\delta^{15}N$ patterns in net-plankton in relation to $\delta^{15}N$ in nitrate

The waters off Vietnam can be divided into a coastal near upwelling area and a riverine-influenced offshore area during southwest monsoon seasons (SWM, Fig. 3.3.1). No such division of the system is apparent during spring intermonsoon (SpIM), when neither upwelling nor low salinity waters were detectable. Upwelling occurred within a 40 - 50 km wide band off Vietnam, in the following termed inshore, along the coast off southern central Vietnam, where the nutricline was found in approximately 20 m depth (Fig. 3.3.2). Outside the upwelling area, in the following termed offshore, a deeper nutricline at 40 to 60 m prevailed. Net-plankton outside the upwelling area generally was depleted in $\delta^{15}N$ by ca 2 ‰ compared to size fractions in the upwelling region during southwest monsoon (Fig. 3.3.4). No such offset was found during spring intermonsoon season (SpIM) 2004. This indicates that net-plankton utilized two different nitrogen sources during SWM, whereas during SpIM possibly only a single nitrogen source contributed to planktonic nitrogen.

   The phytoplankton food source is generally assumed to reflect the isotope value of the nitrate consumed. We found no spatially significant differences in $\delta^{15}N$ of nitrate$_{sub}$ between in- and offshore stations (Fig. 5.3). The mean $\delta^{15}N$ nitrate$_{sub}$ was 3.5 ± 0.3 ‰ (SWM 2003), 2.9 ± 0.9 ‰ (SpIM 2004), and 3.7 ± 0.6 ‰ (SWM 2004) from the three cruises. We assume they reflect the $\delta^{15}N$ value of nitrate from the source of upwelling in ca. 125 m depth (Vo 1997). Net-plankton caught during SpIM 2004 and within the upwelling area during SWM 2003 and 2004 had higher $\delta^{15}N$ values than the respective nitrate$_{sub}$ (Fig. 3.3.4). Outside the upwelling area only larger size fractions > 1000 µm had higher $\delta^{15}N$ values than nitrate$_{sub}$, whereas smaller net-plankton was depleted. This implies that plankton with $\delta^{15}N$ values below the $\delta^{15}N$-nitrate$_{sub}$ utilize a light nitrogen source. The only possible nitrogen source with $\delta^{15}N$ lower than nitrate$_{sub}$ is nitrogen from nitrogen fixation. Congruent nitrogen fixation patterns by Voss et al. (2006) strongly support this conclusion.

Current view is, that nitrogen from nitrogen fixation is passed on to diatoms, dinoflagellates, and their grazers via ammonium from decomposed cyanobacteria, dissolved organic nitrogen (DON) exudates, or in some cases direct grazing (Sellner 1997). Voss et al. (2006) determined the nitrogen fixation rates from bulk seawater of the same samples filtered for $\delta^{13}C$ analysis in POM in this study. It is not clear in what form nitrogen from nitrogen fixation was transferred into the herbivore food chain, but the significant differences in $\delta^{13}C$ between POM and net-plankton rule out a direct consumption of cyanobacteria.

Utilization of nitrate$_{sub}$ leads to $\delta^{15}N$ values of the assimilating organism, e.g. diatoms, that may be up to 12 ‰ enriched than the source nitrate (Needoba et al. 2003, Altabet 1996). Important factors affecting isotope fractionation in phytoplankton are species composition, swimming abilities, light regime and the assimilatory activity of nitrate reductase (Granger et al. 2004, Needoba and Harrison 2004). $\delta^{15}N$-net-plankton values higher than the nitrate$_{sub}$ therefore possibly reflect the fractionation effect during nitrate uptake.

We generally observed an increase in $\delta^{15}N$ with plankton size (Fig. 3.3.4). Enrichments in $\delta^{15}N$ with increasing plankton size are attributed to trophic fractionation effects (Rolff 2000, Fry and Quinones 1992). However, the observed increases in $\delta^{15}N$ between the consecutive size fractions of average 0.2 ‰ (± 0.6, n = 263) were much smaller than the reported 2 to 3.5 ‰ increase between consumer and diet (Peterson and Fry 1987). One reason may be the insufficient resolution of trophic levels and the overlap within one size fraction. Furthermore $\delta^{15}N$ in bulk plankton may be altered by a variety of factors such as species composition (Montoya et al. 1992), food quality or quantity (Adams and Sterner 2000), nitrogen turnover (Montoya et al. 1991), or amino acid composition (McClelland and Montoya 2002). For example, the salp *Salpa aspera* can feed effectively on a broad range of particle sizes since it uses a mucus net to filter suspended particles out of the sea water (Montoya et al. 1992). The copepod *Pareuchaeta norvegica* selectively feeds on copepods and other small zooplankton and has higher $\delta^{15}N$ values than the salp. The $\delta^{15}N$ in different zooplankton species therefore varies depending on their feeding habits (Montoya et al. 1992). Nutritional stress can cause increases in $\delta^{15}N$ of up to 0.4 ‰ in *Daphnia magna,* which are significantly correlated with the C:N ratio of the food (Adams and Sterner 2000). As the nitrogen content of the food source decreases from a C:N of 6 to 25, the corresponding $\delta^{15}N$ values of the daphnids feeding on the algae increased from 1 to 4 ‰ (Adams and Sterner 2000). However, we found no correlation between C:N ratios and $\delta^{15}N$ of the net-plankton samples.

The natural abundance of ^{15}N in various components of an ecosystem can change markedly on a time scale of days (Montoya et al. 1991). Differences in nitrogen turnover will

lead to different kinetics in the isotope responses of plankton species to changes in $\delta^{15}N$ of the food source (Montoya et al. 2002). E.g. the turnover time of *Acartia tonsa* was estimated to be 7.6 ± 0.6 days, whereas the ctenophore *Mnemiopsis leidyi* was assumed to have much slower turnover times according to less variable $\delta^{15}N$ values (Montoya et al. 1991). Furthermore $\delta^{15}N$ in bulk plankton may alter by variations in $\delta^{15}N$ of amino acids attributed to internal processing or variations in the acquired food source (McClelland and Montoya 2002). But although amino acids like glutamic acid, alanine, aspartic acid, isoleucine, leucine, proline, and valine are up to 7 ‰ enriched in the consumer compared to the diet they always seem to reflect the trophic increase in bulk $\delta^{15}N$ (McClelland and Montoya 2002). Despite these factors only trophic fractionation can cause the general increase in $\delta^{15}N$ with size and is confirmed by other studies (e.g. Montoya et al. 2002, Fry and Quinones 1992).

Simple two source mixing model

Based on the assumption that size fraction 55-166 µm was dominated by phytoplankton, the median $\delta^{15}N$ values in this size fraction from stations outside the upwelling area (2.9 and 3.1 ‰ for SWM 2003 and 2004, respectively) may be a mixture of nitrate in the source upwelling water ($\delta^{15}N$=3.5 ± 0.3 and 3.7 ± 0.6 ‰ for SWM 2003 and 2004, respectively) and that regenerated from nitrogen fixers (-1 ‰, Montoya et al. 2002). According to the rule of proportion the $\delta^{15}N$ in phytoplankton is composed of 13 % nitrogen from N_2-fixation and 87 % subthermocline nitrate. The contribution from N_2-fixation is much less than in the oligotrophic North Atlantic, where N_2-fixation was estimated to contribute in average 51 % to the organic N in particles in the upper 100 m and in average between 30 to 40 % to the organic N in zooplankton size fractions of 250-500, 500-1000, 1000-2000, and 2000-4000 µm (Montoya et al. 2002). However our estimation is four times more the contribution estimated by Voss et al. (2006) based on concomitant rate measurements. According to their findings N_2-fixation contributed 4.1 ± 3.1 % and 1.5 ± 1.5 % of N demand. The rather large contribution may indicate the accumulative effect of regenerated N from nitrogen fixers in larger phytoplankton with slow nitrogen turnover times.

The $\delta^{15}N$ value of the subthermocline nitrate itself is the result of mixing between the two new nitrogen sources N_2 and deep nitrate. The theoretical $\delta^{15}N$ value of deep nitrate is 4.5 ‰, the $\delta^{15}N$ of N_2 is 0 ‰. According to the rule of proportion the $\delta^{15}N$ in subthermocline nitrate is composed to 14 to 29 % of nitrogen from N_2-fixation and to 86 to 71 % of deep nitrate. Our estimation is in the range of the contribution of nitrogen from nitrogen fixation in the

Kuroshio Water (20 ± 9 %) and in the North Atlantic Ocean (25 %) according to Liu et al. (1996).

3.3.4. Conclusion

The dominance of different phytoplankton species in POM and the net-plankton seemed to be a most important factor determining stable carbon and nitrogen distribution in the planktonic food web off southern central Vietnam. Based on significant differences in $\delta^{13}C$ values between POM and net-plankton we assumed that POM was dominated by nano-and picoplankton as opposed to micro-and mesoplankton in the net-plankton. The carbon transfer between both communities seemed to be limited. $\delta^{15}N$-net-plankton values above the nitrate_{sub} values indicate a preferential use of nitrate as nitrogen source in the upwelling area and during SpIM. The depletion of $\delta^{15}N$ values of net-plankton outside compared to inside the upwelling area indicated the additional utilization of nitrogen from nitrogen fixation. Concomitant findings of high N_2-fixation rates by Voss et al. (2006) and $\delta^{15}N$ of the presumed primary producers below the $\delta^{15}N$ values of nitrate_{sub} strongly support this conclusion. We estimated that nitrogen fixation accounted between 14 to 29 % of nitrate_{sub} and 13 % of the N-demand in microphytoplankton.

3.4 Nitrogen Stable Isotopes in Amino Acids of Different Plankton Size Fractions from the South China Sea

The results presented in this chapter are part of the manuscript "Nitrogen Stable Isotopes in Amino Acids of Different Plankton Size Fractions from the South China Sea" by N. Loick, M. Gehre, and M. Voss. This manuscript is in preparation for Ecology. My share in this manuscript constitutes 90 % and includes the plankton sampling on board and the isotope analysis of bulk plankton and amino acids in the lab, the discussion of the results, as well as the writing of the manuscript.

3.4.1 Introduction

Nitrogen limitation in natural marine zooplankton assemblages is difficult to detect. Whereas deflections from the Redfield ratio of nitrogen and phosphate in seawater (N:P ratios < 16) are often used to indicate potential phytoplankton N-deficiency (Beardall et al. 2001), C:N ratios have often been used to determine and model nitrogen limitation in zooplankton (Kuijpers 2004, Pertola et al. 2002). Several laboratory studies as well as models support this theory (Pertola et al. 2002, Anderson 1992). Marine zooplankton generally has C:N ratios between 3 and 6 (Le Fèvre-Lehoerff et al. 1993), because their C:N requirements for growth exceed those available in food, e.g. phytoplankton that may have C:N ratios between 6.6 to 8 (Landry 1993). The relatively stable C: N elemental ratio in zooplankton, therefore, may be used as a proxy to identify nitrogen limitation in secondary production under low food conditions. N content is a mix of proteins, DNA, RNA, free amino acids, and others. The analysis of individual N-containing compounds are likely to better reflect the nitrogen status of an organism under changing nutritional conditions as shown for the protein content and free amino acids in copepods (Helland et al. 2000, 2003; Guisande et al. 1999, 2000). Under favourable feeding conditions copepods selectively feed on algae and reflect their distinct amino acid patterns (Guisande et al. 2002). In response to starvation, the protein content of *Calanus finmarchicus* females decreased after 10 days due to the sequential catabolism of endogenous nutrients during starvation from 65 µg protein per female to 10 µg protein per female (Helland et al. 2003).

Primary production in the upwelling area off southern central Vietnam can be nitrogen limited during times of weak upwelling according to N:P ratios < 16 (Pham et al. 2002, Dippner et al. subm.). Upwelling regularly fertilizes a 40 to 50 km wide strip along the coast off southern central Vietnam during summer monsoon (Hu et al. 2001, Dippner et al. subm.). During southwest monsoon (SWM) 2003 and 2004 chlorophyll *a* distribution clearly reflected

the division of the system into coastal near upwelling and offshore non-upwelling sites. Whereas subthermocline nitrate was the principle N source for primary production along the coast, nitrogen from N_2- fixation were higher at offshore sites and may have contributed up to 13 % of the N-demand in phytoplankton (Voss et al. 2006, Loick et al. 2006). The utilization of different nitrogen sources was also reflected by significant decreases in bulk $\delta^{15}N$ values of small net-plankton size fractions of ca. 1.7 ‰ (Loick et al. 2006). Here we show stable nitrogen isotope ratios in seven amino acids of six plankton size fraction and discuss the differences we found in their signatures from upwelling influenced sites compared to those from non-upwelling stations.

3.4.2 Results

The results of this chapter are based on the material and methods described in detail in chapter 2.5.

Hydrography

Stations 33a, 33 and 65 were in the vicinity of Mekong-influenced waters with surface salinities < 33.2 (Fig. 2.3 in chapter 2.5).
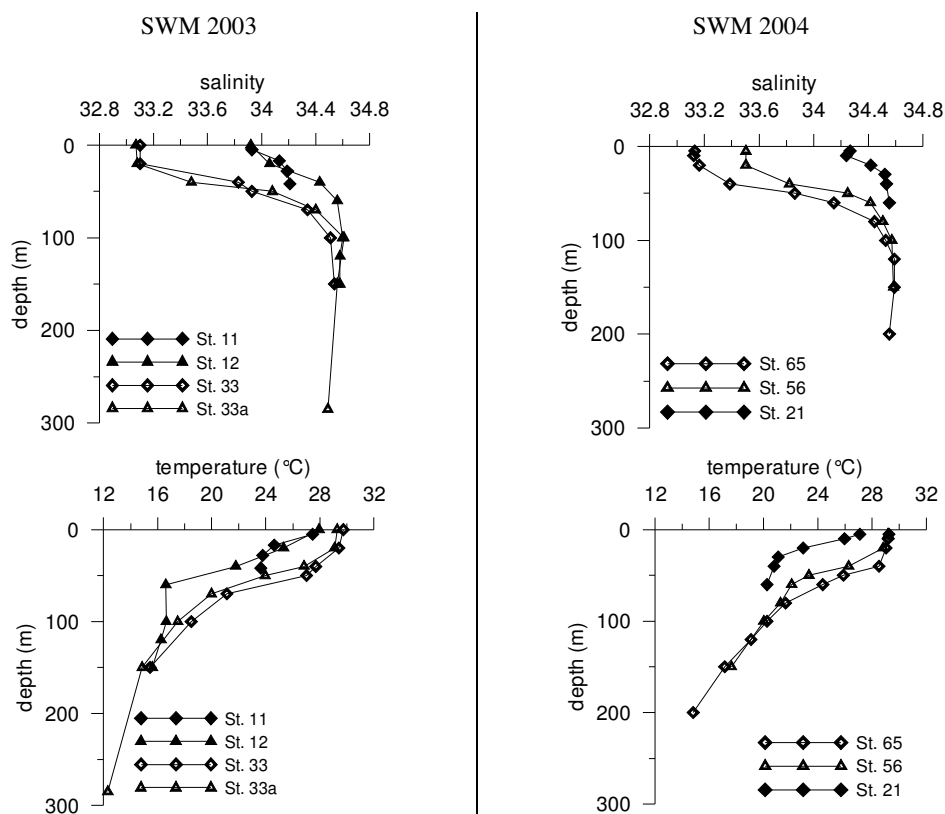
Fig. 3.4.1: Vertical salinity, temperature, nitrate, and chlorophyll *a* distributions at stations within (closed symbols) and outside (open symbols) the upwelling area during SWM 2003 (left panels) and SWM 2004 (right panels). Note the different chlorophyll *a* scales for 2003 and 2004 data. *Continued on the next page.*
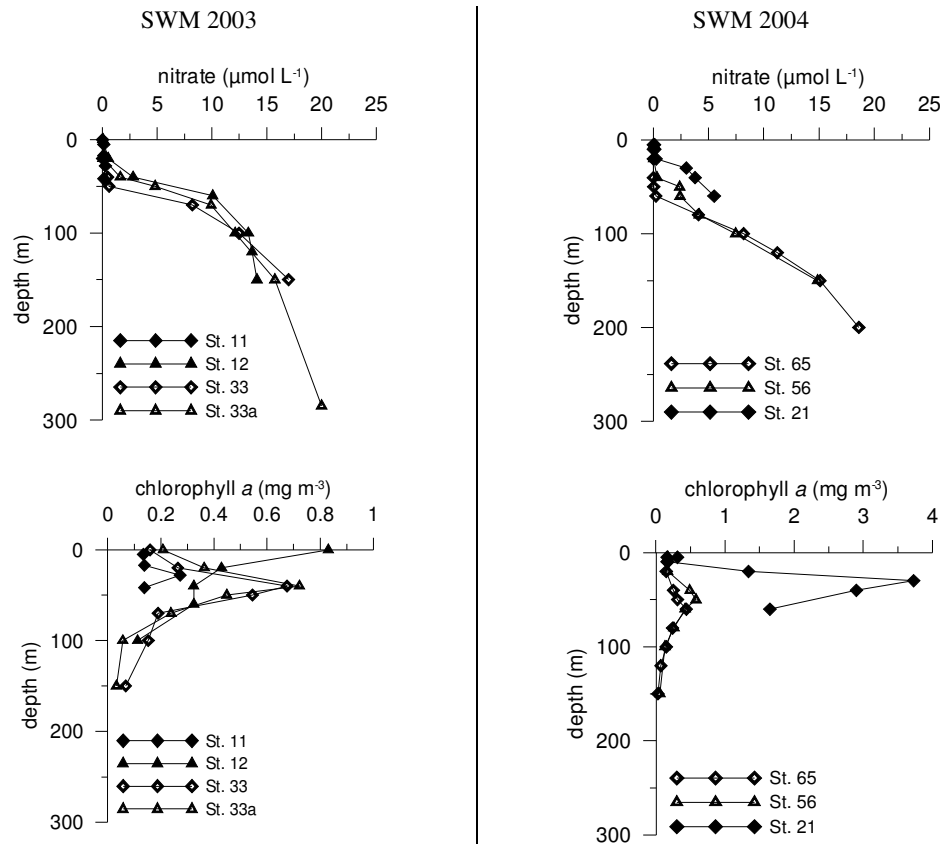
Fig. 3.4.1: *Continued from the previous page.*

The inshore stations 11, 12 and 21 had higher salinities of > 33.9 (St. 11 and 12) and > 34.2 (St. 21) and lower temperatures of < 28 °C in the upper 100 m compared to salinities > 33.0 (St. 33a and 33), > 33.5 (St. 56), > 33. 1 (St. 65) and temperatures < 29 °C at the offshore stations (Fig. 3.4.1). The nitrate concentrations were depleted in the upper 40 m, except for stations 12 and 21, where only the upper 20 m were depleted (Fig. 3.4.1). Below the nutricline nitrate concentrations generally increased to > 17 µmol l^{-1} below 150 m. Chlorophyll *a* profiles showed subthermocline maxima at 40 to 50 m depths. Only at station 12, a surface maximum was found. Although an in-offshore trend is less visible from the vertical Chl. *a* profiles, the depth normalized (to maximum 70 m depth) integrated Chl. *a* concentrations show higher values in the upwelling area with concentrations > 0.5 mg m^{-2} compared to offshore waters, thus reflecting the differences in productivity (Fig. 3.4.2). In July 2003 the maximum value of 0.8 mg Chl. *a* m^{-2} was much lower than the maximum value during 2004 of 2.1 mg Chl. *a* m^{-2}, indicating the weak upwelling intensity during 2003 as discussed in detail in chapter 3.1. Stations 11 and 12 had integrated Chl. *a* values of 0.5 mg m^{-3} compared to slightly lower values around 0.3 mg m^{-3} at stations 33a and 33 in July 2003. A stronger

difference between in- and offshore values was found in July 2004, when St. 21 had an integrated Chl. *a* value of 2.1 mg m^{-2} compared to < 0.4 mg m^{-2} at stations 56 and 65.
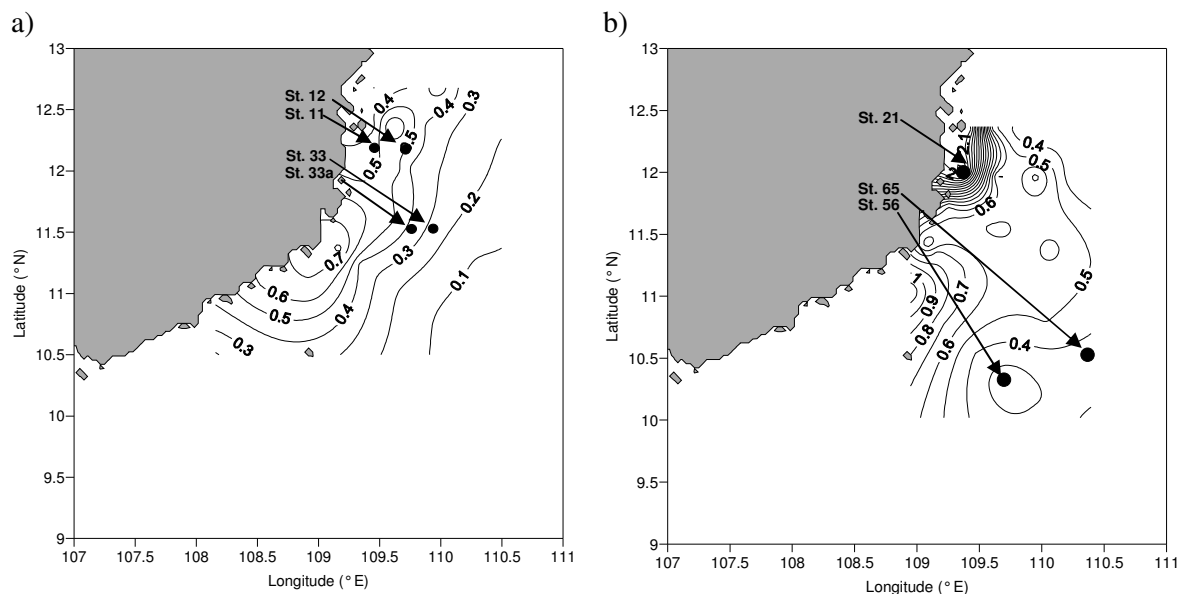
Fig. 3.4.2: Normalized depths integrated chlorophyll *a* values over the upper 70 m of the water column from (a) SWM 2003 and (b) SWM 2004. The black dots mark the position of the sampling stations for the amino acid analysis. Contour interval = 0.1 mg m^{-3}.

$\delta^{15}N$ in Plankton

Bulk $\delta^{15}N$ values generally increased logarithmically with plankton size (Fig. 2.4 in chapter 2.5). Plankton from upwelling influenced sites was 1.7 to 3 ‰ enriched compared to plankton from outside the upwelling area during both years. In July 2004 $\delta^{15}N$ values of the three smallest size fractions (55-166 µm, 330-1000 µm, 1000-1500 µm) from the offshore sites were 2 ‰ lower than in July 2003, whereas the $\delta^{15}N$ values from inside the upwelling area were rather similar between 4.5 to 6 ‰.

$\delta^{15}N$ in the amino acids alanine, aspartic acid, glutamic acid, and leucine increased logarithmically with plankton size throughout the area (Fig. 3.4.3a to d). $\delta^{15}N$ in tyrosine only increased significantly in the upwelling area, whereas proline significantly increased only outside the upwelling area (Fig. 3.4.3f and g). In contrast to the other amino acids, $\delta^{15}N$ in glycine did not increase with plankton size (Fig. 3.4.3e). Although most of the seven amino acids increased with size like the bulk plankton $\delta^{15}N$, they did not reflect the lower $\delta^{15}N$ values outside the upwelling area as found in bulk $\delta^{15}N$. Only $\delta^{15}N$ in tyrosine followed this pattern and had $\delta^{15}N$ values that were 2 to 6 ‰ depleted outside compared to inside the upwelling area (Fig. 3.4.3f).

a) alanine

in: $p < 0.01$

off: $p < 0.05$
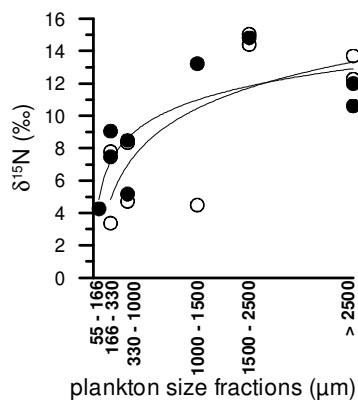
b) aspartic acid

in: $p < 0.01$

off: $p < 0.01$
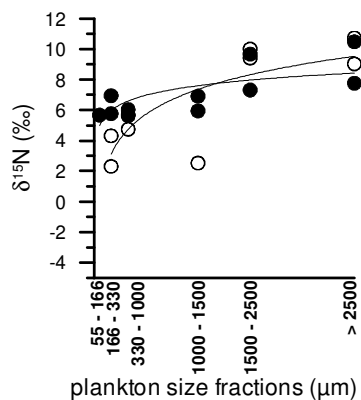
c) glutamic acid

in: $p < 0.01$

off: $p < 0.05$
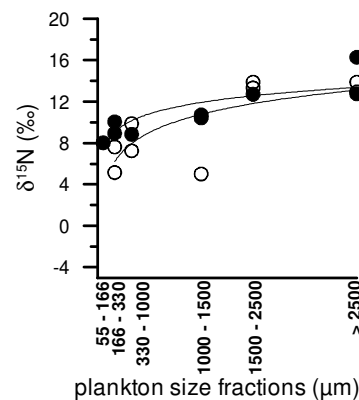
d) leucine

in: $p < 0.05$

off: $p < 0.01$
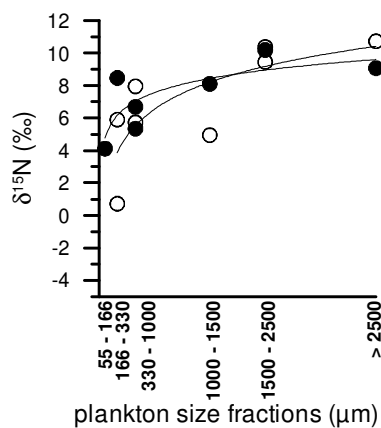
e) glycine

in: $p = ns$

off: $p = ns$
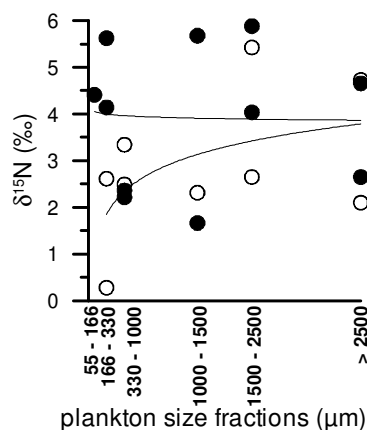
f) tyrosine

in: $p < 0.05$

off: $p = ns$
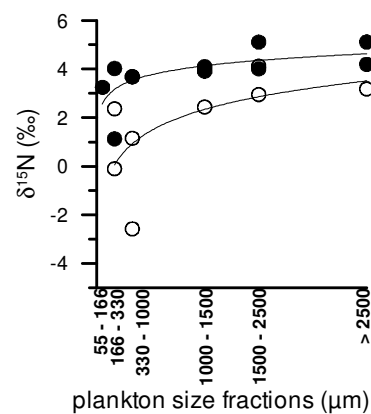
g) proline

in: $p = ns$

off: $p < 0.05$
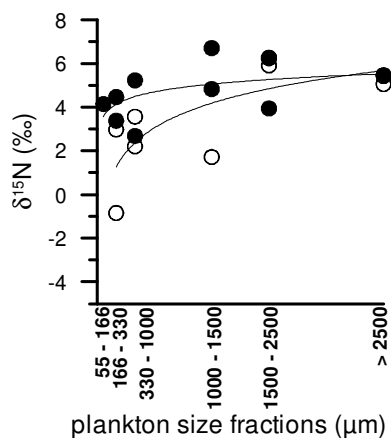
Fig. 3.4.3: $\delta^{15}N$ of different amino acids from six plankton size fractions covering a size range from 55 to > 2500 µm comprised from both SWM seasons. Black cycles (●) indicate samples from upwelling influenced stations, open cycles (O) from non-upwelling influenced stations. Black lines show natural logarithm-regression lines.

3.4.3   Discussion

δ^{15}N-amino acid ratios at in- and offshore sites

Our data suggest that secondary production of mesoplankton may have been N-limited outside compared to inside the upwelling area. The depth of the nutricline was 20 to 40 m deeper outside than inside the upwelling area (Fig. 3.4.1) and lower integrated Chl. *a* values point to less primary production offshore (Fig. 3.4.2). Furthermore increased N_2-fixation rates outside compared to inside the upwelling area point to enhanced cyanobacteria growth and reduced growth of other phytoplankton like diatoms at these sites. Only few zooplankton species directly feed on cyanobacteria (Sellner 1997) and reduced growth of e.g. diatoms may cause food and N-limitation in zooplankton at offshore sites. Contrary to expectations C:N ratios in zooplankton did not differ in- and outside the upwelling area (not shown), and no differences in the δ^{15}N values of the different amino acids in the six size fractions were found between in- and offshore sites (Fig. 3.4.3). However, we found striking differences between upwelling and non-upwelling sites when correlating the δ^{15}N of the essential amino acid leucine (leu) to the non-essential amino acids alanine (ala), aspartic acid (asp), glutamic acid (glu), glycine (gly), tyrosine (tyr), and proline (pro, Fig. 3.4.4, Tab. 3.4.1).
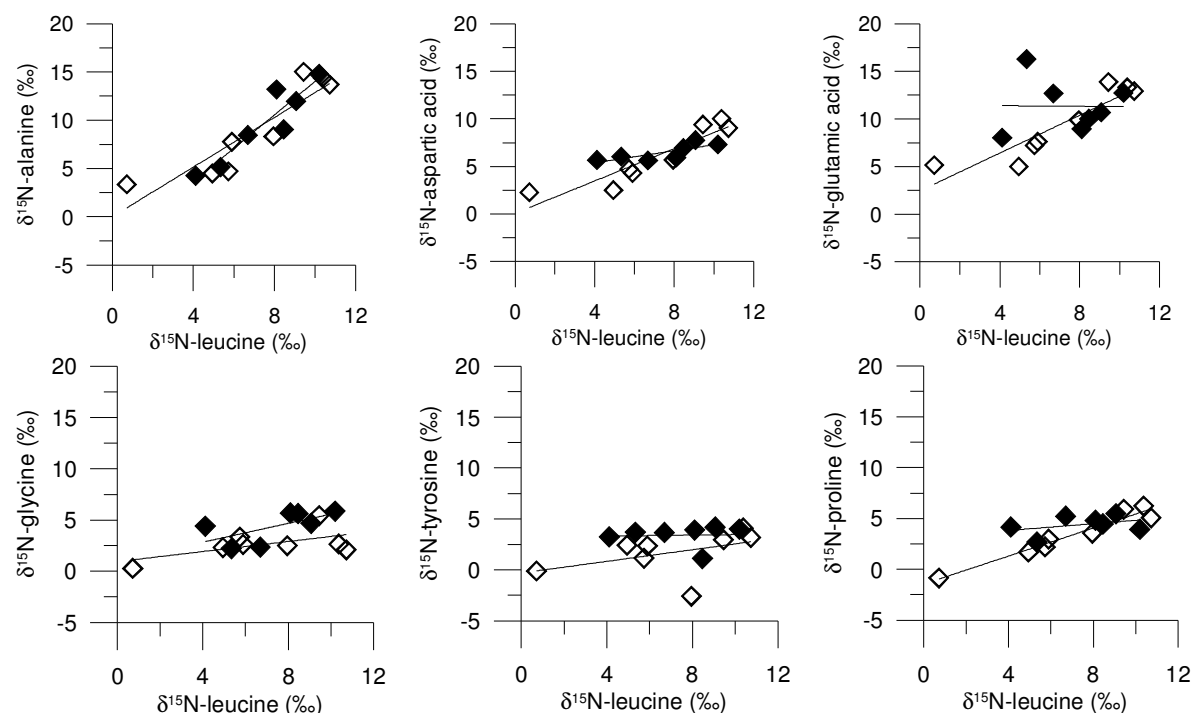
Fig. 3.4.4: Correlations of δ^{15}N of different amino acid from increasing plankton size fractions (55 to > 2500 µm) from stations inside (filled symbols) and outside (open symbols) the upwelling area from SWM 2003 and 2004. Data points are comprised from six different plankton size fractions from SWM 2003 and 2004. Black lines give the linear correlations of the different ratios. For details see Tab. 3.4.1.

Table 3.4.1: Regression equations (y) for linear correlations between the $\delta^{15}N$ ratios of six different non-essential amino acids and leucine from upwelling and non-upwelling sites. Degrees of freedom (d. f.) were chosen according to Bärlocher (1999). n = number of samples, r^2 = correlation coefficient, p = significance level; n.s. = not significant.

	amino acid	y	d.f. (= n-2)	r^2	p
inside the upwelling area	alanine	1.7x-3.3	6	0.8665	< 0.001
	aspartic acid	0.3x+4.1	6	0.6302	< 0.05
	glutamic acid	-0.01x+11.5	6	0.0001	n.s.
	glycine	0.5x+1	6	0.4045	n.s.
	tyrosine	0.02x+3.2	6	0.0024	n.s.
	proline	0.2x+3.2	6	0.1486	n.s.
outside the upwelling area	alanine	1.3x+0.004	5	0.815	< 0.01
	aspartic acid	0.8x+0.1	5	0.8421	< 0.01
	glutamic acid	1x+2.5	5	0.8337	< 0.01
	glycine	0.3x+0.9	5	0.3338	n.s.
	tyrosine	0.3x-0.3	5	0.1976	n.s.
	proline	0.7x-1.5	5	0.9418	< 0.01

The classification into essential and non-essential amino acids is according to Guillaume (1997). The $\delta^{15}N$ of ala, asp, glu, and pro were highly significantly correlated to the $\delta^{15}N$ of leu outside the upwelling area (Fig. 3.4.4, Table 3.4.1). In contrast no such correlations were found in the upwelling area, except for $\delta^{15}N_{leu}$: $\delta^{15}N_{ala}$ and $\delta^{15}N_{leu}$: $\delta^{15}N_{asp}$ (Fig. 3.4.4). The details of the regression lines are given in Table 3.4.1.

The only other data set, besides this one, on $\delta^{15}N$ in amino acids from plankton size fractions is from McClelland and Montoya (2002) who used a different amino acid derivatization method. Hofmann et al. (2003) showed that the two derivatization methods lead to $\delta^{15}N$ values that differ between 0.1 to 1.8 ‰ among amino acids. Therefore the comparison between data from this study to data from McClelland and Montoya (2002) has to be taken with some caution. McClelland and Montoya (2002) measured the $\delta^{15}N$ of amino acids in three plankton size fractions (250-500 µm, 500-1000 µm, 1000-2000 µm) at two stations (21, 30) from the tropical North Atlantic Ocean (NA). The hydrological conditions at the sampling sites in the tropical NA may have been different to our sampling sites. Nevertheless in conjunction with plankton nitrogen dynamics we think it is reasonable to compare the NA data to our data from the SCS, because in both areas N_2 and NO_3^- are the principal new nitrogen sources for primary production (McClelland et al. 2003, Loick et al. 2006). N_2 was a new N-source for primary production at NA station 30, whereas at the other station, N_2 was

no additional N-source and NO_3^- may have been the principal new N-source for primary production. Therefore station 30 may be comparable to our sampling site outside the upwelling area, whereas NA station 21 may be comparable to our sampling site inside the upwelling area.

In the following we correlate the $\delta^{15}N$ amino acid data from McClelland and Montoya (2002) in the same way as we did our SCS data. We therefore relate the $\delta^{15}N$ of leu to the $\delta^{15}N$ of ala, asp, glu, gly, tyr, and pro from NA station 21 plankton and compare these correlations to those generated from NA station 30 plankton. The results obtained are compared to the ratios found in our SCS data.

At NA station 30 positive correlations between the ratios of $\delta^{15}N_{leu}$ to the $\delta^{15}N$ of ala, asp, glu, tyr, and pro in the three plankton size fractions were found (Fig. 3.4.5). However NA correlations are statistically less significant due to only three data points (Tab. 3.4.2). In contrast no correlations were found between the $\delta^{15}N_{leu}$ and the $\delta^{15}N$ of ala, asp, glu, gly and tyr in plankton from NA station 21 (Fig. 3.4.5).
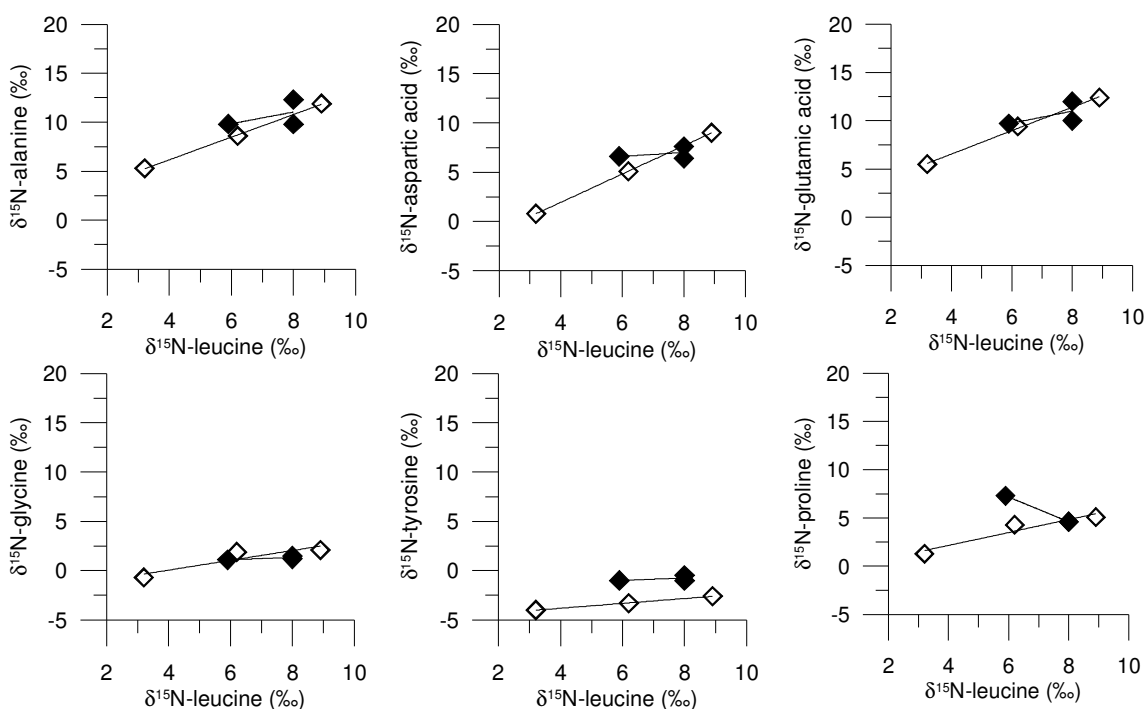
Fig. 3.4.5: Correlations of $\delta^{15}N$ of different amino acid from three plankton size fractions (250 to 2000 µm) from station 21 (closed symbols) and station 30 (open symbols) from the tropical North Atlantic from McClelland and Montoya 2002.

Remarkable similarities in the $\delta^{15}N_{leu}$ to $\delta^{15}N$ of the other tested amino acids can be found between our two sampling sites from the SCS and the two sampling stations from the NA (McCelland and Montoya 2002). Similar to the ratios outside the upwelling area in the SCS,

the δ^{15}N of ala, asp, glu and pro from NA station 30 were positively correlated to the δ^{15}N of leu and the δ^{15}N of gly was not correlated to the δ^{15}N of leu. In contrast thereto and similar to the ratios inside the upwelling area from the SCS, no correlations were found in plankton from NA station 21, except for $\delta^{15}N_{pro}$ that was negatively correlated with $\delta^{15}N_{leu}$.

Table 3.4.2: Regression equations (y) for linear correlations between the δ^{15}N ratios of six different non-essential amino acids and leucine from station 21 and 30 from the North Atlantic from McClelland and Montoya (2002). Degrees of freedom (d. f.) were chosen according to Bärlocher (1999). n = number of samples, r^2 = correlation coefficient, p = significance level; n.s. = not significant.

	amino acid	y	d.f. (= n-2)	r^2	p
Station 21	alanine	0.6x+6.3	1	0.25	n.s.
	aspartic acid	0.2x+5.5	1	0.129	n.s.
	glutamic acid	0.6x+6.1	1	0.3603	n.s.
	glycine	0.1x+0.4	1	0.4807	n.s.
	tyrosine	0.1x-1.7	1	0.25	n.s.
	proline	-1.3x+14.9	1	1	< 0.001
Statation 30	alanine	1.2x+1.5	1	0.9991	< 0.05
	aspartic acid	1.4x-3.8	1	0.9999	< 0.001
	glutamic acid	1.2x+1.7	1	0.9979	< 0.05
	glycine	0.5x-1.9	1	0.8268	n.s.
	tyrosine	0.2x-4.8	1	0.9991	< 0.05
	proline	-1.3x+14.9	1	0.9170	n.s.

Amino acids in zooplankton are taken up with the food and Guisande et al. (2002) showed that zooplankton reflects the amino acid composition of its food. Theoretically the δ^{15}N of a compound is determined by the discrimination against ^{15}N by the respective enzyme catalyzing the reaction which forms this compound (Fry in press). However, if the pool is exhausted, no discrimination will take place and the compound will reflect the δ^{15}N of the source pool (Fry in press). We suggest that the digestive enzymes are responsible for the linear correlations between the δ^{15}N in leu to the δ^{15}N of the ala, asp, glu and pro that were found at some sites of the SCS and NA and not at others. Mayzaud and Poulet (1978) and Hassett and Landry (1983) showed that ingestion rates of food and digestive enzyme activity was linearly related to ambient particle concentrations. Sabrowski and Buchholz (1999) compared the activity levels of the digestive enzymes chitinase, NAGase, protease, cellulose, and laminariase in the stomach and the midgut gland of krill under hunger, when fed with the non-chitinous green algae *Dunaliella bioculata* or with the chitinous diatom *Cyclotella cryptica*. They found that most enzymes were only weakly correlated and some negative

correlations also appeared. However, statistically significant correlations were found for protease in starved animals and animals fed with *D. bioculata*. Furthermore the correlation analysis between all stomach enzymes within one feeding condition showed, for starved animals, statistically significant relations of chitinase to NAGase, protease and cellulose. The other correlation coefficients for laminariase during hunger and for all analysed enzymes when fed with *D. bioculata* were comparatively high and always positive. In contrast in animals fed with *C. cryptica*, the correlation coefficients were lower and some negative correlations appeared. In the midgut gland only few statistically significant correlations were found as compared to the stomach. Sabrowski and Buchholz (1999) interpreted their findings with increased enzyme activities in the stomach when species starve for a longer period.

No correlations between the $\delta^{15}N_{leu}$ and the $\delta^{15}N$ of gly and tyr were found. This may be related to the comparatively complex synthesis of gly from serine and the hydroxylation of tyr from phenylalanine, an essential amino acid for crustaceans. Compared thereto the metabolism of the non-essential amino acids is closely related to each other with glutamic acid in addition to 2-oxoglutarate, pyruvate, oxalacetate as central compounds for synthesis of proline, alanine, and aspartic acid (Lehninger 1987).

Trophic fractionation effects on the $\delta^{15}N$ of the amino acids

The $\delta^{15}N$ of most amino acids increased significantly with plankton size at stations from in- and outside the upwelling area (Fig. 3.4.3). The increase in bulk $\delta^{15}N$ with plankton size can generally be attributed to the dominance of higher trophic level organism in larger plankton size fractions (Fry and Quinones 1992). Furthermore ^{15}N enrichment in daphnids was found to be strongly linearly related to the C:N of their diet *Scenedesmus acutus* (Adams and Sterner 2000). Increases in bulk $\delta^{15}N$ with size were reflected by significant increases $\delta^{15}N$ in the amino acid ala, asp, glu, and leu with size at all stations (Fig. 3.4.3 a to d). These same amino acids are fractionated by more than 3 ‰ during consumption (Tab. 3.4.1, McClelland and Montoya 2002).

Accordingly to the findings by McClelland and Montoya (2002) $\delta^{15}N$ in glycine did not increase with plankton size (Fig. 3.4.3e). Increases in the $\delta^{15}N$ values from food source to consumer have been attributed to fractionation during transamination and desamination so that ^{15}N excess appeared to be greatest in amino acids which are extensively involved in nitrogen transfer (Macko et al. 1987, Gannes et al. 1998). Little fractionation for glycine with increasing plankton size may indicate that the glycine pool in the organisms of the different size fractions remains rather unaltered. Different to the findings by McClelland and Montoya

(2002) δ^{15}N in tyrosine increased significantly with size at the inshore stations (Fig. 3.4.3f), whereas proline increased significantly with size only at the offshore stations (Fig. 3.4.3g). Animals synthesise tyrosine from the essential amino acid phenylalanine. According to McClelland and Montoya (2002) no fractionation occurs during phenylalanine consumption, whereas *B. plicatilis* was 0.9 ‰ depleted in δ^{15}N-tyr compared to *T. suecica* (Tab. 3.4.3).

Table 3.4.3: Fractionation factors for ^{15}N- in different amino acids associated with consumption of *Tetraselmis suecica* by *Brachionus plicatilis* (McClelland and Montoya 2002).

amino acid	ε	amino acid	ε
alanine	5 ‰	glycine	0.9 ‰
aspartic acid	4.5 ‰	tyrosine	-0.9 ‰
glutamic acid	6.7 ‰		
leucine	3.4 ‰		
proline	4.0 ‰		

Nevertheless, the increase in δ^{15}N generally by 2 ‰ in plankton ranging from 55 to > 2500µm in our samples is only 0.6 ‰ different from the increase by 1.4 ‰ from 250 to 2000 µm of field samples from the tropical North Atlantic. This indicates that different fractionation factors may exist for tyrosine uptake in the field compared to laboratory conditions.

Increases in δ^{15}N$_{pro}$ with size at the offshore stations may not only be due to trophic fractionation, but may also be due to internal catabolism. The δ^{15}N values of the different amino acids comprise free amino acid (FAA) as well as protein-bound amino acid stable nitrogen isotope data. According to Helland et al. (2003) the FAA pool in marine copepods amounts to 15 - 30 % of the proteinic amino acids content. Glycine, proline, and alanine belong to the few amino acids (besides taurine and ß-alanine) that are found to be without major inhibiting or activating effects on enzymatic activity and therefore can function as osmolytes in marine invertebrates (Yancey et al. 1982, Goolish and Burton 1989). Although the concentrations of proline, alanine and glycine in the FAA pool of our samples are not known, changes in their pool hold the potential to alter the δ^{15}N values in amino acids of plankton. Maybe they can also function as internal nitrogen store that is utilized when nitrogen becomes a limiting factor for an animal.

3.4.4   Conclusion

This is the first approach to correlate the δ^{15}N of an essential amino acid (leu) to six non-essential amino acids (ala, asp, glu, gly, tyr, pro) from different size fractions. We showed that there are spatial differences in these correlations between plankton from inside and

outside the upwelling area. Whereas outside the upwelling area four of the six amino acids correlated highly significantly ($p < 0.01$) with leu, this was the case for only one amino acid inside the upwelling area. A comparison with data from McClelland and Montoya (2002) indicates that these patterns are not random, but can be found in the NA as well. Supported by the similarities between the SCS and NA sites and physiological starvation studies we interpret the strong correlations of $\delta^{15}N_{leu}$ to $\delta^{15}N$ in ala, asp, glu, and pro at the offshore sites in the SCS as indication for food or N-limitation in zooplankton. In contrast no or weak correlations may indicate no or less food or N-limitation for zooplankton inside the upwelling area of the SCS.

In consensus with laboratory and field studies the increases in $\delta^{15}N$ in ala, asp, glu, and leu reflected the trophic enrichment in $\delta^{15}N$ with plankton size, whereas glycine was not fractionated. Furthermore deflections from the expected $\delta^{15}N$ distribution in pro and tyr indicate that besides trophic fractionation, other factors my influence the $\delta^{15}N$ amino acid distribution in natural plankton size fractions.

4.   Final Conclusions and Future Outlook

N_2-fixation has rarely been documented in upwelling areas in which traditionally N-supply for primary production is attributed to NO_3^- or NH_4^+ uptake. This may be the reason why only few studies address N_2-fixation in upwelling areas (Voss et al. 2004, Walsh 1996). The rate measurements in this work have proven that N_2-fixation also occurs near and in the centre of the Vietnamese upwelling area. It has been calculated that 13 % of primary production in the herbivore food web close to the upwelling area was supported by N from N_2-fixation (Fig. 4.1).
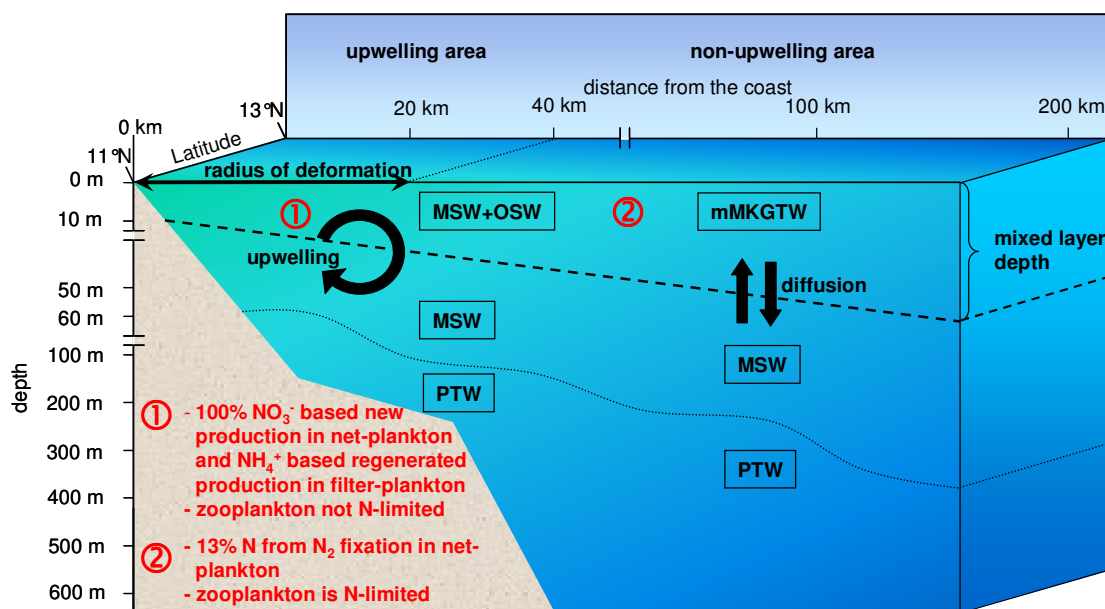
Fig. 4.1: Sketch summarizing the spatial distribution of the production regimes and the hydrological conditions during upwelling season off Vietnam. Upwelling of nutrient rich Maximum Salinity Water (MSW) principally occurs within a ca. 40 km wide stripe, the radius of deformation, along the coast off southern central Vietnam. Larger phytoplankton uses upwelled NO_3^- as principal N-source, whereas smaller nano- and picoplankton seem to primarily rely on NH_4^+ or other reduced N-species as N source. Further offshore Mekong Gulf of Thailand Water (MKGTW) leads to an additional deepening and stabilization of the thermocline. Here, larger phyto-plankton uses NO_3^- that diffuses into the euphotic zone from MSW into Open Sea Water (OSW) or MKGTW and cyanobacteria use N_2 as new nitrogen source. Zooplankton feeds on larger phytoplankton rather than on nano- and picoplankton at in and offshore sites. Nevertheless, nitrogen from N_2-fixation may have been transferred from the microbial into the herbivore food web and in higher trophic levels. During non-upwelling season NO_3^- appears to be the only new nitrogen source throughout the system.

The pool size of fixed nitrogen is one of the greatest unknown variables in recent global marine nitrogen budget (Brandes and Devol 2002). At the moment N_2-fixation rates account for maximum 110 Tg N yr^{-1} (Tg = 10^{12} g; Capone 2001, Gruber and Sarmiento 1997) implying that 170 Tg N yr^{-1} are missing to balance the denitrification sinks of 280 Tg N yr^{-1} (Brandes and Devol 2002). Serious underestimations of global N_2-fixation rates seem to be

the principal reason for the "missing" N to balance the budget (Brandes and Devol 2002). The stochastic nature of the cyanobacterial blooms and, until recently, a lack of pure cultures for physiological studies complicates the quantification of N_2-fixation (Karl et al. 2002). The North Atlantic is a well studied area in terms of N_2-fixation and Brandes and Devol (2002) re-estimated studies by Montoya et al. (2002), Sigman (1998), and Carpenter et al. (1999) that one sixth (16.6 %) of all nitrogen used by surface producers may be derived from nitrogen fixation. Capone et al. (2005) estimated – based on 154 stations in the tropical and subtropical North Atlantic - that *Trichodesmium* alone may account for 33.6 Tg N yr^{-1}. However, due to the paucity of data from other areas like the South Atlantic, South Pacific or South Indian Oceans the amount of global marine nitrogen fixation could not yet be assessed (Brandes and Devol 2002).

N_2-fixation rates in this study varied considerably during SWM and SpIM seasons. So far it is not clear why these differences between upwelling and non-upwelling seasons occur, although indications were found, that entering of MKGTW from the south into the investigation area may play an important role. It is also not clear, why the lowest contribution of N from N_2-fixation was determined during SpIM, a time when repeatedly mass occurrences of *Trichodesmium* spp. have been reported (Nguyen and Doan 1996).

According to Vitousek et al. (2002) the main controls of the rates of nitrogen transformation from N_2 to cyanobacterial N and to other primary producers include (a) ecophysiological factors like phosphate (PO_3^{4-}), iron (Fe), molybdenum (Mo), oxygen (O_2), light, or temperature and (b) ecological controls like the competition with other primary producers and grazing on growing cyanobacteria, that in case of heterocyst containing cyanobacteria may prevent the accumulation of enough photosynthetic cells to support the energetic requirements of N_2-fixation in heterocysts. The upwelling area is an excellent site for further field and simulated *in-situ* studies of the above mentioned factors because of the seemingly explicit off-on switch of N_2-fixation at times when MKGTW is deflected into the area.

In this study the first estimations of the amount of N_2-fixation for primary production and higher trophic levels from the southern part of the SCS were presented. This is up to now a "white spot" on the global map of N_2-fixation. Future research should aim to characterize the different groups of cyanobacteria that cause the spatial heterogeneity in N_2-fixation rates and explore mechanisms that could keep N fixers from responding to N deficiency in the ecosystem e.g. as found during SpIM. This could be done by mesocosm experiments of natural plankton communities in mixtures of OSW, MKGTW, MSW and Mekong Water.

Additionally, fertilization with PO_3^{4-}, Fe, or Mo may shade more light on the limiting factor of N_2-fixation off Vietnam.

Results of this thesis support the hypothesis of a tight coupling of nitrogen cycling between diazotrophs and other primary producers as suggested by Carpenter et al. (1999) and Villareal (1994) for other oceanic regions. It may be worthy to reconsider that "other primary producers" may belong to two different food webs, the microbial and the herbivore as reviewed by Kiørboe (1993). Whereas the carbon cycling in both food webs may proceed independently, the nitrogen cycling may be tightly coupled between them. E.g. $\delta^{15}N$ values of filter and net-plankton indicated that regenerated nitrogen plays an important role as intermediate for the transfer of nitrogen from nitrogen fixation into higher trophic levels, whereas $\delta^{13}C$ values in the different plankton size fractions indicated no direct consumption of smaller plankton by zooplankton of higher trophic levels. These interactions between the microbial and herbivore food web off Vietnam need more detailed characterization. This includes the identification of the dominant species and their spatial distribution in both communities and a systematic investigation on the fate of N_2 once it is fixed by microorganisms. The extent of interaction between both food webs, especially when N_2 is used as additional new N-source at offshore sites, may be an important determinant for the degree of nitrogen limitation in the herbivore food web. In that respect the symbioses between the cyanobacteria *Richelia* spp. and the diatoms *Hemiaulus* spp. and *Rhizosolenia* spp. may be important. Incubation experiments with ^{15}N-labeled NH_4^+ and ^{15}N-labeled DON together with predator-prey experiments could help to identify and quantify the role of regenerated nitrogen as intermediate between the microbial and herbivore food webs.

In this study it was hypothesized for the first time that the correlation of $\delta^{15}N_{leu}$ to the $\delta^{15}N$ of non-essential amino acids indicates N-limitation in zooplankton. This approach holds the potential to test whether intense N_2-fixation by cyanobacteria may reduce N-limitation in other plankton. However, prior to any application, this theory has to be verified. This could be done e.g. by starvation experiments with zooplankton in which the effect of N-limitation on the correlation of $\delta^{15}N_{leu}$ to other amino acids can be examined.

Besides natural controls, marine N-cycling may also be affected by anthropogenic perturbations. Since 1986 Vietnam became one of the fastest growing economies in the world, averaging around 8 percent annual gross domestic product (GDP) growth from 1990 to 1997 (FAO 2005). Aquaculture products are one of the most important export products of Vietnam and increased annually by 17.7 % between 1993 and 2003. Intensified aquaculture led to the

eutrophication of the bays and harmful algae blooms (HABS) e.g. of *Trichodesmium erythraeum* or *Noctiluca scintillans* (Larsen and Nguyen 2004). Future increases in eutrophication may even cause an expansion of these species from the bays into the upwelling area. A consequence could be massive fish and invertebrate kills that have been associated with toxic blooms of *N. scintillans* (Fonda Umani et al. 2004). Although the species does not produce toxins, it has been found to accumulate toxic levels of ammonia, which is then excreted into the surrounding waters, possibly acting as the killing agent in blooms (Okaichi and Nishio 1976, Montani et al. 1998 cf. Fonda Umani et al. 2004).

Future climate change will enhance frequencies of ENSO events and may lead to changes in precipitation in South East Asia (Christensen et al. 2001). ENSO events seem to have a major effect on N_2-fixation off Vietnam as indicated by lower N_2-fixation rates during post-ENSO SWM 2003 compared to 2004. We are just beginning to understand the current functioning of this ecosystem and are far from predicting future changes coming along with the above mentioned expectable environmental changes. The major goal of future work should be the incorporation of the physiological and ecological controls of N_2-fixation into regional and global ecosystem models, which would allow more realistic long term prediction of global environmental change (Vitousek et al. 2002).

5.   References

Adams, T.S., Sterner, R.W., 2000. The effect of dietary nitrogen content on trophic level ^{15}N enrichment. *Limnology and Oceanography* 45 (3): 601 – 607.

Altabet, M.A., Francois, R. 1994. Sedimentary nitrogen isotopic ratio records surface ocean NO_3 – utilization. *Global Biogeochemical Cycles* 8: 103 – 116.

Altabet, M.A., 1996. Isotopic fractionation during biochemical reactions. In: Ittekot, Schäfer, Honjo, Depetris (Eds.), Scope: Particle flux in the ocean. John Wiley and Sons Ltd, Chichester, pp. 156 – 183.

Anderson, T.R., 1992. Modelling the influence of food C: N ratio and respiration on growth and nitrogen excretion in marine zooplankton and bacteria. *Journal of Plankton Research* 14: 1645 – 1671.

Bärlocher, F., 1999. Biostatistik - Praktische Einführung in Konzepte und Methoden. Georg Thieme Verlag Stuttgart, New York. pp 206.

Bé, A., 1968. Measuring total plankton biomass. In: Zooplankton sampling, Monographs on oceanographic methodology 2. UNESCO, Imprimeries Populaires, Genève, p. 174.

Beardall, J., Young, E., Roberts, S., 2001. Approaches for determining phytoplankton nutrient limitation. *Aquatic Science* 63: 44 – 69.

Brandes, J. A., Devol, A. H., 2002. A global marine-fixed nitrogen isotopic budget: Implications for the Holocene nitrogen cycling. *Global Biochemical Cycles* 16 (4), 1120, doi: 10.1029/2001GB001856.

Brink, K.H., 1983. The near-surface dynamics of coastal upwelling. *Progress in Oceanography* 12: 223 – 257.

Broecker, W. S., Patzert, W. C., Toggweiler, J. R., Stuive, M., 1986. Hydrography, chemistry, and radioisotopes in the southeast Asian basins. *Journal of Geophysical Research* 91: 14345 – 14354.

Burns, B.D., Beardal J., 1987. Utilization of inorganic carbon by marine microalgae. *Journal of Experimental Marine Biology and Ecology* 107:75 – 86.

Capone, D.G., Farrier, M.D., Carpenter, E.J., 1994. Amino acid cycling in colonies of the planktonic marine cyanobacterium *Trichodesmium thiebautii*. *Applied Environmental Microbiology* 60:3989 – 3995.

Capone, D.G., Zehr, J.P., Paerl, H.W., Bergman, B., Carpenter, E.J.,1997. Trichodesmium: A globally significant marine cyanobacterium. *Science*. 276:1221 – 1229.

Capone, D.G., Subramaniam, A., Montoya, J.P., Voss,M., Humborg, C. Johansen, A., Siefert, R.L., Carpenter, E.J., 1998. An extensive bloom of the N_2 fixing cyanobacterium, *Trichodesmium erythraeum*, in the central Arabian Sea during the spring intermonsoon. *Marine Ecology Progress Series* 172: 281 – 292.

Capone, D. G., 2001. Marine nitrogen fixation: What´s the fuss? Current Opinion in Microbiology 4 (3): 341 – 348.

Capone, D.G., Burns, J.A.,Montoya, J.P.,Subramaniam, A., Mahaffey, C., Gundersoen, T., Michaels, A.F.,Carpenter, E.J., 2005. Nitrogen fixation by *Trichodesmium* spp.: An important source of new nitrogen to the tropical and subtropical North Atlantic Ocean. *Global Biogeochemical Cycles* 19: GB2024, doi:10.1029/2004GB002331.

Carpenter, E.J., Romans, K., 1991. Major role of the cyanobacterium Trichodesmium in nutrient cycling in the North Atlantic Ocean. *Science* 254: 1356 – 1358.

Carpenter, E. J., Harvey, H. R., Fry, B., Capone, D., 1997. Biogeochemical tracers of the marine cyanobacterium Trichodesmium. Deep-Sea Research I 44 (1): 27 – 38.

Carpenter, E.J., Montoya, J.P., Burns, J., Mulholland, M.R., Subramaniam, A., Capone, D.G., 1999. Extensive bloom of a N_2-fixing diatom/cyanobacterial association in the tropical Atlantic Ocean. *Marine Ecology Progress Series* 185: 273 – 283.

Chao, S.Y., Shaw, P.T., Wu, S.Y., 1996. El Nino modulation of the South China Sea circulation. *Progress in Oceanography* 38: 51 – 93.

Checkley, D.M.Jr., Miller, C.A., 1989. Nitrogen isotope fractionation by oceanic zooplankton. *Deep-Sea Research Part A (Oceanographic Research Papers)* 36 (10): 1449 – 1456.

Chen, Y.-L.L., Chen, H.Y., Lin, Y.H., 2003. Distribution and downward flux of Trichodesmium in the South China Sea as influenced by the transport from the Kuroshio Current. *Marine Ecology Progress Series* 259: 47 – 57.

Chen, Y.-L.L., Chen, H.Y., Karl, D.M., Takahashi, M., 2004. Nitrogen modulates phytoplankton growth in spring in the South China Sea. *Continental Shelf Research* 24 (4-5): 527 – 541.

Chen, C.T.A., Wang, S.L., Wang, B.J., Pai, S.C., 2001. Nutrient budgets for the South China Sea basin. *Marine Chemistry* 75 (4): 281 – 300.

Christensen, M. J., Hulme, M., Von Storch, H., Whetton, P., Jones, R., Fu, C., 2001. Regional climate information – Evaluation and Projections. In: Climate Change 2001, The Scientific Basis. Houghton J. T., Ding, Y., Griggs, D.J., Noguer, M., van der Linden, P. J., Dai, X., Maskell, K., Johnson, C. A. (Eds.). Contribution of Working group I to the third assessment report of the intergovernmental panel on climate change, pp. 583 – 639.

Cifuentes, L. A., Fogel, M. L., Pennock, J. R., Sharp, J. H., 1989. Biogeochemical factors that influence the stable nitrogen isotope ratio of dissolved ammonium in the Delaware Estuary. *Geochimica et Cosmochima Acta* 53: 2713 – 2721.

Conley, D.J., 1997. Riverine contribution of biogenic silica to the oceanic silica budget, *Limnology and Oceanography* 42: 774 – 777.

Cooper, T. G., Wood, H. G., 1971. The carboxylation of phosphoenolpyruvate and pyruvate. II. The active species of CO2 utilized by phosphoenolphyruvate carboxylase and pyruvate carboxylase. *Journal of Biological Chemistry* 246: 5488 – 5490.

Culberson, C.H., 1991. Dissolved Oxygen. WHP Operations and Methods WHP Office Report WHPO 91-1. WOCE Report No. 68/91. Woods Hole, Mass., USA.

Dale, W.L., 1956. Wind and drift current in the South China Sea. *Malayan Journal of Tropical Geography* 8: 1 – 31.

Deetae, S., Wisespongpand, P., 2001. Sub-thermocline Chlorophyll maximum in the South China Sea, area IV: Vietnamese waters. Proceedings of the SEAFDEC Seminar on Fisheries Resources in the South China Sea 4: Vietnamese Waters: 251 – 264.

Descolas-Gros,C., Fortugne, M. R., 1985. Carbon fixation in marine phytoplankton: carboxylase activities and stable carbon isotope ratios; physiological and paleoclima-tological aspects. *Marine Biology* 87: 1-6.

Descolas-Gros,C., Oriol, L., 1992. Variations in carboxylase activity in marine phytoplankton cultures. ß-carboxylation in carbon flux studies. *Marine Ecology Progress Series* 85: 163 – 169.

Dippner, J., Nguyen, K.V., Hein, H., Ohde, T., Loick, N., submitted 2006. Monsoon Induced Upwelling off the Vietnamese Coast. *Ocean Dynamics*.

Dugdale, R.C., Goering, J.J., 1967. Uptake of new and regenerated forms of nitrogen in primary productivity. *Limnology and Oceanography* 12: 196 – 206.

Falkowski, P. G., 1991. Species variability in the fractionation of ^{13}C and ^{12}C by marine phytoplankton. *Journal of Plankton Research* 13 (suppl.): 21 – 28.

Fang, W., Fang, G., Shi, P., Huang, Q., Xie, Q., 2002. Seasonal structure of upper layer circulation in the southern South China Sea from in situ observations. *Journal of Geophysical Research* 107 (C11), 3202, doi:1029/2002JC001343.

FAO, 2005a. Selected indicators of food and agriculture development in Asia-pacific Region 1994-2004. RAP Publication 20. (Available at www.fao.org/ documents/show_cdr.asp? url_file=/docrep/008/ae937e/ae937e00.htm)

Fonda Umani, S., Beran, A., Parlato, S., Virgilio, D., Zollet, T., De Olazabal, A., Lazzarini, B., Cabrini, M., 2004. *Noctiluca scintillans* MACARTNEY in the Northern Adriatic Sea : long-term dynamics, relationships with temperature and eutrophication, and role in the food web. *Journal of Plankton Research* 26 (5): 545 – 561.

Fry, B., Wainright, S. C., 1991. Diatom sources of ^{13}C-rich carbon in marine food webs. *Marine Ecology Progress Series* 76: 146 – 157.

Fry, B., Quinones, R.B., 1994. Biomass spectra and stable isotope indicators of trophic level in zooplankton of the Northwest Atlantic. *Marine Ecology Progress Series* 112 (1-2): 201 – 204.

Fry, B. in press. Stable Isotope Ecology. ISBN 0387305130.

Gannes, L. Z., Martinez del Rio, C., Koch, P., 1998. Natural abundance variations in stable isotopes and their potential uses in animal physiological ecology. *Comparative Biochemistry and Physiology* 119: 725 – 737.

Glibert, P.M., Bronk, D. A., 1994. Release of dissolved organic nitrogen by marine diazotrophic cyanobacteria, *Trichodesmium* spp. *Applied Environmental Microbiology* 60: 3996 – 4000.

Goericke, R., Fry, B., 1994. Variations of marine plankton ^{13}C with latitude, temperature, and dissolved CO_2 in the world ocean. *Global Biogeochemical Cycles* 8: 85 – 90.

Goericke, R., Montoya, J. P., Fry, B., 1994. Physiology of isotopic fractionation in algae and cyanobacteria. In: Methods in Ecology, Stable Isotopes in Ecology and Environmental Science. Lajtha, K., Michener, R. H. (Eds.). Blackwell Scientific Publications, Oxford, pp. 187 – 221.

Goering, J., Alexander, B., Haubenstock, N., 1990. Seasonal variability of stable carbon and nitrogen isotope ratios in organisms in a North Pacific Bay. *Estuarine, Coastal and Shelf Science* 30: 239 – 260.

Gong, G. C., Liu, K. K., Liu, C. T., Pai, S. C., 1992. The chemical hydrography of the South China Sea west of Luzon and a comparison with the west Philippine Sea. *Terrestrial, Atmospheric and Oceanic Sciences* 3: 587 – 602.

Goolish, E. M., Burton, R. S., 1989. Energetics of osmoregulation in an intertidal copepod: effects of anoxia and lipid reserves on the pattern of free amino acid accumulation. *Functional Ecology* 3: 81 – 89.

Granger, J., Sigman, D.M., Needoba, J.A., Harrison, P.J., 2004. Coupled nitrogen and oxygen isotope fractionation of nitrate during assimilation by cultures of marine phytoplankton. *Limnology and Oceanography* 49 (5): 1763 – 1773.

Grasshoff, K., Ehrhardt, M., Kremling, K., 1983. Methods of Seawater Analysis. Verlag Chemie, Weinheim, pp. 419.

Grasshoff K., Ehrhardt M., Kremling K., 1999. Methods of Seawater Analysis. Wiley-Verlag Chemie, Weinheim, pp. 600.

Gruber, N., Sarmiento, J. L., 1997. Global patterns of marine nitrogen fixation and denitrification. *Global Biogeochemical Cycles* 11 (2): 235 – 266.

Guillaume, J., 1997. Protein and amino acids. In: D'Abramo, L.R., Conklin, D.E., Akiyama, D.M. (Eds.). Crustacean Nutrition. Adv. World Aquaculture 6, Baton Rouge, LA, USA, pp. 26 – 50.

Guisande, C., Maneiro, I., Riveiro, I. 1999. Homeostasis in the essential amino acid composition of the marine copepod *Euterpina acutifrons*. *Limnology and Oceanography* 44 (3): 691 – 696.

Guisande, C., Riveiro, I., Maneiro, I., 2000. Comparisons among the amino acid composition of females, eggs and food to determine the relative importance of food quantity and food quality to copepod reproduction. *Marine Ecology Progress Series* 202: 135 – 142.

Guisande, C., Maneiro, I., Riveiro, I., Barreiro, A., Pazos, Y., 2002. Estimation of copepod trophic niche in the field using amino acids and marker pigments. *Marine Ecology Progress Series* 239: 147 – 156.

Guy,.R.D., Vandlerberghe, G.C., Turpin, D.H., 1989. Significance of phosphoenolpyruvate carboxylase during ammonium assimilation. *Plant Physiology* 89: 1150 – 1157.

Hagen, E., 2001. Northwest African upwelling scenario. *Oceanologica Acta* 24: 1-17.

Hansell, D.A., Bates, N.R., Olson, D.B., 2004. Excess nitrate and nitrogen fixation in the North Atlantic Ocean. *Marine Chemistry* 84: 243 – 265.

Hassett, R. P., Landry, M. R., 1983. Effects of food-level acclimation on digestive enzyme activities and feeding behaviour of Calanus pacificus. *Marine Biology* 75: 47 – 55.

Helland, S., Triantaphyllidis, Fyhn, H.J., Evjen, M.S., Lavens, P., Sorgeloos, P., 2000. Modulation of the free amino acid pool and protein content in populations of the brine shrimp *Artemia* spp. *Marine Biology* 137: 1005 – 1016.

Helland, S., Nejstgaard, J.C., Fyhn, H.J., Egge, J.K., Båmstedt, U., 2003. Effects of starvation, season, and diet on the free amino acid and protein content of *Calanus finmarchicus* females. *Marine Biology* 143 (2): 297 – 306.

Hellerman, S., Rosenstein, M., 1983. Normal monthly wind stress over the world ocean with error estimates. *Journal of Physical Oceanography* 13: 1093 – 1104.

Hoch, M. P., Fogel, M. L., Kirchman, D. L., 1992. Isotope fractionation associated with ammonium uptake by a marine bacterium. *Limnology and Oceanography* 37:1447 – 1459.

Hofmann, D., Gehre, M., Jung, K., 2003. Sample preparation techniques fort he determination of natural ^{15}N/ ^{14}N variations in amino acids by Gas Chromatography-Combustion-Isotope ratio mass spectrometry (GC-C-IRMS). *Isotopes in Environment and Health Studies* 39 (3): 233 – 244.

Horrigan, S. G., Montoya, J. P., Nevins, J. L., McCarthy, J.J., 1990. Natural isotopic composition of dissolved inorganic nitrogen in the Chesapeake Bay. *Estuarine, Coastal, and Shelf Science* 30: 393 – 410.

Hu, J., Hong, H., Qi, Y., 2000. A review on the currents in the South China Sea: Seasonal circulation, South China Sea Warm Current and Kuroshio Intrusion. *Journal of Oceanography* 56: 607 – 624.

Hu, J., Kawamura, H., Hong, H., Kobayashi, F., Wang, D., 2001. 3-6 months variation of sea surface height in the South China Sea and its adjacent ocean. *Journal of Oceanography* 57 (1): 69 – 78.

Huppe, H. C., Turpin, D.H., 1994. Effect of nitrogen limitation and resupply on the glucose 6-phosphate dehydrogenase from *Chlamydomonas reinhardtii*. *Plant Physiology* 108 (2): 127 – 127.

Hwang, C., Chen, S.A., 2000. Circulation and eddies over the South China Sea derived from TOPEX/Poseidon altimetry. *Journal of Geophysical Research* 105 (C3): 23943 – 23965.

Isobe, A., Namba, T., 2001. The circulation in the upper and intermediate layers of the South China Sea. *Journal of Oceanography* 57(1): 93 – 104.

Javelle, A., Merrick, M., 2005. Complex formation between AmtB and GlnK: an ancestral role in prokaryotic nitrogen control. *Biochemical Society Transactions* 33: 174 – 176.

Jeffrey, S.W., Humphrey, G.F., 1975. New spectrophotometric equation for determining chlorophyll a, b, c1 and c2. *Biochemie und Physiology der Pflanzen* 167: 194 – 204.

Jivaluk, J., 2001. Composition, abundance and distribution of zooplankton in the South China Sea, Area IV: Vietnamese waters. Proceedings of the SEAFDEC Seminar on Fisheries Resources in the South China Sea 4: Vietnamese Waters: 77 – 93.

John, H.C., Zelck, C., Erasmi, W., 2000. Poleward transport of equatorial fish larvae in the Atlantic Eastern boundary current system. *Archive of Fishery and Marine Research* 48: 61 – 88.

John, H.C., Mohrholz, V., Lutjeharms, J.R.E., Weeks, S., Cloete, R., Kreiner, A., daSilva Neto, A ., 2004. Oceanographiv and faunistic structures across an Angola Current intrusion into northern Nabmibian waters. *Journal of Marine Systems* 46: 1 – 22.

Karl, D., Letelier, R., Tupas, L., Dore, J., Christian, J., Hebel, D., 1997. The role of nitrogen fixation in biogeochemical cycling in the subtropical North Pacific Ocean. *Nature* 388 (6642): 533 – 538.

Karl, D., Michaels, A., Bergman, B., Capone, D., Carpenter, E., Letelier, R., Lipschultz, F., Pearl, H., Sigman, D., Stal, L., 2002. Dinitrogen fixation in the world´s ocean. *Biogeochemistry* 57/ 58: 47 – 98.

Kiørboe, T., 1993. Turbulence, phytoplankton cell size, and the structure of pelagic food webs. *Advances in Marine Biology* 29: 1 – 72.

Kohl, J.-G., Nicklisch, A., 1988. Ökophysiologie der Algen - Wachstum und Ressourcennutzung. Akademie-Verlag Berlin, pp. 253.

Körtzinger, A., 2003. A significant CO_2 sink in the tropical Atlantic Ocean associated with the Amazon River plume. *Geophysical Research Letters* 30 (24): 2287, doi:10.1029/ 2003GL018841.

Kronzucker, H.J., Britto, D.T., Davenport, R.J., Tester, M., 2001. Ammonium toxicity and the real cost of transport. *Trends in Plant Science* 6(8): 335 – 337.

Kroopnik, P.M., 1985. The distribution of $\delta^{13}C$ of CO_2 in the world oceans. *Deep-Sea Research* 32: 57 – 84.

Kuijper, L.D.J., Anderson, T.R., Kooijman, S.A.L.M., 2004. C and N gross growth efficiencies of copepod egg production studied using a dynamic energy budget model. *Journal of Plankton Research* 26 (2): 213 – 226.

Landry, M.R., 1993. Predicting excretion rates of microzooplankton from carbon metabolism and elemental ratios. *Limnology and Oceanography* 38 (2): 468 – 472.

Larsen, J., Nguyen, N. L., 2004. Potentially toxic microalgae of Vietnamese waters. *Opera Botanica* 140, pp. 216.

Le Fèvre-Lehoerff, G., Erard-le Denn E., Arzul, G., 1993. Planktonic ecosystems in the Channel: trophic relations. *Oceanologica Acta* 16: 661 – 670.

Legendre, L., Le Fèvre, J., 1991. From individual plankton cells to pelagic ecosystems and to global biogeochemical cycles. In: Demers, S. (Ed.), Particles Analysis in Oceanography, Springer Verlag, Berlin, pp. 261 – 300.

Lehninger, A. L., 1987. Prinzipien der Biochemie. De Gruyter, Berlin, New York. pp 1117.

Levitus, S., 1984. Annual cycle of temperature and heat storage in the world ocean. Journal of *Physical Oceanography* 14: 727 – 746.

Lindzen, R.S., 1979. Atmospheric Tides. *Annual Review of Earth and Planetary Science* 7: 199 – 225.

Liu, K.K., Kaplan, I.R., 1989. The eastern tropical Pacific as a source of ^{15}N-enriched nitrate in seawater off southern California. *Limnology and Oceanography* 34 (5): 820 – 830.

Liu, K.K., Su, M.J., Hsueh, C.R., Gong, G.C., 1996. The nitrogen isotopic composition of nitrate in the Kuroshio Water northeast of Taiwan: evidence for nitrogen fixation as a source of isotopically light nitrate. *Marine Chemistry* 54 (3-4): 273 – 292.

Liu, K.K., Chao, S.Y., Shaw, P.T., Gong, G.C., Chen, C.C., Tang, T.Y., 2002. Monsoon-forced chlorophyll distribution and primary production in the South China Sea: observations and a numerical study. *Deep-Sea Research* I 49 (8): 1387 – 1412.

Loick, N., Dippner, J., Doan, H.N., Liskow, I., Voss, M., 2006. Pelagic nitrogen dynamics in the Vietnamese upwelling area. Eos Trans. AGU, 87(36). Ocean Science Meeting Supplement, Abstract OS11I-05: 47.

Lomas, M. W., 2004. Nitrate reductase and urease enzyme activity in the marine diatom *Thalassiosira weissflogii* (Bacillariophyceae): interactions among nitrogen substrates. *Marine Biology* 144: 37 – 44.

Macko, S. A., Lee, W. Y., Parker, P. L., 1982. Nitrogen and carbon stable isotope fractionation by two species of marine amphipods: laboratory and field studies. *Journal of Experimental Marine Biology and Ecology* 63: 45 – 49.

Macko, S. A., Fogel (Estep), M. L., Hare, P. E., Hoering, T. C. 1987. Isotopic fractionation of nitrogen and carbon in the synthesis of amino acids by microorganisms. *Chemical Geology* 65: 79 – 92.

Margalef, R., 1978. Phytoplankton communities in upwelling areas. The example of NW Africa. *Oecologica Aquatica* 3: 97 – 132.

Mariotti, A., Germon, J.C., Hubert, P., Kaiser, P. Letolle, R., Tardieux, A., Tardieux P., 1981. Experimental determination of nitrogen kinetic isotope fractionation: some principles, illustration for the denitrification and nitrification processes. *Plant and Soil* 62: 413 – 430.

Mayzaud, P., Poulet, S. A., 1978. The importance of the time factor in the response of zooplankton to varying concentrations of naturally occurring particulate matter. *Limnology and Oceanography* 23 (6): 1144 – 1154.

McCarthy, J.J., Taylor, W. R., Jay, L., Taft, J. L., 1977. Nitrogenous Nutrition of the Plankton in the Chesapeake Bay. 1. Nutrient Availability and Phytoplankton Preferences. *Limnology and Oceanography* 22 (6): 996 – 1011.

McCarthy, J. J., Goldman, J. C., 1979. Nitrogenous nutrition of marine phytoplankton in nutrient-depleted waters. *Science* (Wash.) 203 (4381): 670 – 672.

McClelland, J. W. Montoya, J. P., 2002. Trophic relationships and the nitrogen isotopic composition of amino acids in plankton. *Ecology* 83 (8): 2173 – 2180.

McClelland, J. W., Holl, C. M., Montoya, J. P., 2003. Relating low δ^{15}N values of zooplankton to N_2-fixation in the tropical North Atlantic: insights provided by stable isotope ratios of amino acids. *Deep-Sea Research I* 50: 849-861.

Metzger, E.J., Hurlburt, H.E., 1996. Coupled dynamics of the South China Sea, the Sulu Sea, and the Pacific Ocean. *Journal of Geophysical Research* 101: 12331 – 12352.

Meybeck, M., Carbonnel, J.P., 1975. Chemical transport by the Mekong river. *Nature* 255: 134 – 136.

Michener, R.H., Schell, D.M. 1994. Stable isotope ratios as tracers in marine aquatic food webs. In: Lajtha and Michener (Eds.). Stable Isotopes in Ecology and Environmental Science. Methods in Ecology. Blackwell, Boston: 138 – 157.

Miflin, B.J., Lea, P.J., 1977. Amino acid metabolism. *Annual Review of Plant Physiology* 28: 199 – 329.

Milliman, J. D., 1991. Flux and fate and fluviatile sediment and water in coastal seas. In: Mantura, R. F. C., Martin, J. M., Wollast, R. (Eds). Ocean Margin Processes and Global Change. Wiley and Sons, Chichester, pp. 69 – 89.

Minagawa, M., Wada, E., 1984. Stepwise enrichment of ^{15}N along food chains: further evidence and the relation between ^{15}N and animal age. *Geochimica et Cosmocimica Acta* 48: 1135 – 1140.

Minagawa, M., Wada, E., 1986. Nitrogen isotope ratios of red tide organisms in the East China Sea: a characterization of biological nitrogen fixation. *Marine Chemistry* 19: 245 – 259.

Mittelstaedt, E., 1976. On the currents along the Northwest African coast south of 22°N. *Deutsche hydrographische Zeitschrift* 29: 97 – 117.

Mittelstaedt, E., 1991. The ocean boundary along the northwest African coast. Circulation and oceanographic properties at the sea surface. *Progress in Oceanography* 26: 307 – 355.

Mohrholz, V., Schmidt, M., Lutjeharms, J.R.E., 2001. The hydrography and dynamics of the Angola-Benguela Frontal Zone and environment in April 1999. *South African Journal of Science* 97: 199 – 208.

Montani, S., Pithakpol, S., Tada, K., 1998. Nutrient regeneration in coastal seas by *Noctiluca scintillans*, a red tide-causing dinoflagellate. *Journal of Marine Biotechnology* 6: 224-228.

Montoya, J.P., Horrigan, S.G., McCarthy, J.J., 1991. Rapid, storm-induced changes in the natural abundance of ^{15}N in a planktonic ecosystem, Chesapeake Bay, USA. *Geochimica et Cosmochimica Acta* 55: 3627 – 3638.

Montoya, J.P., Wiebe, P.H., McCarthy, J.J., 1992. Natural abundance of ^{15}N in particulate nitrogen and zooplankton in the Gulf Stream region and warm-core ring 86A. *Deep-Sea Research Part A (Oceanographic Research Papers)* 39 (1A suppl.): S363 – S392.

Montoya, J. P., McCarthy, J. J., 1995. Isotopic fractionation during nitrate uptake by phytoplankton grown in continuous culture. *Journal of Plankton Research* 17 (3): 439-464.

Montoya, J. P., Voß; M., Kähler,P., Capone, D.G., 1996. A simple, high precision tracer assay for dinitrogen fixation. *Applied Environmental Microbiology* 62: 986 – 993.

Montoya, J.P., Carpenter, E.J., Capone, D.G., 2002. Nitrogen fixation and nitrogen isotope abundances in zooplankton of the oligotrophic North Atlantic. *Limnology and Oceanography* 47 (6): 1617 – 1628.

Montoya, J.P., Holl, C.M., Zehr, J.P., Hansen, A., Villareal, T.A., Capone, D.G., 2004. High rates of N_2 fixation by unicellular diazotrophs in the oligotrophic Pacific Ocean. *Nature* 430 (7003): 1027 – 1032.

Morimoto, A., Yoshimoto, K., Yanagi, T., 2000. Characteristics of the Sea Surface Circulation and Eddy Field in the South China Sea Revealed by Satellite Altimetric Data. *Journal of Oceanography* 56(3): 331 – 343.

Mulholland, M. R., Capone, D. G., 1999. Nitrogen fixation, uptake and metabolism in natural and cultured populations of *Trichodesmium* spp. *Marine Ecology Progress Series* 188: 33 – 49.

Mulholland, M. R., Ohki, K., Capone, D. G., 2001. Nutrient controls on nitrogen uptake and metabolism by natural populations and cultures of Trichodesmium (cyanobacteria). *Journal of Phycology* 37: 1001 – 1009.

Murphy, J., Riley, J.P., 1962. A modified single solution method for the determination of phosphate in natural waters. *Analytica Chimica Acta* 27: 31 – 36.

Needoba, J.A., Waser, N.A., Harrison, P.J., Calvert, S.E., 2003. Nitrogen isotope fractionation in 12 species of marine phytoplankton during growth on nitrate. *Marine Ecology Progress Series* 255: 81 – 91.

Needoba, J.A., Harrison, P.J., 2004. Influence of low light and A light: Dark cycle on NO_3^- uptake, intracellular NO_3^-, and nitrogen isotope fractionation by marine phytoplankton. *Journal of Phycology* 40 (3): 505 – 516.

Needoba, J.A., Sigman, D. M., Harrison, P.J., 2004. The mechanism of isotope fractionation during algal nitrate assimilation as illuminated by the $^{15}N/^{14}N$ of intracellular nitrate. *Journal of Phycology* 40 (3): 517 – 522.

Nguyen, C, Nguyen, A. K., 2002. Distribution of zooplankton in the East Sea – Results of the Vietnam-Philippines joint oceanographic and marine scientific research cruise, 2000. In: Nguyen TA and Nguyen HP (Eds.) Collection of Marine Research Work, Special Issue on the Occasion of the 80th Anniversary of the Institute of Oceanography (1922 -2002). National Centre for Natural Science and Technology of Vietnam Institute of Oceanography, Vol. XII, pp. 159 – 166.

Nguyen, N.L., 1996. Species composition and cell density of phytoplankton in the coastal strong upwelling of Ninh Thuan – Binh Thuan provinces. In: Vo, V. L., Nguyen, T.A, Nguyen, V.L., Le, P. T., Nguyen, H.P., Nguyen, K. V. (Eds.), Contributions on coastal strong upwelling in southern central Vietnam, Science and Technics Publishing House, Nha Trang, pp. 131 – 142. (in Vietnamese with English Abstract)

Nguyen, N.L., Doan, N.H., 1996. Harmful marine phytoplankton in Vietnam waters. In: Yasumoto, T., Oshoma, I., and Fukuyo, Y. (Eds.), Harmful and Toxic algal blooms, Intergovermental Oceanic Commission, UNESCO, Paris, pp. 45 – 48.

Nguyen, N. L., 1999. *Trichodesmium erythraeum* bloom, Harmful Algae News, 19: 13. (Available at http://ioc.unesco.org/iocweb/IOCpub/iocpdf/ han19.pdf.).

Nguyen, T.A., Vo, D.S., 1999. Hydrographic and biogeochemical studies in the Mekong delta, Vietnam. In: Ittekkot V, Subramaniam V, Annadurai S. (Eds.) Biogeochemistry of Rivers in Tropical South and Southeast Asia. *Mitteilungen aus dem Geologisch-Paläontologischen Institut der Universität Hamburg* 82: 285 – 297.

Nguyen, T.A., Hoang, D.T., 2001. Studies on phytoplankton pigment: chlorophyll, total carotenoids and degradation products in Vietnamese waters (The south China Sea, Area IV) Proceedings of the SEAFDEC Seminar on Fisheries Resources in the South China Sea, Area 4: Vietnamese Waters, pp. 1 – 18.

Nguyen, T.C., Vu, M.H., 2001. Distribution and species composition of Phytoplankton in the Vietnamese waters. Proceedings of the SEAFDEC Seminar on Fisheries Resources in the South China Sea, Area 4: Vietnamese Waters, pp. 265 – 291.

Nguyen, V.C., 1990. Estuary Dynamics of Rivers of Vietnam. Dr. Sc. Thesis, Moskow State University, Russia, pp. 379. (in Russian)

Nitterouer, C.A., Brunskill, G.J., Figueiredo, A.G., 1995. Importance of tropical coastal environments. *Geo-marine Letters* 15: 121 – 126.

Oberhuber, J.M., 1988. An atlas based on the "COADS" data set: The budget of heat, buoyancy, and turbulent kinetic energy at the surface of the global ocean. *MPI Report* 15. pp. 198.

Okaichi, T., Nishio, S., 1976. Indentification of ammonia as the toxic principle of red tide of *Noctiluca militaris. Bulletin of the Plankton Society of Japan* 23: 75-80.

Pertola, S., Koski, M., Viitasalo, M., 2002. Stochiometry of mesozooplankton in N- and P-limited areas of the Baltic Sea. *Marine Biology* 140 (2): 425 – 434.

Pesant, S., Legendre, L., Gosselin, M., Bjornsen, P.K., Fortier, L., Michaud, J., Nielsen,, T.G., 2000. Pathways of carbon cycling in marine surface waters: the fate of small-sized phytoplankton in the Northeast Water Polynya. *Journal of Plankton Research* 22 (4): 779 – 801.

Peterson, B.J., Fry, B., 1987. Stable isotopes in ecosystem studies. *Annual Review of Ecology and Systematics* 18: 293 – 320.

Pham, V.T., Nguyen, T.A., Hoang, T.D., 2002. Some remarks on the distribution of nutrients along the transect Nha Trang-Luzon (Vietnamese-Philippines cooperative investigation, JOMSRE II, May 2000). In: Nguyen TA (Ed), Collection of marine Research Works XII, pp 91 – 102.

Pohlmann, T., 1987. A three-dimensional circulation model of the South China Sea. In: Nihoul JJ, Jamart B (Eds.) Three-Dimensional Models of Marine and Estuarine Dynamics, Elsevier New York, pp. 245 – 268.

Proctor, L. M. 1997. Nitrogen-fixing, photosynthetic, anaerobic bacteria associated with pelagic copepods. *Aquatic Microbiological Ecology* 12: 105 – 113.

Qu, T., 2000. Upper layer circulation in the South China Sea. *Journal of Physical Oceanography* 30: 1450 – 1460.

Quesada, A., Hidalgo, J., Fernandez, E., 1998. Three Nrt2 genes are differentially regulated in *Chlamydomonas reinhardtii*. *Molecular and General Genetics* 258: 373 – 377.

Rau, G.H., Teyssie, J.L., Rassoulzadegan, F., Fowler, S.W., 1990. ^{13}C/ ^{12}C and ^{15}N/ ^{14}N variations among size-fractionated marine particles: Implications for their origin and trophic relationships. *Marine Ecology Progress Series* 59 (1-2): 33 – 38.

Redfield, A., Ketchum, B., Richards, F., 1963. The influence of organisms on the composition of sea water. In: Hill N. (Ed.) The Sea 2 Interscience, New York, pp. 224 – 228.

Rojana-anawat, P., Pradit, S., Sukramongkol, N., Siriraksophon, S., 2001. Temperature, salinity, dissolved oxygen and water masses of Vietnamese waters. Proceedings of the SEAFDEC Seminar on Fisheries Resources in the South China Sea, Area 4: Vietnamese Waters, pp. 346 – 355.

Rolff, C., 2000. Seasonal variation in δ^{13}C and δ^{15}N of size-fractioned plankton at a coastal station in the northern Baltic proper. *Marine Ecology Progress Series* 203: 47 – 65.

Sabrowski, R., Buchholz, F., 1999. A laboratory study on digestive processes in the Antarctic krill, Euphausia superba, with special regard to chitinolytic enzymes. *Polar Biology* 21: 295 – 304.

Schemainda, R., Hagen, E., 1983. On steady state intermediate vertical currents induced by Mozambique Current. *Océanographie Tropicale* 18: 81 – 88.

Schott, F.A., McCreary, Jr. J.P., 2001. The monsoon circulation of the Indian Ocean. *Progress in Oceanography* 51: 1 – 123.

Sellner, K.G., 1997. Physiology, ecology, and toxic properties of marine cyanobacteria blooms. *Limnology and Oceanography* 42 (5): 1089 – 1104.

Shamsudin, L., 1998. Seasonal variation of fatty acid content in natural microplankton from the Tumpat coastal waters of the South China Sea. *Archives of Physiology and Biochemistry* 106(3): 253 – 260.

Shamsudin, L., Mohamad, K., Noraslizan, S., Kasina, M. 2001. Nanoplankton distribution and abundance in the Vietnamese waters of the South China Sea. Proceedings of the SEAFDEC Seminar on Fisheries Resources in the South China Sea, Area IV: Vietnamese Waters, pp. 198 – 232.

Shaw, P.T., Chao, S.Y., 1994. Surface circulation in the South China Sea. *Deep-Sea Research I* (41): 1663 – 1683.

Sieburth, J.McN., 1979. Sea Microbes. Oxford University Press, New York, pp. 491.

Sigman, D.M., Altabet, M.A., Michener, R., McCorkle, D.C., Fry, B., Holmes, R.M., 1997. Natural abundance-level measurement of the nitrogen isotopic composition of oceanic nitrate: An adaptation of the ammonia diffusion method. *Marine Chemistry* 57 (3-4): 227 – 242.

Sigman, D. M. 1998, The role of biological production in Pleistocene atmospheric carbon variations and the nitrogen isotope dynamics of the Southern Ocean. Ph. D. thesis, WHOI, Boston, Mass., USA.

Sigman, D.M., Casciotti, K.L., 2001. Nitrogen isotopes in the ocean. In: Thorpe, S., Threbion, K. (Eds.), Encyclopedia of Ocean Sciences, Elservier Verlag, New York, pp. 1884 – 1894.

Slutz, R.J., Lubker, S.J., Hiscox, D.J., Woodruff, S.D., Jenne, R.L., Joseph, D.H., Steurer, P.M., Elms, J.D., 1985. Comprehensive Ocean-Atmosphere Data Set. Release 1. NOAA Environmental Research Laboratory, Climate Research Program Boulder, Colorado, pp. 268.

Smith, R.L., 1968. Upwelling. *Oceanography and Marine Biology : an Annual Review* 6: 11 – 46.

Song, B, Ward, B.B., 2004. Molecular characterization of the assimilatory nitrate reductase gene and its expression in the marine green alga *Dunaliella tertiolecta* (Chlorophyceae). *Journal of Phycology* 40 (4): 721 – 731.

Stolte, W., Mc Collio, T., Noordeloos, A.A.M., Reigman, R., 1994. Effect of N source on the size distribution within marine phytoplankton populations. *Journal of Experimental Marine Biology and Ecology* 184: 83 – 97.

Syrett, P.J., 1981. Nitrogen metabolism of microalgae. In Platt, T. (Ed.). Physiological Bases of Phytoplankton Ecology. *Canadian Bulletin of Fisheries and Aquatic Sciences* 210: 182 – 210.

Takabayashi, M., Wilkerson, F.P, Robertson, D., 2005. Response of Glutamine Synthetase Gene Transcription and Enzyme Activity to External Nitrogen Sources in the diatom *Skeletonema costatum* (Bacillariophyceae). *Journal of Phycology* 41 (1): 84 – 94.

Tang, D.L., Kawamura, H., Dien, T.V., Lee, M.A., 2004. Offshore phytoplankton biomass increase and its oceanographic causes in the South China Sea. *Marine Ecology Progress Series* 268: 31 – 41.

Tischner, R. 2000. Nitrate uptake and reduction in higher and lower plants. *Plant Cell and Environment* 23: 1005 – 1024.

Vanlerberghe, G.C., Schuller, K.A., Smith, R.G., Feil, R., Plaxton, W.C., Turpin, D.H., 1990. Relationship between NH_4^+ assimilation rate and *in vivo* phosphoenolpyruvate carboxylase activity: Regulation of anaplerotic carbon flow in the green alga *Selenastrum minutum. Plant Physiology* 94: 284 – 290.

Villareal, T. A., 1994. Widespread occurrence of Hemiaulus-Cyanobacterial symbiosis in the Southwest North-Atlantic Ocean. *Bulletin of Marine Science* 54 (1): 1 – 7.

Vitousek, P. M., Cassman, K., Cleveland, C., Crews, T., Field, C. B., Grimm, N. B., Howarth, R. W., Marino, R., Martinelli, L., Rastetter, E.B., Sprent, J. I., 2002. Towards an ecological understanding of biological nitrogen fixation. *Biogeochemistry* 57/ 58: 1 – 45.

Vo, V.L., 1997. Atlas of natural condition, ecology and bioproduction of strong upwelling sea region in southern central Vietnam. Vo, VL and Nguyen, TA (Eds.), Science and Technics Publishing House, Nha Trang, p. 2.

Vo, V.L., Dang, V.H., 2002. The southward cold current along the coast of central Vietnam. In: Nguyen TA and Nguyen HP (Eds.) Collection of Marine Research Work, Special Issue on the Occasion of the 80th Anniversary of the Institute of Oceanography (1922 -2002). National Centre for Natural Science and Technology of Vietnam Institute of Oceanography, Vol. XII, pp. 91 – 102.

Voss, M., Dippner, J. W., Montoya, J. P. 2001. Nitrogen isotope patterns in the oxygen-deficient waters of the Eastern Tropical North Pacific Ocean. *Deep-Sea Research, Part I* 48 (8): 1905 – 1921.

Voss, M., Croot, P., Lochte, K., Mills, M., Peeken, I., 2004. Patterns of Nitrogen Fixation along 10°N in the Tropical Atlantic. *Geophysical Research Letters* 31: L23S09: doi: 10.1029/204GL020127.

Voss, M., Bombar, D., Loick, N., Dippner, J.W., 2006. Riverine influence on nitrogen fixation in the upwelling region off Vietnam, South China Sea. *Geophysical Research Letters* 33, L07604, doi: 10.1029/2005GL025569.

Wafar, M., L′Helguen, S., Raikar, V., Maguer, J-F., Le Corre, P., 2004. Nitrogen uptake by size-fractionated plankton in a permanently well-mixed temperate coastal waters. *Journal of Plankton Research* 26 (19): 1207 – 1218.

Walsh, J. J., 1996. Nitrogen fixation within a tropical upwelling ecosystem: Evidence for a Redfield budget of carbon/ nitrogen cycling by total phytoplankton community. *Journal of Geophysical Research* 101 (C9): 20,607 – 20,616.

Waser, N. A., Harrison, P. J., Nielsen, B., Calvert, S. E., Turpin, D. H. 1998. Nitrogen isotope fractionation during the uptake and assimilation of nitrate, nitrite, ammonium and urea uptake by a marine diatom. *Limnology and Oceanography* 43 (2): 215 – 224.

Wefer, G., Fischer, G., 1993. Seasonal patterns of vertical particle flux in equatorial and coastal upwelling areas of eastern Atlantic. *Deep-Sea Research* 40: 1613 – 1645.

White, P.J., 1996. The permeation of ammonium through a voltage-independent K^+ channel in the plasma membrane of rye roots. *Journal of Membrane Biology* 152: 89 – 99.

Wikner, J., Hagström, Å, 1988. Evidence for a tightly coupled nanoplanktonic predator-prey link regulating the bacteriovores in the marine environment. *Marine Ecology Progress Series* 50: 137 – 145.

Woodruff, S.D., Slutz, R.J., Jenne, R.L., Steurer, P.M., 1987. A comprehensive ocean-atmosphere data set. *Bulletin of the American Meteorological Society* 68: 1239 – 1250.

Wu , J., Calvert, S. E., Wong, C. S., 1997. Nitrogen isotope variations in the subarctic northeast Pacific: Relationships to nitrate utilization and trophic structure. *Deep-Sea Research* 44: 287 – 314.

Wu, J., Chung, S., Wen, L., Liu, K., Chen, Y.L., Chen, H., Karl, D.M., 2003. Dissolved inorganic phosphorus, dissolved iron, and Trichodesmium in the oligotrophic South China Sea. *Global Biogeochemical Cycles* 17(1), 1008, doi:10.1029/2002GB001924.

Wu, C.R., Shaw, P. T., Chao, S. Y.,1998. Seasonal and interannual variations in the velocity field of the South China Sea. *Journal of Oceanography* 54 (4): 261 – 372.

Wu, S.-G., Wong, H. K., Luo, Y.-L., Liang, Z.-R., 1999. Distribution and origin of sediments on the northern Sunda Shelf, South China Sea. *Chinese Journal of Limnology* 17 (1): 28 – 40.

Wyrtki, K., 1961. Physical oceanography of the Southeast Asian waters. In: NAGA Report 2, Scientific Results of Marine Investigations of the South China Sea and Gulf of Thailand 1959-1961, Scripps Institution of Oceanography, University of California, San Diego, La Jolla, pp. 195.

Xue, H., Chai, F., Pettigrew, N., Xu, D., Shi, M., Xu, J., 2004. Kuroshio intrusion and the circulation in the South China Sea. *Journal of Geophysical Research (C Oceans)* 109 (C2), C02017, doi:10.1029/2002JC001724.

Yancey, P.H., Clark, M.E., Hand, S.C., Bowlus, R.D., Somero, G.N., 1982. Living with water stress: evolution of osmolyte systems. *Science* 217: 1214 – 1222.

Yang, H.J., Liu, Q.Y., 1998. A summary on ocean circulation study of the South China Sea. *Advance in Earth Sciences* 13(4): 364 – 368. (in Chinese with English abstract)

Yang, H., Liu, Q., Liu, Z., Wang, D., Liu, X., 2002. A general circulation model study of the dynamics of the upper layer ocean circulation of the South China Sea. *Journal Geophysical Research* 1007 (C7), doi:10.1029/2001JC1084.

Yoshida, K., Mao, H.-L., 1957. A theory of upwelling of large horizontal extent. *Journal of Marine Research* 16: 40 – 53.

Yoshida, K., 1967. Circulation in the Eastern Tropical Ocean with Special References to Upwelling and Undercurrents. *Japanese Journal of Geophysics* 4: 1 – 75.

Zehr, J. P., Carpenter, E. J., Villareal, T. A., 2000. New perspectives on nitrogen-fixing microorganisms in tropical and subtropical oceans. *Trends in Microbiology* 8: 68 – 73.

Zehr, J. P., Waterbury, J. B., Turner, P. J., Montoya, J. P., Omoregie, E., Steward, G. F., Hansen, A., Karl, D. M., 2001. Unicellular cyanobacteria fix N_2 in the subtropical North Pacific Ocean. *Nature* 412: 635-638.

Zehr, J. P., Ward, B. B., 2002. Minireview: Nitrogen Cycling in the Ocean: New Perspectives on Processes and Paradigms. *Applied and Environmental Microbiology* 68: 1015 – 1024.

Zhang, R., 2000. Features of the East Asian monsoon during El Niño Episode. *CLIVAR Exchanges* 5: 21 – 22.

Erklärung

Hiermit versichere ich, dass ich die vorliegende Arbeit selbstständig angefertigt und ohne fremde Hilfe verfasst habe, keine ausser den von mir angegebenen Hilfsmitteln und Quellen dazu verwendet habe und die den benutzten Werken inhaltlich und wörtlich entnommenen Stellen als solche kenntlich gemacht habe.

Rostock, den

Natalie Loick, Dipl.-Biol.

born on 03. July 1976 in Bottrop, Germany

Workings

May 2003 – April 2006	PhD candidate and research associate in the bilateral project "Pelagic processes and biogeochemical fluxes in the South China Sea off southern central Vietnam"
Sep. 2002 – Apr. 2003	Research associate in the international JGOFS-Indic (Joint Global Ocean Flux Study) project
Sep. 2001 – Aug. 2002	Elaboration of the DFG-Project (German Research Foundation) "Characterization of ecophysiological and behavioural strategies of dominant zooplankton in the northern Benguela upwelling area" – defeated Feb. 2003

Studies

July 2000 – Apr. 2001	Preparation of the master thesis "Horizontal and vertical distribution of different calanoid copepod species in the Angola-Benguela Front System" at the Center for Tropical Marine Ecology (ZMT) in Bremen
Okt. 1997 – Apr. 2001	Postgraduate studies and final examinations in Marine Biology, Ecology and Zoology at the University of Bremen
Okt. 1995 – Sept. 1997	Undergraduate studies and Vordiplom in Biology at the University of Rostock

School

1982 – 1986	Elementary school: Urbanusgrundschule in Rhade
1986 – 1995	Secondary school: Gymnasium Remigianum in Borken (Westf.)
1992 – 1993	Year abroad: Burlington High School in Vermont, USA

Attachment

Computed heat flux budget from J. W. Dippner, Baltic Sea Research Institute Warnemünde, Germany:

The turbulent surface heat fluxes, the sensible heat flux Q_H and latent heat fluxes Q_L, are estimated by the bulk formulations:

$$Q_H = \rho_a c_{p,air} c_H W (T_a - T_s) \tag{2.1}$$

$$Q_L = \rho_a L_w c_L W (q_a - q_s) \tag{2.2}$$

where ρ_a is the density of dry air, T_a is is the dry air temperature, T_s the sea surface temperature (SST), q_a the air specific humidity and q_s the specific humidity close to the surface assuming saturation. $c_{p,air} = 1005$ Ws kg^{-1} K^{-1} is the specific heat of air and $L_W = 2.5$ x 10^6 Ws kg^{-1} the latent heat evaporation. W is the wind speed. c_H and c_L are bulk transfer coefficients according to Kondo (1975). At the sea surface, the specific humidity is given by the vapour pressure e and the atmospheric surface pressure p.

$$e = 611 x 10^{(T-273.16)/(T-35.86)} \tag{2.3}$$

$$q = \frac{0.622e}{p - 0.378e} \tag{2.4}$$

e and p are in Pascal, T is in Kelvin. Details are given in Oberhuber (1988). The net effect of long wave radiation at the surface is taken from Berliand and Berliand (1952):

$$QB = \varepsilon \sigma T_a^3 [T_a F + 4(T_s - T_a)] \tag{2.5}$$

where $\varepsilon = 0.97$ is the emissivity of water, $\sigma = 5.67$ x 10^{-8} W/m^{2}K^4 the Stefan-Boltzmann constant. The cloud and vapour pressure correction is a Brunt type correction function:

$$F = (0 - 39 - 0.05\sqrt{e/100})(1 - \chi n^2) \tag{2.6}$$

where n is the relative cloud cover and χ is a function of geographical latitude according to Budyko (1974)

$$\chi = 0.5 + 0.4(\min(|\phi|, 60°))/90° \tag{2.7}$$

The upwelling dynamics is analysed with respect to the peculiarities of Vietnamese upwelling. According to Hagen (2001) the velocity of the wind induced upwelling or Ekman pumping can be estimated by

$$w_E = \frac{1}{f\rho_0}\frac{\partial \tau^y}{\partial x} = \frac{\tau^y}{Lf\rho_0} = \frac{E^x}{L} \tag{2.8}$$

where f is the Coriolis parameter, ρ_0 a reference density, τ^y the north-south component of the wind stress, E_x the offshore Ekman volume transport and L the width of the shelf. Considering upwelling at the shore and keeping in mind that the shelf is very narrow between 11 °N and 16 °N, the shelf width L must be replaced by the first mode of the radius of deformation R: $w_E = E^x/R$.

To analyse the influence of dynamical upwelling, the northward component of relative vorticity is computed. Defining $\eta = \partial u/\partial z - \partial w/\partial x$, the frictionless system:

$$\frac{\partial u}{\partial t} + u\frac{\partial u}{\partial x} + v\frac{\partial u}{\partial y} + w\frac{\partial u}{\partial z} - fv = -\frac{1}{\rho}\frac{\partial p}{\partial x} \tag{2.9}$$

$$\frac{\partial w}{\partial t} + u\frac{\partial w}{\partial x} + v\frac{\partial w}{\partial y} + w\frac{\partial w}{\partial z} - f^*u = -\frac{1}{\rho}\frac{\partial p}{\partial z} - g \tag{2.10}$$

becomes after cross differentiation and subtraction:

$$\frac{d\eta}{dt} = -\eta\left(\frac{\partial u}{\partial x} + \frac{\partial w}{\partial z}\right) - \frac{\partial v}{\partial z}\frac{\partial u}{\partial y} + \frac{\partial v}{\partial x}\frac{\partial w}{\partial y} + f\frac{\partial v}{\partial z} + f^*\frac{\partial u}{\partial x} + \frac{1}{\rho^2}\left(\frac{\partial \rho}{\partial z}\frac{\partial p}{\partial x} - \frac{\partial \rho}{\partial x}\frac{\partial p}{\partial z}\right) \tag{2.11}$$

Here u, v, and w are the three components of the velocity field, p is the pressure, ρ is the density and g is the gravity acceleration. The Coriolis parameters are f = 2ωsinφ and f* = 2 ωcosφ, where ω is the frequency of earth rotation and φ the geographical latitude. The terms on the right hand side of equation 2.11 are the production term of relative vorticity: the divergence term, two tilting terms, two Coriolis terms and the solenoid term. Since $\partial w/\partial y$ is small, the second tilting term is four times smaller than the first tilting term and can be neglected. Using the equation of incompressibility, equation 2.11 becomes:

$$\frac{d\eta}{dt} = \eta\frac{\partial v}{\partial y} - \frac{\partial v}{\partial z}\frac{\partial u}{\partial y} + f\frac{\partial v}{\partial z} + f^*\frac{\partial u}{\partial x} + \frac{1}{\rho^2}\left(\frac{\partial \rho}{\partial z}\frac{\partial p}{\partial x} - \frac{\partial \rho}{\partial x}\frac{\partial p}{\partial z}\right) \tag{2.12}$$

This equation is used for analysis. Assuming steady state, Equation 2.11 can be written as:

$$\frac{\partial w}{\partial z} = -\frac{\partial u}{\partial x} - \frac{1}{\eta}\frac{\partial v}{\partial z}\frac{\partial u}{\partial y} + \frac{1}{\eta}\frac{\partial v}{\partial x}\frac{\partial w}{\partial y} + \frac{f}{\eta}\frac{\partial v}{\partial z} + \frac{f^*}{\eta}\frac{\partial u}{\partial x} + \frac{1}{\eta\rho^2}\left(\frac{\partial \rho}{\partial z}\frac{\partial p}{\partial x} - \frac{\partial \rho}{\partial x}\frac{\partial p}{\partial z}\right) \tag{2.13}$$

Stepwise integration of Equation 2.13 over the water column results in the dynamical upwelling velocity which is computed from the observations.

References

Berliand, M.E., Berliand, T.G., 1952. Determining the net long-wave radiation with consideration of the effect of cloudiness. *Izvestia Akademia Nauk SSSR Series Geofisica* 1: 64 – 78 (in Russian).

Budyko, M.I., 1974. Climate and life. In: Int. Geophys. Ser. Academic Press, pp. 508.

Kondo, J., 1975. Air-Sea bulk transfer coefficients in diabatic conditions. *Boundary-Layer Meteorology* 9: 91 – 112.